ABSTRACT

LUIS, JANE MARIAN SA-ONG. Sexual Reproduction and Enhancing the Efficacy of Biocontrol of Aflatoxin Contamination by *Aspergillus flavus*. (Under the direction of Dr. Peter S. Ojiambo and Dr. Ignazio Carbone).

Aflatoxigenic strains of *Aspergillus flavus* contaminate maize with carcinogenic aflatoxins and exposure to contaminated food and feed can negatively impact human and livestock health. The fungus survives in its asexual state as conidia, hyphae or mycelia. Under unfavorable conditions, the fungus can produce thick-walled sclerotia that can bear ascospore-bearing ascocarps when fertilized by conidia of the opposite mating type. The shift from asexual to sexual states affects the survival, morphology and genetic diversity of the fungus, but the transition from asexual to sexual state is not well understood. Reciprocal crosses with high and low female fertility were used to examine changes in the morphology, secondary metabolite expression, and gene transcription within the sclerotia/stromata over a period of 8 weeks. Scanning electron micrographs showed progressive development of sexual structures over time, starting with formation of ascocarps and internal hyphae at 4 weeks of incubation followed by development of asci and ascospores at 6 to 8 weeks of incubation. The development of these structures was accompanied by distinctive secondary metabolite and transcriptomic profiles in stromata from high and low fertility crosses. These results provide insights on a possible mechanism of sexual reproduction in *A. flavus* and broaden our knowledge on sexual development in this fungus and other filamentous fungi that were strictly thought to be asexual. The impact of candidate biocontrol strain RMb10 on the population dynamics of native *A. flavus* was tested in replicated large-scale field trials in Alabama, Mississippi, North Carolina, and Texas in 2016 and 2017. Unlike all currently reported biocontrol strains of *A. flavus* which are of the mating type *MAT1-2*, RMb10 has a *MAT1-1* mating type. A total of 780 *A. flavus* isolates were collected from soil samples at each state prior to

biocontrol application and at harvest. These isolates were screened for colony morphology, sclerotia production (+/-), mating type (*MAT1-1* or *MAT1-2*) and aflatoxin gene cluster type (full, partial, or missing). Selected isolates (n = 311) were then subjected to next generation multi-locus sequence typing using five loci (*aflM*, *aflW*, *amdS*, *mfs* and *trpC*). Population genetic analysis showed that the *A. flavus* populations collected during each sampling period in each state and year exhibited signatures of recombination consistent with sexual reproduction. Increase in the frequency of isolates belonging to the same multi-locus haplotype as RMb10 and Afla-Guard® as well as in the number of isolates with missing aflatoxin gene cluster at harvest suggests successful proliferation of the biocontrol strains into the field populations. Further, RMb10 had comparable performance with that of the commercial biocontrol product Afla-Guard® in reducing aflatoxin contamination in Texas in 2016 when environmental conditions were conducive for aflatoxin contamination. Results of the study provide insights in developing new biocontrol strategies for sustainable reduction of aflatoxin contamination.

Sexual Reproduction and Enhancing the Efficacy of Biocontrol of Aflatoxin Contamination by *Aspergillus flavus*

by
Jane Marian Sa-ong Luis

A dissertation submitted to the Graduate Faculty of
North Carolina State University
in partial fulfillment of the
requirements for the degree of
Doctor of Philosophy

Plant Pathology

Raleigh, North Carolina
2019

APPROVED BY:

Dr. Peter S. Ojiambo Committee Co-Chair	Dr. Ignazio Carbone Committee Co-Chair
Dr. Shuijin Hu	Dr. Ralph A. Dean

DEDICATION

To my loving family who inspires me to work hard and find joy in all things.

BIOGRAPHY

Jane Marian Sa-ong Luis was born in the strawberry and vegetable-growing town of La Trinidad, Benguet, Philippines. Her interest in agriculture started when her parents, who are both agriculture professors, exposed her to the world of mycology and animal science at an early age. She moved to Los Baños, Laguna to obtain her bachelor's degree in agriculture from the University of the Philippines Los Baños. Her undergraduate thesis involved studying the effect of moisture and incubation time in the productivity of shiitake mushroom when grown in alnus logs. She worked for three years in Cambodia then joined the Department of Plant Pathology at the University of Georgia to obtain her master's degree. Her research involved phenotyping different peanut genotypes for drought stress tolerance, strain-typing *Aspergillus* isolates and quantifying aflatoxin contamination in peanuts. The global impact of aflatoxin motivated her to pursue a doctoral degree in the same field. She then joined the Department of Entomology and Plant Pathology at North Carolina State University, where her research involved characterizing sexual reproduction in *Aspergillus flavus* and examining the potential of a locally-selected *A. flavus* strain as biocontrol agent against aflatoxin contamination in maize.

ACKNOWLEDGEMENTS

I would like to express my deepest gratitude to many people who made my PhD life both full of intensive learning and enjoyable moments. To my co-advisers Drs. Peter Ojiambo and Ignazio Carbone; committee members Drs. Shuijin Hu and Ralph Dean; and Drs. Gary Payne and Marc Cubeta, who used their expertise in their own fields to guide me in my research and widen my scientific skills. They also offered encouraging words of wisdom, abundant support and valuable insights during the duration of my graduate study. To our collaborators from USDA-ARS SRRC at New Orleans including Drs. Jeffrey Cary, Matthew Lebar, Geromy Moore and Deepak Bhatnagar for their involvement in my study regarding the morphology, secondary metabolite expression and transcriptomic profiles of *A. flavus* crosses with different levels of female fertility. To our AMCOE collaborators including Drs. Ron Heiniger, Mark Weaver, Thomas Isakeit, and Kira Bowen for sending soil samples and maize kernels for my biocontrol study.

I greatly appreciate the help of Samah Ameen, Vicki Cornish, Greg O'Brian, James White, Yeonyee Oh, Richard Gell and Megan Molo in conducting my laboratory experiments, collecting soil samples from the field, and/or running data analysis programs. I also appreciate my lab members, fellow graduate students and friends including Wendy Britton, Thomas Keever, Lucky Mehra, Anna Thomas, Katie Neufeld, Urmila Adhikari, Maureiq Ojwang', Aydin Beseli, Isaack Kikway, Mengying Wang, Jing Jin, Johnny Balidion and many more for their friendship, kindness and invitations for social activities. I thank my parents and siblings for their constant support, encouragement, and many ways of making me feel loved. Last but not the least, I would like to thank my husband Xing Wei for his unending care and support, and my daughter Jasmine Hanna for adding more joy to our lives.

TABLE OF CONTENTS

LIST OF TABLES

CHAPTER 2

CHAPTER 3

CHAPTER 4

LIST OF FIGURES

CHAPTER 2

CHAPTER 3

CHAPTER 4

CHAPTER 1

Literature Review

1.0. Origin and Importance of Maize

Maize (*Zea mays* L.) is one of the most widely distributed grain crops around the world. It is believed to have been domesticated from a subspecies of the wild grass teosinte, *Zea mays ssp. parviglumis*, about 9,000 years ago (Doebley 1990; Matsuoka et al. 2002). The wild progenitor of maize which is native to the Central Balsas River Valley in Mexico (Hastorf 2009; Ranere et al. 2009) is characterized by a tall stalk, long lateral branches, broad leaves, and ears consisting of 5 to 12 kernels individually sealed in a hard fruit case (Doebley 2004). Domestication was initiated when ancient farmers in Mexico selected kernels with desirable characteristics to be planted the next season. Continuous selection over many seasons led to the development of modern ears which bear 500 or more exposed kernels attached to the central axis of the cob (Beadle 1939; Doebley 2004). Maize subsequently became a major part of the diet of most native people in Mexico. From Mexico, domesticated maize dispersed northward into southwestern United States and Canada, and southward into Guatemala, South America and the Andes Mountains (Matsuoka et al. 2002). Contact between Native Americans and European colonists in the 15th century paved way for the spread of maize to different parts of the world. With the exemption of Antarctica, maize is now cultivated on all continents from 58^{o} North to 40^{o} South (OGTR 2008; Encyclopedia Britannica 2018; ICGA 2018).

Maize production worldwide has increased over time due to enhancements regarding seed varieties, fertilizers, pesticides, and equipment as well as improvements in production practices including reduced tillage, irrigation, crop rotations, and pest management systems (USDA-ERS

2018). Maize serves as the main staple diet in many countries in sub-Saharan Africa and Latin America, while it is consumed in substantial quantities in Asia and Europe. In the United States, high proportion of the produce is used for livestock feed as green chop, dry forage, silage or grain (OGTR 2008; NCGA 2018; USDA-ERS 2018). Maize also serves as a big component of alcohol production (fuel ethanol), pharmaceutical supplies (antibiotics, vitamin carriers), and industrial products (paper, soap, textiles) (OGTR 2008; ISU 2009).

In 2018, maize ranked as the highest produced grain in the world. It was cultivated on 179.6 million hectares of land with a total production of 1.1 billion metric tons (Statista 2018a; Statista 2018b; USDA-FAS 2018). United States (376.6 million metric tons, 34%) is the highest producer, where more than half of its total production is from the Midwestern states of Iowa, Illinois, Nebraska and Minnesota. China (215.9 million metric tons, 20%) and Brazil (94.5 million metric tons, 9%) rank as the second and third highest producers, respectively (NCGA 2018; USDA-NASS 2018).

The average price of maize runs around $3.25 per bushel (NCGA 2018), but the price received by maize growers and suppliers from food and feed companies is influenced by the quality and safety of the grain. Contamination with mycotoxins, particularly aflatoxin, can lower the price or even lead to rejection of contaminated maize lots. Additional costs may be incurred from mycotoxin testing and potential lawsuits from consumers (Mitchell et al. 2016). Hence, there is a constant need to develop management strategies that either prevent or limit mycotoxin contamination and sustain high grain quality.

2.0. Genus *Aspergillus*

2.1. Taxonomy

Aspergillus is a large genus belonging to phylum Ascomycota, subphylum Pezizomycotina, class Eurotiomycetes, order Eurotiales, and family Trichocomaceae. The phylum Ascomycota (sac fungi) consists of 'meiosporic' species that have the ability to reproduce sexually, either through heterothallic (obligate outbreeding) or homothallic (self-fertile) breeding mechanisms. Ascomycetes produce four to eight ascospores (teleomorph spores) within a saclike structure called an ascus. This is in contrast to the 'mitosporic' species traditionally classified under phylum Deuteromycota, which are known to only reproduce asexually (Taylor et al. 1999; Taylor et al. 2006; Dyer and O'Gormann 2012). The subphylum Pezizomycotina consists of all filamentous ascomycetes that produce ascospores within a fruiting body (ascoma or ascocarp). Many form closed fruiting bodies, while some lost the ability to undergo meiosis and no longer produce asci (Spatofora 2007; Holt and Iudica 2013). Members of the class Eurotiomycetes and order Eurotiales produce small, evanescent asci scattered within a fully closed, spherical ascocarp (cleistothecium) rather than gathered in a spore-bearing hymenium (Geiser et al. 2006). Members of the family Trichocomaceae are most commonly observed in their anamorph state and are typically recognized by their complex phialide-bearing structures (*Aspergillus, Paecilomyces* and *Penicillium*). Most members have opportunistic lifestyles that rapidly invade uncolonized substrata. In many species, sexual reproduction typically occurs at the end of their proliferative stage after fully colonizing their substrata (Malloch and Cain 1972; Malloch 1986). The genus *Aspergillus* is comprised of more than 250 recognized species that are collectively called the 'Aspergilli' (Geiser et al. 2007; Dyer and O'Gormann 2012). The genus is divided into eight subgenera and 22 sections (Peterson et al. 2008). Among these, section *Flavi* (under subgenus

Circumdati) is one of the most economically important because it contains *A. flavus* and *A. parasiticus* which are the main producers of aflatoxin in harvested produce (Diener et al. 1987; CAST 2003). The teleomorphs of *A. flavus* and *A. parasiticus* are named *Petromyces flavus* and *P. parasiticus*, respectively, to indicate the production of one to multiple ascocarps borne within a larger structure known as sclerotium. Ascospores are released following natural breakdown of the ascus wall and outer wall (peridium) of the ascocarp instead of being forcefully discharged (Malloch and Cain 1972; Dyer and O'Gormann 2012).

2.2. Morphology

Aspergillus was originally described by Pier Antonio Micheli in 1729 (Micheli 1729). He noted that the spores of the fungus radiated from a central structure similar to an 'aspergillum' used by Roman Catholic clergy to sprinkle holy water in the church (Ainsworth 1976). This structure is now referred to as the vesicle and is the defining characteristic of the genus (Bennet 2010).

The vegetative mycelium of *Aspergillus* consists of a network of septate hyphae that can be hyaline, bright colored, light brown, or colored in localized areas. The formation of a conidial structure starts with the enlargement of a thick-walled hyphal cell (foot cell). A septate or aseptate conidiophore (stalk) branch out perpendicularly from the foot cell and the surface of the substrate. When the conidiophore reaches its maximum height, the tip swells to form a globose, hemispherical, elliptical, or long clavate vesicle that provides expanded surface for the attachment of reproductive cells. In uniseriate species, the vesicle gives rise to a single layer of conidium-producing sterigmata (phialides), while in biseriate species, the vesicle gives rise to a base layer (metulae) and secondary layer (phialides) of sterigmata (Raper and Fennel 1965). The tips of the

sterigmata successively produce unbranched chains of conidia to craft globose, radiate, or columnar shaped conidial heads (Raper and Fennel 1965).

Sclerotia are produced by some *Aspergillus* species, but are lacking in many. These structures are hardened, normally darkly pigmented hyphal masses that are capable of remaining dormant in the soil for long periods of time during which they can survive harsh environmental conditions with limited nutritional need (Dyer and O'Gormann 2012; Chang et al. 2014). Sclerotia are composed of polyhedral, thick-walled cells that assume globose to subglobose shapes when mature (Raper and Fennel 1965).

Ascocarp formation in the majority of ascosporic Aspergilli is initiated by the formation of a terminally coiled ascogone (Raper and Fennell 1965). The ascocarps of different species similarly arise from ascocarp initials but differ in gross appearance. *A. glaucus* (teleomorph: *Eurotium herbariorum*) produces small, yellow, naked ascocarps borne on a single stalk-like hypha that are loosely suspended in a network of pigment-encrusted mycelia (Rapper and Fennell 1965). The ascocarps of *A. nidulans* (*Emericella nidulans*) are dark-purple and produced in a nest-like arrangement that is completely enveloped by or associated with thick-walled hölle cells (Fennell and Warcup 1959; Rapper and Fennell 1965; Sharma 2005). *A. fischeri* (*Neosartorya fischeri*) produces globose, white to cream ascocarps covered by abundant sterile hyphae that develop within a cottony mycelial matrix (Rapper and Fennell 1965; Sarbhoy 1985). *A. alliaceus* (*Petromyces alliaceus*) produces one to several, variably-sized, globose ascocarps within a dark-walled and persistently hard, sclerotium-like body (Rapper and Fennell 1965; Sarbhoy 1985). Unlike the above species, *A. athecius* (*Eurotium athecium*) fails to develop walled ascocarps and produce asci in naked clusters on undifferentiated mycelium (Rapper and Fennel 1965; Sharma 2005). An atheridium may be present or not, and may or may not display obvious fusion with the

ascogone (Raper and Fennell 1965). The nuclei from a heterothallic partner, or nucleus in a homothallic species, normally form the maternal tissues and ascocarp wall while the compatible partner provides the fertilizing nucleus that passes into the ascogenous hyphae (Dyer and O'Gormann 2012). Fusing of compatible hyphae gives rise to crozier tips and non-linear asci (Raper and Fennell 1965). The ascocarps are usually thin walled and produce asci and ascospores within a few weeks. Conversely, ascocarps that are borne within sclerotia necessitate longer time (usually months) for maturation. In the latter case, the ascocarps become embedded in a matrix of vegetative hyphae (stroma) consisting of pseudoparenchymatous hyphae (stromal matrix). Flattened cells make up the outer wall of the ascocarp (peridium). The ascocarps may contain up to 100,000 asci that individually enclose, with very rare exceptions, eight ascospores (Dyer and O'Gormann 2012). Ascospores are hyaline in all species except *A. nidulans* for which they are red-brown through purple-red to violet and *A. ornatus* in which they are red-brown shades when mature. Mature ascospores resemble a double convex lens. Upon germination of ascospores, the two valves part completely and allow the growth of a germ tube (Raper and Fennell 1965).

2.3 Distribution and Significance

Aspergillus species are ubiquitous in nature. They can survive in a wide range of temperature (6 to 55^{o}C) and feed on a large variety of plant, animal and man-made substrates (Krijgsheld et al. 2013). Their effective dispersal mechanism through massive conidia production makes them the most dominant fungal structures in the air. Air movement, and possibly insects, transports them over short and long distances where they can establish new colonies (Hedayati et al. 2007; Bennet 2010). Members of section *Flavi* are most abundantly found in warm and humid

climates, and hence they are particularly common in agricultural soils of subtropical and warm temperate regions (Horn 2003).

The ability of many *Aspergillus* species to secrete high amounts of enzymes and organic acids makes them beneficial in food and industrial processes. For example, kojic acid produced by *A. oryzae* is used in food fermenting processes, while cellulases and hemicellulases produced by *A. niger* are utilized in textile, pulp and paper production (Polizeli et al. 2016). On the other hand, many *Aspergillus* species pose a high health and economic risk as opportunistic pathogens and toxin producers. *A. fumigatus* is the most predominant cause of allergic bronchopulmonary aspergillosis in immunocompromised patients (Chaudhary and Marr 2011). Many species grow on fresh and processed plant produce, and are thus, known as common food spoilage molds (Krijgsheld et al. 2013). *A. flavus* causes *Aspergillus* ear rot in maize and the fungus can also contaminate maize kernels with toxic secondary metabolites such as aflatoxin (Smart et al. 1990).

3.0. *Aspergillus flavus*

3.1. Distinguishing characteristics

A. flavus produces B aflatoxins (AFB_1 and AFB_2) and cyclopiazonic acid (CPA), but not G aflatoxins (AFG_1 and AFG_2). The inability to produce G aflatoxins is due to a deletion in its *cypA* gene that is predicted to encode a cytochrome P450 monooxygenase in the aflatoxin gene cluster (Ehrlich et al. 2004).

Conidia of *A. flavus* are globose to subglobose when mature and their size can range from 3.5 to 4.5 μm in diameter. Its conidial wall is relatively thin with fine to moderately roughened ornamentations. This is in contrast to the conidia of *A. parasiticus* that are more spherical in shape and possess noticeably echinulate or spinulose conidial walls. *A. flavus* produces velvety colonies

composed of yellow-green to green or brown sporulation and goldish to red-brown reverse. The conidiophores are hyaline, usually roughened but can vary from smooth to coarsely roughened. Sterigmata can be uniseriate or biseriate, with both conditions normally seen within the same strain or vesicle. *A. flavus* produces sclerotia that are dark red-brown to purple-brown or black at maturity, and vary in shape as globose, subglobose or vertically elongate (Raper and Fennell 1965).

3.2. Diversity within *A. flavus*

A. flavus has two sclerotia morphotypes and different chemotypes. Strains that produce sclerotia are classified as either "S" or "L" morphotype strain based on production of small or large sized sclerotia, respectively. The L morphotype strain, that is also most common, typically produces sclerotia that are greater than 400 μm in diameter. The S morphotype strain, which is less common, produces relatively more abundant sclerotia that are lesser than 400 μm in diameter and fewer conidial heads than the L morphotype strains (Cotty 1989; Geiser et al. 2000; Chang et al. 2014). Mycotoxin production in *A. flavus* is highly variable and can range from atoxigenic to potent producers of AFB_1, AFB_2 and CPA. The atoxigenic populations are normally found coexisting with toxigenic populations in plant tissues and in soil (Payne and Widstrom 1992; Horn 2003). For example, an intensive field sampling conducted by Horn and Dorner (1999) showed that 12% of the *A. flavus* L strains along a wide transect within the United States were non-aflatoxigenic, while 88% were toxigenic. L morphotype strains in the United States exist in high densities in the southern, wetter regions and are more variable in aflatoxin and CPA production. S morphotype strains exist in high densities in the northern, drier regions next to the Sahara Dessert and generally produce high levels of AFB_1. All S morphotype strains identified in the United States

produce B aflatoxins only (S_B), while those from Argentina, West Africa, Southeast Asia and Australia produce both B and G aflatoxins (S_{BG}) (Horn and Dorner 1999).

Isolates of *A. flavus* can also be categorized into vegetative compatibility groups (VCGs), also called heterokaryon compatibility groups. Vegetative compatibility is indicated by the formation of a zone of dense growth and heavy sporulation at the intersection of the two colonies (Horn and Greene 1995). Vegetative compatibility functions as a multi-locus measure of genetic diversity because the multiple, unlinked heterokaryon incompatibility (*het*) loci distributed across the genome of the paired colonies must all be identical for anastomosis to occur (Horn and Greene 1995). Isolates within the same VCG are clonal, thereby, are morphologically similar and variation in mycotoxin profile is lesser within a VCG than between VCGs (Bayman and Cotty 1993). The diversity of VCGs in a given location is high and the populations of VCGs can change even over a short period of time (Scheidegger and Payne 2003).

Phylogenetic analysis based on restriction fragment length polymorphisms (RFLPs) of nuclear-coding genes and DNA sequences identified two reproductively isolated clades within *A. flavus* that cannot be readily separated by morphology and metabolite production (Geiser et al. 2000). Group I includes L sclerotia that produce B aflatoxins (L_B) and S_B isolates, while Group II includes S_B and S_{BG} isolates. Group I is further subdivided into lineages IA, IB and IC. Lineage IA contains S_B and L_B isolates. Lineage IB contains non-aflatoxigenic L isolates and *A. oryzae*. Lineage IC contains L isolates that produce and do not produce aflatoxins (Geiser et al. 2000). Multi-locus analysis using 21 regions in the aflatoxin gene cluster of *A. flavus* confirms that lineage IB contains only non-aflatoxigenic species with complete or partial deletions in their aflatoxin gene cluster. This lineage also includes NRRL 21882, which is the active ingredient of the commercial biocontrol product Afla-Guard®. Lineage IC contains both aflatoxigenic and non-

aflatoxigenic isolates and share a more recent common ancestor with *A. parasiticus* than lineage IB. Lineage IC includes NRRL 18543, which is the active ingredient of AF36 (Moore et al. 2009).

Observed diversity in morphology, toxicity and genetic composition within *A. flavus* has been attributed to several factors. These factors include movement of individuals between locations, current practices of intensive agriculture, dominant crops grown in the area, mutation, and sexual recombination between compatible genotypes (Bayman and Cotty 1991; Horn 2007; Olarte et al. 2012).

3.3. Life cycle and reproduction

The ubiquitousness of *A. flavus* in the soil led to the conclusion that soil is its primary habitat (Horn 2007). The fungus spends a large portion of its life cycle as soil saprobe, where it plays an important role as a decomposer and nutrient recycler of plant and animal debris (Hedayati et al. 2007). Under certain circumstances, *A. flavus* can become an opportunistic pathogen of developing seeds (Payne 2016). It produces a large array of degrading enzymes to utilize temporarily available plant materials including cellulose, pectin, lignin, tannins, cutin, starch, lipid and proteins (Horn 2007).

A. flavus produces numerous conidia that are easily dispersed aerially by wind and insects over short and long distances. During adverse conditions such as lack of adequate water or nutrients, the fungus produces resistant structures called sclerotia (Hedayati et al. 2007). Populations in the soil (conidia, hyphae, sclerotia) serve as the primary inocula for infection when conidia land on the surface of susceptible maize (Horn 2003). The susceptibility of maize to infection by the fungus commences at the emergence of silks. Conidia of *A. flavus* that land on the silk can either penetrate silks directly, enter through cracks and intercellular gaps, or moved by

insects into the ear (Payne and Widstrom 1992). Populations that infect the ear replenish the populations in the soil when infected maize ears fall on the soil surface during the growing season or at harvest. Pre-infection of the ears before dropping on the ground gives the fungus a competitive advantage over other microorganisms in the soil. Secondary infection can occur when conidia from southern regions of Northern America is wind dispersed to crops in the northern areas. The fungus overwinters as mycelium or sclerotium in soil or infected corncobs, which later serve as source of primary inoculum for infection of next season's crop (Hedayati et al. 2007; Horn 2007).

A. flavus was originally considered to be strictly asexual. This was thought to explain the strong clonal structure of populations, in which vegetative compatibility was believed to be a strong barrier of genetic exchange (Chang et al. 2014; Ehrlich 2014). However, populations of *A. flavus* show considerable genetic, morphological and chemotype diversity within vegetative compatibility groups. Populations are also dynamic and the dominant VCG group in an area can shift from year to year (Bayman and Cotty 1991). This observed diversity was first attributed to parasexuality, which involves the exchange of genetic material between two haploid strains and formation of heterokaryons. However, the parasexual cycle has only been observed under laboratory conditions and hyphal fusion would primarily occur between genetically similar individuals of the same VCG (Chang et al. 2014).

The discovery of the sexual stage of *A. flavus* showed that VCG is not a strong barrier to genetic exchange and outcrossing among VCGs leads to formation of new VCGs (Olarte et al. 2012). *A. flavus* was identified to be heterothallic, where each individual contain one of the two mating type idiomorphs, *MAT1-1* or *MAT1-2*, at a single locus. *MAT1-1* encodes an α-domain transcription factor, while *MAT1-2* encodes a high mobility group-domain (HMG) transcription

factor (Ramirez-Prado et al. 2008). Successful crosses between individuals of opposite mating types and different VCGs lead to the formation of ascospore-bearing ascocarps embedded within the matrix of the sclerotia after an extended incubation of five to seven months in dark conditions (Horn et al. 2014). *A. flavus* was also identified to be hermaphroditic with respect to male and female roles during sexual reproduction (Horn et al. 2016). The sclerotium functions as the female by providing nutrient sources and bearing the ascocarps and ascospores, while the conidium functions as the male by fertilizing the sclerotium. The degree of fertility or sterility of the cross is dictated by the parental source of conidium and sclerotium (Horn et al. 2016). Recombinant progenies are produced through independent assortment of chromosomes and crossing over within the aflatoxin gene cluster or other portions of the genome (Olarte et al. 2012).

4.0. Aflatoxin

4.1. Background and description

Aflatoxins are hepatotoxic, carcinogenic and immunosuppressive secondary metabolites produced mainly by *A. flavus* and *A. parasiticus* (Diener et al. 1987; CAST 2003). These toxins are chemically composed of dihydrofuran or tetrahydrofuran moieties that are fused to a coumarin ring (Hussein and Brasel 2001). The four major types of aflatoxins (AFB_1, AFB_2, AFG_1, AFG_2) are identified based on their blue (B) or green (G) fluorescence under ultraviolet light and relative chromatographic mobility (1 or 2). Among the four, AFB_1 is the most toxic when studied on experimental animals and clinical patients (Chu 2003). AFB_2 and AFG_2 are hydroxyl-derivatives of AFB_1 and AFB_2, respectively, and remain relatively nontoxic unless metabolically oxidized *in vivo* (Kensler et al. 2011). An additional aflatoxin, AFM_1, can be metabolized from AFB_1 when

lactating animals ingest contaminated feed. AFM_1 is metabolized by the hepatic system of animals and becomes absorbed in their milk (Ghanem and Orfi 2009).

Aflatoxin continues to be the most problematic and heavily regulated mycotoxin in the United States and other parts of the world (Mitchell et al. 2016). Awareness of the harmful effects of aflatoxin started in the mid-1960s when Brazilian peanut meals infected by *A. flavus* and contaminated with high levels of aflatoxin were identified as the causative agents of Turkey "X" disease. This epidemic killed 100,000 turkey poults that were being raised around 500 farms in England (Wannop 1961; Kensler et al. 2011). Continuous consumption of food or feed products with high aflatoxin concentrations have also been associated with high mortality in other avian flocks, reduced milk production in cattle, lesser egg yield in poultry, stunted growth in children, and hepatocellular carcinoma (liver cancer) in elder adults (CAST 2003; Wild 2007).

Due to the above health risks, over 100 nations have established regulatory limits for aflatoxin contamination. The United States Food and Drug Administration established a maximum level of 100 to 300 parts per billion (ppb) total aflatoxin content for maize and peanut products intended for beef cattle, swine and mature poultry consumption; 20 ppb for human and immature animals; and, 0.5 ppb AFM_1 in milk (FDA 2000). European countries established a much stricter cut-off of 4 ppb total aflatoxin content in all cereals and dried fruits intended for direct human consumption or use as ingredients in foodstuffs; and, 0 ppb in milk or milk-based products (FAO 2004; FAO 2006).

4.2. Aflatoxigenic species of *Aspergillus*

A. flavus and *A. parasiticus* are the two major producers of aflatoxin on a number of substrates. *A. flavus* typically produces AFB and cyclopiazonic acid (CPA) and is the most

commonly found aflatoxin-producing fungus in maize, peanuts, cottonseed and tree nuts. In contrast, *A. parasiticus* produces AFB and AFG but not CPA. It occurs more frequently in peanuts than other crops but is typically outcompeted by *A. flavus* when both fungi are present (Payne and Widstrom 1992; Payne 1998; Horn and Dorner 1999).

Aflatoxin production necessitates a substantial expenditure of energy that involves around 25 genes arranged in a complex biosynthetic cluster. These genes encode for the proteins necessary for the oxidative, reductive, and regulatory processes in aflatoxin biosynthesis. The aflatoxin gene cluster in *A. flavus* is located within a 70kb DNA region in the subtelomeric region of chromosome III (Yu et al. 2004). Since polymorphism for aflatoxin production is maintained by balancing selection (Carbone et al. 2007), it has been postulated that aflatoxin production provides some benefits to the fungus. Some of the proposed benefits include competitive mechanism (Bilgrami et al. 1988), feeding deterrents against arthropods for resource competition or protection from fungivory (Drott et al. 2017), pathogenicity mechanism (Horn 2007), adaptation to ecological niche (Horn and Dorner 2002), and alleviation of environmental stress (Fountain et al. 2014).

Other *Aspergillus* species that produce aflatoxins have been reported. These include *A. nomius, A. pseudonomius*, *A. bombycis, A. pseudotamarii, A. pseudocaelatus, A. ochraceoroseus* and *A. rambellii*. *A. nomius* is often found in soil and on dead or diseased insects. It is morphologically similar to *A. flavus* and produces AFB and AFG but not CPA. *A. pseudonomius* was isolated from insects and soil in the United States and produces AFB (Varga et al. 2011). *A. bombycis*, which was isolated along with *A. nomius* from insect frass in silkworm-rearing houses in Japan and Indonesia, also produces AFB and AFG but not CPA (Peterson et al. 2001). *A. pseudotamarii*, collected from a tea field soil in Japan and Brazil, produces AFB (Ito et al. 2001). *A. pseudocaelatus*, isolated from *Arachis burkartii* leaf in Argentina, produces AFB,

AFG and CPA (Varga et al. 2014). *A. ochraceoroseus* and *A. rambellii* were isolated from soil detritus in Africa and produce AFB_1 (Moore et al. 2015). All the abovementioned species infrequently contaminate agricultural crops, and thus they are not considered to pose a significant economic risk.

4.2. Impact to the maize industry in the United States

Aflatoxin has been detected in maize kernels at different stages of development and maturity from late milk stage until harvest (Anderson et al. 1975). Drought stress accompanied by elevated temperatures during seed development promotes *A. flavus* invasion and subsequent aflatoxin contamination. More rapid accumulation of aflatoxin occurs when kernels are naturally wounded or damaged by insects (Payne and Widstrom 1992; Horn and Dorner 1999). Not all kernels need to be contaminated with aflatoxin before losses due to contamination are incurred. A single heavily contaminated kernel can bring the average concentration of 10,000 seeds to a dangerous level and even lead to the rejection of the whole lot (Schroeder 1969). Contamination can ensue during postharvest when inadequately dried grains are stored or where storage conditions favor the growth of the fungus and production of aflatoxin (Ojiambo et al. 2018).

Annually, a large acreage of maize in the United States is under threat of aflatoxin contamination. This acreage ranges from Texas to Oklahoma in the south and Alabama to North Carolina in the southeast (Mitchell et al. 2016; Reus 2016). During intense drought conditions, the threat of aflatoxin contamination can extend northward into the midwestern states of Kansas, Missouri and Illinois (Ingwersen 2013). Extremely severe losses occurred in Mississippi, Louisiana and Texas in 1998 (Cardwell et al. 2001), which forced growers to either destroy or sell their crops at significantly reduced prices. The high risk of aflatoxin contamination also abolished

the potential for maize to be used as a rotational crop in Arizona and Corpus Christi, Texas. Aflatoxin contamination in the Corn Belt states of Indiana, Illinois, Iowa, Missouri, Nebraska and Kansas arises sporadically but can be extreme when droughts occur (Cardwell et al. 2001). The regional differences in aflatoxin contamination has been attributed to climatic conditions and agricultural practices that increase the susceptibility of the crop to *A. flavus* invasion (Horn and Dorner 1999).

The annual loss due to aflatoxin contamination in maize in the United States is estimated to be around $163 million. Around $31 million comes from maize rejected for food and around $132 million from maize rejected for feed and through livestock losses (Wu 2006). Losses to the maize industry can even reach up to $1.68 billion annually if climate changes causes more regular aflatoxin contamination in the maize-growing states in the Corn Belt (Mitchell et al. 2016).

5.0. Biological Control of Aflatoxin Contamination in Maize

Several management strategies ranging from pre-harvest to storage options have been suggested to prevent or minimize the possibility of aflatoxin contamination in maize. Some pre-harvest strategies include biological control, host resistance, plant density, and good agricultural practices such as crop rotation, pesticide application, soil amendment and moisture management (Ojiambo et al. 2018). Among these, biological control, which involves application of atoxigenic strains of *A. flavus* to competitively outcompete toxigenic strains, has one of the greatest impacts (Ojiambo et al. 2018). The other strategies are either still in their early stage of development, do not reduce the risk of *A. flavus* invasion and resultant aflatoxin contamination significantly relative to the regulatory limits, or may not be practical in areas where resources are limited. Some postharvest strategies include proper timing of harvest, maintenance of appropriate kernel moisture

(<14%), alteration of storage conditions to reduce fungal activity, and cleaning and sorting of grain prior to storage (Ojiambo et al. 2018).

Two commercially available biocontrol strains, AF36 and Afla-Guard®, are currently used in the United States to reduce aflatoxin contamination. *A. flavus* strain NRRL 18543 used as the active ingredient in AF36 was isolated from an upland cotton in Arizona (Cotty 1989) and is currently registered for use in cotton (Arizona, California, Texas), maize (Arizona, Texas) and pistachio (Arizona, California, New Mexico, Texas) (EPA 2015). Despite having a full aflatoxin gene cluster, it does not produce aflatoxin due to a point mutation in its polyketide synthase (*pksA*) gene that introduces a premature stop codon to prevent formation of norsolorinic acid and aflatoxin accumulation (Ehrlich and Cotty 2004). Conversely, NRRL 18543 produces the mycotoxin cyclopiazonic acid (CPA) that was linked as a probable co-contaminant of the peanut meal associated with the Turkey "X" disease in the mid-1960s (King et al. 2011). *A. flavus* strain NRRL 21882 used as active ingredient in Afla-Guard® was isolated from peanut in Georgia (Dorner 2005) and is currently registered for use in maize and peanut in the United States (EPA 2013). This strain does not produce aflatoxin nor CPA due to complete deletion of its entire aflatoxin and CPA gene clusters (Chang et al. 2005; King et al. 2011).

Application of these commercial biocontrol strains has been reported to reduce aflatoxin contamination by up to 98% (Ehrlich 2014). High concentrations of atoxigenic strain of *A. flavus* are coated in nutrient-supplying carriers, such as barley for Afla-Guard® and wheat for AF36, then applied in high densities to the plant canopy or soil surface. The treated grain absorbs moisture and allows the atoxigenic strain to sporulate profusely. The spores disperse to the developing maize prior to occupation of toxigenic strains, thus physically excluding toxigenic strains from infecting the target kernels and producing aflatoxin. This mechanism is generally referred to as 'competitive

exclusion' (Chang et al. 2014; Damann 2015). In order to maintain efficacy, the biocontrol product needs to be applied annually (Lewis et al. 2019). Further studies are needed to determine whether the biocontrol strains truly displace the native aflatoxin-producing population in the field (Moore et al. 2013a). Another mechanism called 'thigmo-down regulation of aflatoxin synthesis' (Huang et al. 2011) proposes that aflatoxin is inhibited only when appropriate atoxigenic and toxigenic isolates, with certain specificities, come in contact in the first day of growth. Such interaction initiate an unknown signaling pathway, perhaps related to specific and consistent component of programmed development, that prevents or down regulates the biosynthesis of aflatoxin which normally develops after three days of fungal growth (Huang et al. 2011).

6.0. Rationale and Objectives

6.1. Sexual reproduction in *A. flavus*

While useful information regarding mycelium growth, sclerotium production, and the teleomorphic stage of *A. flavus* is available in literature (Horn et al. 2009; Wu et al. 2014; Horn et al. 2016), comprehensive details on the actual process of sexual reproduction are still lacking. For example, there is no information about the mechanism on how conidia fertilize the sclerotia during sexual reproduction in *A. flavus*. Additional research is also needed to determine how the interaction between conidia and sclerotia leads to the formation of ascocarps, asci and ascospores. Unlike other heterothallic fungi, no receptor nor specialized structures for fertilization have been observed on the surface of the *A. flavus* sclerotia (Horn et al. 2016).

As conidia and sclerotia come in contact during sexual reproduction, the sclerotia are also transitioning from asexual to sexual structures. This transition can affect the survival and genetic diversity of the fungus. It may also affect the quantity and diversity of secondary metabolites,

including aflatoxin, produced by the fungus. To the best of our knowledge, there is little to no information available on changes in morphology, secondary metabolism, and transcription during the fertilization of sclerotia and the formation of sexual structures. In addition, while the degree of female fertility is dependent upon the sclerotial strain, it is not known how female fertility could influence morphological, metabolomic, and transcriptional changes during sexual reproduction in *A. flavus*. Understanding the biology and sexual cycle of *A. flavus* could be useful in identifying additional biological strategies to control toxigenic strains of *A. flavus* or facilitate design of novel biocontrol agents. For example, depending on the prevailing genetic structure of the native population, a highly fertile or a low fertility biocontrol strain would be more effective in reducing aflatoxin contamination. A highly fertile *MAT1-2* biocontrol strain could be applied in a field whose native population is primarily composed of *MAT1-1* toxigenic strains (or vice versa) so as to encourage recombination and drive the population towards atoxigenecity. In populations with mixed chemotypes and mating types, the density of the predominant non-aflatoxigenic native strain could be inflated by applying a low fertility biocontrol strain of the same mating type. An increased density of non-aflatoxigenic population would lead to decreased levels of aflatoxin in the crop (Cotty 1994). In such a case, information on the metabolomic and transcriptional changes could be useful in screening and rapid selection of biocontrol strains with the desired level of female fertility.

6.2. A novel strain for biocontrol of aflatoxin contamination in maize

Despite the persistent risk of aflatoxin contamination in the maize-growing areas of the United States, only two commercial biocontrol products (AF36 and Afla-Guard®) are available in the United States. Use of AF36 in maize is restricted to Arizona and Texas (EPA 2015), leaving

Afla-Guard® as the solitary option in other states. Currently, there is an increasing interest to identify additional strains and develop sustainable biocontrol approaches to successfully reduce aflatoxin contamination. In addition, both AF36 and Afla-Guard® were developed on the premise that members of different VCGs cannot recombine. With the discovery of sexual reproduction in *A. flavus*, it is important to select and identify biocontrol strains whose recombination potential with native populations will avoid production of high frequency of aflatoxigenic progeny in their area of use.

AF36, Afla-Guard®, and all reported biocontrol strains are of the mating type *MAT1-2* (Moore et al. 2013b), giving the implication that biocontrol strains should be *MAT1-2*. In 2015, we identified a *MAT1-1* strain (RMb10), which has a comparable ability as Afla-Guard® to reduce aflatoxin contamination when co-inoculated with NRRL 3357 in preliminary greenhouse and field trials (J.M. Luis et al., unpublished). This strain was isolated from a maize field in Rocky Mount, North Carolina in 2012. Previous studies showed that mitigation of aflatoxin contamination through biocontrol tends to be more persistent when the applied strain matches the genetic and ecological structure of the native population of *A. flavus* in the soil (Lewis et al. 2019). Availability of a *MAT1-1* biocontrol strain diversifies the choice of biocontrol products that can be used in the field. The goal of this study is to test the effect of RMb10 in changing the distribution of native *A. flavus* populations when applied in large-scale field trials in southern United States.

6.3. Research objectives

Given the abovementioned considerations, the overall goal of this dissertation is to understand the biology of sexual reproduction in *A. flavus* and to improve the efficacy of biocontrol of aflatoxin contamination in maize. The specific objectives of this dissertation are to:

1. Determine morphological changes that occur in fertilized stromata and unmated sclerotia during sexual reproduction in *A. flavus* as influenced by the degree of female fertility (Chapter 2).
2. Characterize differences in secondary metabolite production and gene expression between crosses with high and low levels of female fertility during sexual reproduction in *A. flavus* (Chapter 3).
3. Examine the impact of RMb10 on the population dynamics of native *A. flavus* in maize fields in southern United States (Chapter 4).

Literature Cited

Anderson H.W., Nehring E.W., Wichser W.R. 1975. Aflatoxin contamination of corn in the field. J. Agric. Food Chem. 23: 775-782.

Ainsworth G.C. 1976. Introduction to the history of mycology. Cambridge: Cambridge University Press, pp. 1-351.

Bayman P., Cotty P.J. 1993. Genetic diversity in *Aspergillus flavus*: association with aflatoxin production and morphology. Can. J. Bot. 71: 23-31.

Bayman P., Cotty P.J. 1991. Vegetative compatibility and genetic diversity in the *Aspergillus flavus* population of a single field. Can. J. Bot. 69: 1707-1711.

Beadle G.W. 1939. Teosinte and the origin of maize. J. Hered. 30: 245-247.

Bennett J.W. 2010. An overview of the genus *Aspergillus*. In: *Aspergillus*: molecular biology and genomics. Machida M., Gomi K. (Eds). Portland: Caiser Academic Press, pp. 1-17.

Bilgrami K.S., Sinha S.P., Jeswal P. 1988. Loss of toxigenicity of *Aspergillus flavus* strains during subculturing - a genetic interpretation. Curr. Sci. 57: 551-552.

Carbone I., Jakobek J.L., Ramirez-Prado J.H., Horn B.W. 2007. Recombination, balancing selection and adaptive evolution in the aflatoxin gene cluster of *Aspergillus parasiticus*. Mol. Ecol. 16: 4401-4417.

Cardwell K.F., Desjardins A., Henry S.H., Munkvold G., Robens J. 2001. Mycotoxins: the cost of achieving food security and food quality. Retrieved Oct 3, 2018. Available from http://www.apsnet.org/publications/apsnetfeatures/Pages/Mycotoxins.aspx.

CAST. 2003. Mycotoxins: risks in plant, animal, and human systems. Council for Agricultural Science and Technology. Task Force Report. Ames, IA, pp. 1-199.

Chang P.K., Horn B.W., Abe K., Gomi K. 2014. *Aspergillus*. In: Encyclopedia of food microbiology. Vol 1. Batt C.A., Tortorello M.L. (Eds). Elsevier Ltd, Academic Press, pp. 77-82.

Chang P., Horn B.W., Dorner J.W. 2005. Sequence breakpoints in the aflatoxin biosynthesis gene cluster and flanking regions in nonaflatoxigenic *Aspergillus flavus* isolates. Fungal Genet. Biol. 42: 914-923.

Chaudhary N., Marr K.A. 2011. Impact of *Aspergillus fumigatus* in allergic airway diseases. Clin. Transl. Allergy 1: 4.

Chu F.S. 2003. Mycotoxins | Toxicology. In: Encyclopedia of food sciences and nutrition. Caballero B. (Ed). Oxford: Academic Press, pp. 4096-4108.

Cotty P.J. 1994. Influence of field application of an atoxigenic strain of *Aspergillus flavus* on the populations of *A. flavus* infecting cotton bolls and on the aflatoxin content of cottonseed. Phytopathology 84: 1270-1277.

Cotty P.J. 1989. Virulence and cultural characteristics of two *Aspergillus flavus* strains pathogenic on cotton. Phytopathology 79: 808-814.

Damann K.J. 2015. Atoxigenic *Aspergillus flavus* biological control of aflatoxin contamination: what is the mechanism? World Mycotoxin J. 8: 235-244.

Diener U.L., Cole R.J., Sanders T.H., Payne G.A., Lee L.S., Klich M.A. 1987. Epidemiology of aflatoxin formation by *Aspergillus flavus*. Annu. Rev. Phytopathol. 25: 249-270.

Doebley J. 2004. The genetics of maize evolution. Annu. Rev. Genet. 38: 37-59.

Doebley J. 1990. Molecular evidence and the evolution of maize. Econ. Bot. 44: 6-27.

Dorner J.W. 2005. Biological control of aflatoxin crop contamination. In: Aflatoxin and food safety. Abbas H.K. (Ed). Boca Raton, Florida: CRC Press, pp. 333-352.

Drott M.T., Lazzaro B.P., Brown D.L., Carbone I., Milgroom M.G. 2017. Balancing selection for aflatoxin in *Aspergillus flavus* is maintained through interference competition with, and fungivory by insects. Proc. Biol. Sci. 284: 20172408.

Dyer P.S., O'Gorman C.M. 2012. Sexual development and cryptic sexuality in fungi: insights from *Aspergillus* species. FEMS Microbiol. Rev. 36: 165-192.

Ehrlich K.C. 2014. Non-aflatoxigenic *Aspergillus flavus* to prevent aflatoxin contamination in crops: advantages and limitations. Front. Microbiol. 5: 50.

Ehrlich K.C., Chang P., Yu J., Cotty P.J. 2004. Aflatoxin biosynthesis cluster gene is required for aflatoxin formation. Appl. Environ. Microbiol. 70: 6518-6524.

Ehrlich K., Cotty P. 2004. An isolate of *Aspergillus flavus* used to reduce aflatoxin contamination in cottonseed has a defective polyketide synthase gene. Appl. Microbiol. Biotechnol. 65: 473-478.

Encyclopedia Britannica. 2018. Corn | History, cultivation, uses, & description. Retrieved Sep 25, 2018. Available from https://www.britannica.com/plant/corn-plant.

EPA. 2015. *Aspergillus flavus* AF36 Prevail. United States Environmental Protection Agency. Retrieved Oct 1, 2018. Available from https://www3.epa.gov/pesticides/chem_search/ppls/071693-00002-20150625.pdf.

EPA. 2013. Afla-Guard(R) GR. United States Environmental Protection Agency. Retrieved Oct 17, 2018. Available from https://www3.epa.gov/pesticides/chem_search/ppls/000100-01469-20130805.pdf.

FAO. 2006. Commission Regulation No 1881/2006 setting maximum levels for certain contaminants in foodstuffs. Food and Agriculture Organization of the United Nations. OJEU 364: 5-24.

FAO. 2004. Worldwide regulations for mycotoxins in food and feed in 2003. Food and Agriculture Organization of the United Nations. Food Nutr. Pap. 81: 1-171.

FDA. 2000. Guidance for industry: action levels for poisonous or deleterious substances in human food and animal feed. United States Food and Drug Administration. Retrieved Sep 25, 2018. Available from https://www.fda.gov/food/guidanceregulation/ucm077969.htm#afla.

Fennell D.I., Warcup J.H. 1959. The ascocarps *of Aspergillus alliaceus*. Mycologia 51: 409-415.

Fountain J.C., Scully B.T., Ni X., Kemerait R.C., Lee R.D., Chen Z.Y., Guo B. 2014. Environmental influences on maize-*Aspergillus flavus* interactions and aflatoxin production. Front. Microbiol. 5: 40.

Geiser D.M., Klich M.A., Frisvad J.C., Peterson S.W., Varga J., Samson R.A. 2007. The current status of species recognition and identification in *Aspergillus*. Stud. Mycol. 59: 1-10.

Geiser D.M., Gueidan C., Miadlikowska J., Lutzoni F., Kauff F., Hofstetter V., Fraker E., Schoch C.L., Tibell L., Untereiner W.A., Aptroot A. 2006. Eurotiomycetes: Eurotiomycetidae and Chaetothyriomycetidae. Mycologia 98: 1053-1064.

Geiser D.M., Dorner J.W., Horn B.W., Taylor J.W. 2000. The phylogenetics of mycotoxin and sclerotium production in *Aspergillus flavus* and *Aspergillus oryzae*. Fungal Genet. Biol. 31: 169-179.

Ghanem I., Orfi M. 2009. Aflatoxin M1 in raw, pasteurized and powdered milk available in the Syrian market. Food Control 20: 603-605.

Hastorf C.A. 2009. Rio Balsas most likely region for maize domestication. Proc. Natl. Acad. Sci. USA 106: 4957-4958.

Hedayati M.T., Pasqualotto A.C., Warn P.A., Bowyer P., Denning D.W. 2007. *Aspergillus flavus*: human pathogen, allergen and mycotoxin producer. Microbiology 153: 1677-1692.

Holt J.R., Iudica C.A. 2013. Hierarchical classification of the phylum Ascomycota. Retrieved Sep 28, 2018. Available from https://comenius.susqu.edu/biol/202/fungi/ascomycota/ascomycota-taxonomy.html.

Horn B.W., Gell R.M., Singh R., Sorensen R.B., Carbone I. 2016. Sexual reproduction in *Aspergillus flavus* sclerotia: acquisition of novel alleles from soil populations and uniparental mitochondrial inheritance. PLoS One 11: e0146169.

Horn B.W., Sorensen R.B., Lamb M.C., Sobolev V.S., Olarte R.A., Worthington C.J., Carbone I. 2014. Sexual reproduction in *Aspergillus flavus* sclerotia naturally produced in corn. Phytopathology 104: 75-85.

Horn B.W., Moore G.G., Carbone I. 2009. Sexual reproduction in *Aspergillus flavus*. Mycologia 101: 423-429.

Horn B.W. 2007. Biodiversity of *Aspergillus* section *Flavi* in the United States: a review. Food Addit. Contam. 24: 1088-1101.

Horn B.W. 2003. Ecology and population biology of aflatoxigenic fungi in soil. J. Toxicol. Toxin Rev 22: 351-379.

Horn B.W., Dorner J.W. 2002. Effect of competition and adverse culture conditions on aflatoxin production by *Aspergillus flavus* through successive generations. Mycologia 94: 741-751.

Horn B.W., Dorner J.W. 1999. Regional differences in production of aflatoxin B1 and cyclopiazonic acid by soil isolates of *Aspergillus flavus* along a transect within the United States. Am. Soc. Microbiol. 65: 1444-1449.

Horn B.W., Greene R.L. 1995. Vegetative compatibility within populations of *Aspergillus flavus, A. parasiticus*, and *A. tamarii* from a peanut field. Mycologia 87: 324-332.

Huang C., Jha A., Sweany R., DeRobertis C., Damann K.E.J. 2011. Intraspecific aflatoxin inhibition in *Aspergillus flavus* is thigmoregulated, independent of vegetative compatibility group and is strain dependent. PLoS One 6: e23470.

Hussein H.S., Brasel J.M. 2001. Toxicity, metabolism, and impact of mycotoxins on humans and animals. Toxicology 167: 101-134.

ICGA. 2018. Corn facts. Iowa Corn Growers Association. Retrieved Sep 25, 2018. Available from https://www.iowacorn.org/media-page/corn-facts/.

Ingwersen J. 2013. Grain handlers wary of toxin lingering in '12 U.S. corn harvest. Reuters News. Retrieved Dec 17, 2018. Available from https://www.reuters.com/article/us-usa-crops-aflatoxin/grain-handlers-wary-of-toxin-lingering-in-12-u-s-corn-harvest-idUSBRE93I11I20130419.

ISU. 2009. Corn. Iowa State University. Retrieved Sep 25, 2018. Available from http://www.ncga.com/file/317.

Ito Y., Peterson S.W., Wicklow D.T., Goto T. 2001. *Aspergillus pseudotamarii*, a new aflatoxin producing species in *Aspergillus* section *Flavi*. Mycol. Res. 105: 233-239.

Kensler T.W., Roebuck B.D., Wogan G.N., Groopman J.D. 2011. Aflatoxin: a 50-year odyssey of mechanistic and translational toxicology. Toxicol. Sci. 120: S48.

King E.D., Bassi A.B.J., Ross D.C., Druebbisch B. 2011. An industry perspective on the use of "atoxigenic" strains of *Aspergillus flavus* as biological control agents and the significance of cyclopiazonic acid. Toxin Rev. 30: 33-41.

Krijgsheld P., Bleichrodt R., van Veluw G.J., Wang F., Muller W.H., Dijksterhuis J., Wosten H.A. 2013. Development in *Aspergillus*. Stud. Mycol. 74: 1-29.

Lewis M.H., Carbone I., Luis J.M., Payne G.A., Bowen K.L., Hagan A.K., Kemerait R., Heiniger R., Ojiambo P. 2019. Biocontrol strains differentially shift the genetic structure of indigenous soil populations of *Aspergillus flavus*. Front. Microbiol. 10: 1738.

Malloch D. 1986. The Trichocomaceae: relationships with other ascomycetes. In: Advances in *Penicillium* and *Aspergillus* systematics. Samson R.A., Pitt J.I. (Eds). Boston, MA: Springer, pp. 365-382.

Malloch D., Cain R.F. 1972. The Trichocomataceae: Ascomycetes with *Aspergillus*, *Paecilomyces*, and *Penicillium* imperfect states. Can. J. Bot. 50: 2613-2628.

Matsuoka Y., Vigouroux Y., Goodman M.M., Sanchez J. G., Buckler E., Doebley J. 2002. A single domestication for maize shown by multilocus microsatellite genotyping. Proc. Natl. Acad. Sci. USA 99: 6080-6084.

Mejia D. 2003. Maize: post-harvest operations. Food and Agriculture Organization of the United Nations, INPhO Post-harvest Compendium. Retrieved Sep 24, 2018. Available from http://www.fao.org/fileadmin/user_upload/inpho/docs/Post_Harvest_Compendium_-_MAIZE.pdf.

Micheli P.A. 1729. Nova plantarum genera. Florentiae: Bernardi Paperninii, pp. 1-234.

Mitchell N.J., Bowers E., Hurburgh C., Wu F. 2016. Potential economic losses to the USA corn industry from aflatoxin contamination. Food Addit. Contam. 33: 540-550.

Moore G.G., Mack B.M., Beltz S.B. 2015. Draft genome sequences of two closely related aflatoxigenic *Aspergillus* species obtained from the Ivory Coast. Genome Biol. Evol. 8: 729.

Moore G.G., Elliot J.L., Singh R., Horn B.W., Dorner J.W., Stone E.A., Chulze S.N., Barros G.G., Manjunath K.N., Wright G.C., Hell K., Carbone I. 2013a. Sexuality generates diversity in the aflatoxin gene cluster: evidence on a global scale. PLoS Pathogens 9: e1003574.

Moore G.G., Mack B.M., Beltz S.B. 2013b. Testing the efficacy of eGFP-transformed *Aspergillus flavus* as biocontrol strains. Food Nutr. Sci. 4: 1-11.

Moore G., Singh R., Horn B.W., Carbone I. 2009. Recombination and lineage-specific gene loss in the aflatoxin gene cluster of *Aspergillus flavus*. Mol. Ecol. 18: 4870-87.

NCGA. 2018. World of corn 2018. National Corn Growers Association. Retrieved Sep 24, 2018. Available from http://www.worldofcorn.com/#/.

OGTR. 2008. The Biology of *Zea mays* L. ssp *mays* (maize or corn). Office of the Gene Technology Regulator, DOHA, Australian Gov: 1-80.

Ojiambo P.S., Battilani P., Cary J.W., Blum B.H., Carbone I. 2018. Cultural and genetic approaches to manage aflatoxin contamination: recent insights provide opportunities for improved control. Phytopathology 108: 1024-1037.

Olarte R.A., Horn B.W., Dorner J.W., Monacell J.T., Singh R., Stone E.A., Carbone I. 2012. Effect of sexual recombination on population diversity in aflatoxin production by *Aspergillus flavus* and evidence for cryptic heterokaryosis. Mol. Ecol. 21: 1453-1476.

Payne G.A. 2016. Mycotoxins and product safety. In: Peanuts: genetics, processing and utilization. Stalker T.H., Wilson R.F. (Eds). Elsevier Inc, pp. 347-361.

Payne G.A. 1998. Process of contamination by aflatoxin-producing fungi and their impact on crops. In: Mycotoxins in agriculture and food safety. Shinha K.K., Bhatnagar D. (Eds). New York: Marcel Decker Inc, pp. 279-300.

Payne G.A., Widstrom N.W. 1992. Aflatoxin in maize. Crit. Rev. Plant Sci. 10: 423-440.

Peterson S.W., Varga J., Frisvad J.C., Samson R.A. 2008. Phylogeny and subgeneric taxonomy of *Aspergillus*. In: *Aspergillus* in the genomic era. Varga J., Samson R.A. (Eds). Wageningen, Netherlands: Wageningen Academic Publishers, pp. 33-56.

Peterson S.W., Ito Y., Horn B.W., Goto T. 2001. *Aspergillus bombycis*, a new aflatoxigenic species and genetic variation in its sibling species, *A. nomius*. Mycologia 93: 689-703.

Polizeli M., Vici A.C., Scarcella A., Cereia M., Pereira M.G. 2016. Enzyme system from *Aspergillus* in current industrial uses and future applications in the production of second-generation ethanol. In: New and future developments in microbial biotechnology and bioengineering: *Aspergillus* system properties and applications. Gupta V.K. (Ed). Elsevier, pp. 127-140.

Ramirez-Prado J.H., Moore G.G., Horn B.W., Carbone I. 2008. Characterization and population analysis of the mating-type genes in *Aspergillus flavus* and *Aspergillus parasiticus*. Fungal Genet. Biol. 45: 1292-1299.

Ranere A.J., Piperno D.R., Holst I., Dickau R., Iriarte J. 2009. The cultural and chronological context of early Holocene maize and squash domestication in the Central Balsas River Valley, Mexico. Proc. Natl. Acad. Sci. USA 106: 5014-5018.

Raper K.B., Fennell D.I. 1965. The Genus *Aspergillus*. Baltimore: The Williams & Wilkins Co., pp. 1-686.

Reus A. 2016. Infographic: Mycotoxins in 2016 US corn crop. Retrieved Oct 3, 2018. Available from https://www.wattagnet.com/articles/28963-infographic-mycotoxins-in-2016-us-corn-crop?v=preview.

Sarbhoy A.K. 1985. Cleistothecial states of *Aspergillus* and their taxonomic position. Mycopathologia 91: 133-142.

Scheidegger K.A., Payne G.A. 2003. Unlocking the secrets behind secondary metabolism: a review of *Aspergillus flavus* from pathogenicity to functional genomics. J. Toxicol. Toxin Rev. 22: 423-459.

Schroeder H.W. 1969. Factors influencing the development of aflatoxins in some field crops. J. Stored Prod. Res. 5: 187-190.

Sharma P.D. 2005. Fungi and allied organisms. Oxford: Alpha Science International Ltd., pp. 1-157.

Smart M.G., Wicklow D.T., Caldwell R.W. 1990. Pathogenesis in *Aspergillus* ear rot of maize: light microscopy of fungal spread from wounds. Phytopathology 80: 1287-1294.

Spatofora J. 2007. Pezizomycotina. The Tree of Life Web Project. Retrieved Sep 28, 2018. Available from http://tolweb.org/Pezizomycotina/29296.

Statista. 2018a. Global grain production by type, 2016/2017 | Statistic. The Statistics Portal. Retrieved Sep 25, 2018. Available from https://www.statista.com/statistics/272536/acreage-of-grain-worldwide-by-type/.

Statista. 2018b. Grain production worldwide by type, 2017/2018 | Statistic. The Statistics Portal. Retrieved Sep 25, 2018. Available from https://www.statista.com/statistics/263977/world-grain-production-by-type/.

Taylor J.W., Spatofora J., Berbee M. 2006. Ascomycota: sac fungi. The Tree of Life Web Project. Retrieved Sep 28, 2018. Available from http://tolweb.org/Ascomycota.

Taylor J.W., Jacobson D.J., Fisher M.C. 1999. The evolution of asexual fungi: reproduction, speciation and classification. Annu. Rev. Phytopathol. 37: 197-246.

USDA-ERS. 2018. Corn and other feedgrains. United States Department of Agriculture - Economic Research Service. Retrieved Sep 24, 2018. Available from https://www.ers.usda.gov/topics/crops/corn-and-other-feedgrains.

USDA-FAS. 2018. Grain: world markets and trade. United States Department of Agriculture - Foreign Agricultural Service. Retrieved Sep 24, 2018. Available from https://apps.fas.usda.gov/psdonline/circulars/grain.pdf.

USDA-NASS. 2018. National Statistics for Corn. United States Department of Agriculture - National Agricultural Statistics Service. Retrieved Sep 24, 2018. Available from https://www.nass.usda.gov/Statistics_by_Subject/.

Varga J., Frisvad J.C., Samson R.A. 2011. Two new aflatoxin producing species, and an overview of *Aspergillus* section *Flavi*. Stud. Mycol. 69: 57-80.

Wannop C.C. 1961. The histopathology of Turkey "X" disease in Great Britain. Avian Diseases 5: 371-381.

Wild C.P. 2007. Aflatoxin exposure in developing countries: the critical interface of agriculture and health. Food Nutr. Bull. 28: S380.

Wu X., Zhou B., Yin C., Guo Y., Lin Y., Pan L., Wang B. 2014. Characterization of natural antisense transcript, sclerotia development and secondary metabolism by strand-specific RNA sequencing of *Aspergillus flavus*. PLoS One 9: e97814.

Wu F. 2006. Mycotoxin reduction in Bt corn: potential economic, health, and regulatory impacts. Transgenic Res. 15: 277-289.

Yu J., Chang P., Ehrlich K.C., Cary J.W., Bhatnagar D., Cleveland T.E., Payne G.A., Linz J.E., Woloshuk C.P., Bennet J.W. 2004. Clustered pathway genes in aflatoxin biosynthesis. Appl. Environ. Microbiol. 70: 1253-1262.

CHAPTER 2

Morphological changes within stromata during sexual reproduction in *Aspergillus flavus*

Submitted to *Mycologia*

Jane Marian Luis[a], Ignazio Carbone[a], Gary A. Payne[a], Deepak Bhatnagar[b], Jeffrey W. Cary[b], Geromy G. Moore[b], Matthew D. Lebar[b], Qijian Wei[b], Brian Mack[b], and Peter S. Ojiambo[a]

[a] Center for Integrated Fungal Research, Department of Entomology and Plant Pathology, North Carolina State University, Raleigh, NC 27695

[b] USDA-ARS Southern Regional Research Center, New Orleans, LA 70124

ABSTRACT

Aspergillus flavus contaminates agricultural produce worldwide with carcinogenic aflatoxins that pose health risks to humans and animals. The fungus survives adverse environmental conditions through production of sclerotia. When fertilized by a compatible conidium of an opposite mating type, the sclerotium transforms into stroma leading to the formation of ascocarps, asci and ascospores. This transition from a sclerotium to a stroma, which is also influenced by female fertility (i.e., capability of a strain to produce ascocarps in which meiosis occurs), is not well understood in *A. flavus*. Reciprocal crosses with different (i.e., low vs. high) levels of female fertility and unmated sclerotia, were plated in mixed cereal agar and incubated at 30 C in continuous dark. Samples of mated and unmated sclerotia were harvested at the time of crossing and every 2 weeks until 8 weeks of incubation and examined by microscopy to characterize morphological changes. Hyphal strands of germinated conidia of a green fluorescent protein (GFP)-labeled *MAT1-1* strain were observed growing towards sclerotia of an mCherry (mCH)-labeled *MAT1-2* strain after 24 hours of incubation. A network of interlocking hyphal strands of the GFP- and mCH-labeled strains was observed at the base of the sclerotia (i.e., region in contact with agar surface) after 72 hours of incubation. Intracellular green-fluorescent hyphal strands were observed within the stromatal matrix at 5 weeks of incubation. Morphological differences between unfertilized sclerotia and stromata became apparent at 4 weeks of incubation. Internal hyphae and croziers were detected inside multiple ascocarps that developed within the stromatal matrix of the high fertility cross, but not in the matrix of the low fertility cross or unmated sclerotia. At 6 to 8 weeks of incubation, hyphal tips produced numerous asci, each ascus containing approximately eight ascospores that emerged out of the ascus after breakdown of the ascus wall. These observations broaden our knowledge on early events during sexual reproduction and show

that hyphae from the male parent may be involved in the early stages of sexual reproduction in *A. flavus*. When combined with omics data, these findings could be useful in further exploration of biochemical mechanisms underlying sexual reproduction in *A. flavus* and identify additional factors critical for sexual recombination in the ecology of this fungus.

KEY WORDS: ascospore; ascocarp; female fertility; morphogenesis; stromata

INTRODUCTION

Aflatoxigenic strains of *Aspergillus flavus* (teleomorph: *Petromyces flavus*) are major producers of aflatoxins that contaminate maize, peanut, cottonseed, tree nut and several other agricultural crops worldwide. Exposure through ingestion of produce contaminated with high concentrations of aflatoxins pose a high risk to human health due to its association with immune system suppression, hepatocellular carcinoma, and stunting of growth in children (Khlangwiset et al. 2011; Wild et al. 2015; Paulussen et al. 2016). Further, livestock fed with contaminated produce have reduced milk production, while poultry fed with contaminated feed have increased mortality and reduced egg yield (CAST 2003; Wild 2007). In contrast, non-aflatoxigenic strains of *A. flavus* are used as biocontrol agents to reduce aflatoxin production either by competitively excluding aflatoxigenic strains from nutrients and space (Cotty and Bayman 1993; Damann 2015) or by inhibiting aflatoxin production in aflatoxigenic strains when hyphae of the two strains physically interact during the infection process (Huang et al. 2011).

The life cycle of *A. flavus* is comprised of asexual, parasexual and sexual stages but growth and development of the fungus are predominantly observed in its anamorph state (Ojiambo et al. 2018). Asexual reproduction results in the production and release of numerous conidia that are dispersed by wind and insects to short and long distances from the initial source. Conidia germinate into hyphae that branch to form a patchwork known as mycelia, which in turn produce conidiophores that release more conidia. During adverse conditions such as lack of adequate water or nutrients, several strains of *A. flavus* can produce asexual survival structures known as sclerotia (Hedayati et al. 2007; Bennet 2010). These hardened, darkly pigmented hyphal masses are composed of polyhedral, thick-walled cells that assume globose to subglobose shapes when mature. As an asexual structure, a sclerotium can germinate and give rise to new hyphae or produce

conidia bearing conidiophores (Raper and Fennell 1965; Dyer and O'Gormann 2012; Chang et al. 2014).

Previous studies showed a strong clonal structure for *A. flavus* populations, which led to the conclusion that vegetative compatibility is a strong barrier of genetic exchange between strains (Chang et al. 2014; Ehrlich 2014). Vegetative compatibility is a self/non-self-recognition system that results in stable hyphal fusion between strains whose alleles are identical at all heterokaryon incompatibility (*het*) loci (Saupe 2000). However, populations of *A. flavus* showed considerable genetic, morphological and chemotype diversity among vegetative compatibility groups (VCGs). Populations of this fungus are also dynamic and the dominant VCG group in an area can shift from year to year (Bayman and Cotty 1991). This observed diversity was first attributed to parasexuality, which leads to the formation of heterokaryons and the exchange of genetic material between two haploid strains. However, hyphal fusion occurs primarily between genetically similar individuals of the same VCG. In addition, the parasexual cycle has only been observed in laboratory settings, and direct evidence of its occurrence in nature is still lacking (Chang et al. 2014).

The discovery of the sexual stage of *A. flavus* showed that VCG is not a strong barrier to genetic exchange when outcrossing among VCGs led to formation of new VCGs (Olarte et al. 2012). Indeed, all *A. flavus* crosses that formed fertile ascocarps involved pairs of sexually compatible strains that belonged to different VCGs (Horn et al. 2009). *A. flavus* was identified to be heterothallic, where each individual contains one of the two mating type idiomorphs, *MAT1-1* or *MAT1-2*, at a single locus. *MAT1-1* encodes an α-domain transcription factor, while *MAT1-2* encodes a high mobility group-domain (HMG) transcription factor (Ramirez-Prado et al. 2008). Successful crosses between individuals of the opposite mating types formed ascospore-bearing

ascocarps within the stromatal matrix after an extended incubation of 5 to 7 months in dark conditions (Horn et al. 2014). *A. flavus* was also identified to be hermaphroditic with respect to male and female roles during sexual reproduction, with the conidium being functionally the male fertilizing the sclerotium, while the sclerotium serves functionally as the female by providing nutrient sources and bearing the ascocarps, asci and ascospores (Horn et al. 2016). A key component of sexual reproduction and development in fungi is the ability to produce female organs in which meiosis occurs (Saleh et al. 2012). This ability is referred to as female fertility and sexual reproduction will not occur in the absence of a female-fertile strain. In *A. flavus*, the degree of female fertility of a cross is attributed to fertility factors in the female strain producing sclerotia (Horn et al. 2016).

Fertilization of sclerotia by a compatible conidium-producing strain leading to the formation of ascospores has been reported in *A. flavus* with ascocarps and ascospores forming in the stromatal matrix after 4 to 44 weeks of incubation in the lab or under field conditions (Horn et al. 2009; Horn et al. 2016). However, there is limited information on the morphological changes that occur when a sclerotium first comes in contact with conidia from a compatible strain during the initial phases of sexual reproduction. Receptor structures for fertilization have not been detected on the surface of sclerotia of *A. flavus* (Horn et al. 2016) and it is unclear whether direct contact of the sclerotia with conidia is needed to initiate sexual reproduction. In addition, morphological changes that occur in a sclerotium during sexual reproduction have not been characterized in *A. flavus*. It is not known how the degree of female fertility influences changes in the morphology of sclerotia and stromata during sexual reproduction and development. Such information could provide a better understanding not only of the morphological features during sexual reproduction, but also provide a broader basis for relating biochemical, metabolic and

transcriptomic properties associated with development of sclerotia and stromata in *A. flavus*. Thus, this study was conducted with the following objectives: 1) characterize the morphological changes that occur in sclerotia and stromata during sexual reproduction in *A. flavus*, and 2) determine how the degree of fertility of the sclerotium-producing strain influences morphological features in sclerotia and stromata during sexual reproduction in *A. flavus*.

MATERIALS AND METHODS

Strains of A. flavus. – Two fungal strains, NRRL 21882 and NRRL 29507, were used as parental strains in this study. Strain NRRL 21882 was originally isolated from a peanut seed in Georgia. It is non-aflatoxigenic and used as the active ingredient in the commercially available biocontrol agent Afla-Guard® (Dorner 2004). Strain NRRL 29507 was originally isolated from a peanut field in Georgia (Horn and Green 1995) and is aflatoxigenic. These two strains were selected based on their mating type and vegetative compatibility grouping. Strain NRRL 21882 has the mating type allele *MAT1-2*, while NRRL 29507 has *MAT1-1* (Ramirez and-Prado et al. 2009). The vegetative compatibility group of NRRL 21882 is 24, while NRRL 29507 belongs to VCG 33 (Horn and Green 1995). These strains were previously stored at -80 C in 40% glycerol and sub-cultured on mixed cereal agar (MCA) (McAlpin and Wicklow 2005) at 30 C for use in subsequent experiments described below.

Culture conditions and fertility of reciprocal crosses. – Strains NRRL 21882 and NRRL 29507 were first individually cultured on MCA culture plates and incubated in a growth chamber at 30 C under continuous darkness for 14 days (Horn et al. 2016). Conidia and sclerotia from cultures of each strain were harvested separately. Dry conidia obtained from the cultures were harvested and

suspended in 3 ml distilled water containing 0.01% Triton-X. The resultant conidial suspension was collected, adjusted to 5 x 10^5 conidia/ml, and then 20 µl of the suspension was spread onto new MCA plates. Sclerotia were detached from the agar by adding distilled water containing 0.01% Triton-X and carefully scraping the surface with a transfer loop. The resultant sclerotial suspension was then transferred to 50 ml tubes, thoroughly washed with distilled water by repeated vortexing and decanting, and finally filtered through a Miracloth to remove any residual conidia.

To establish the degree of female fertility, two reciprocal crosses involving strains NRRL 21882 and NRRL 29507 were examined. In the first reciprocal cross, strain NRRL 29507 (*MAT1-1)* was used as the sclerotium-producing female parent, while NRRL 21882 (*MAT1-2*) was used as the conidium-producing male parent (TABLE 2.1). In the second reciprocal cross, strain NRRL 29507 was used as the male parent, while strain NRRL 21882 was used as the female parent. Strains were crossed by overlaying the sclerotia onto the surface of MCA plates containing the conidia of the opposite mating type. Culture plates were sealed with parafilm, enclosed in ziplock bags to prevent desiccation, and incubated in a growth chamber at 30 C in continuous darkness for 2 to 8 weeks. After each incubation period, sclerotia were harvested as described above. A total of 300 sclerotia from each cross were then manually sectioned with a micro-scalpel and examined for the presence of ascocarps under a dissecting stereomicroscope. Sclerotia were considered to be fertilized based on the development of ascocarps within the stromatal matrix. The proportion of stromata that formed ascocarps containing ascospores was used as a measure of female fertility as described by Horn et al (2016). Sclerotia of an unmated strain NRRL 29507 were included as control. Sclerotia from the reciprocal crosses and unmated strain were replicated three times with a sample of 300 sclerotia per replication and the experiment was repeated once.

Morphological features during sexual reproduction. – Interaction between sclerotia and conidia during the initial phase of sexual reproduction and development was examined using fluorescence microscopy as described below. In addition, changes in the morphology of sclerotia produced from the two reciprocal crosses involving strains NRRL 29507 and NRRL 21882 were examined using scanning electron microscopy to capture a wide range of morphological features. Sclerotia and stromata harvested at each time-point were immediately processed for fixation as described below to characterize morphological changes as affected by the degree of female fertility. In both microscopy techniques, sclerotia from the reciprocal crosses were crossed and harvested as described above.

Transformation of test strains and fluorescent microscopy. – Fluorescent strains of NRRL 29507 (*A. flavus* 1582-mCherry) and NRRL 21882 *(A. flavus* 1534-eGFP) were developed at USDA-ARS SRRC in New Orleans and used to observe the interaction between conidia and sclerotia during initial phases of sexual reproduction and development. Overlap fusion PCR was used to generate the gpd-GFP-trpC and gpd-mCherry-trpC reporter constructs for transformation into *A. flavus* 1534 and 1582, respectively (FIG. S2.1). Both of these strains are sensitive to pyrithiamine. The expression of the reporter gene in both constructs was under the control of the *A. nidulans* glyceraldehyde 3-phosphate dehydrogenase (*gpd*) promoter and tryptophan synthase (*trpC*) transcriptional terminator region. The pyrithiamine resistance selectable marker gene, *ptrA*, was amplified using plasmid pPTRI (Takara Bio) as template and primers ptrA-F and ptrA-R (TABLE S2.1). Briefly, the *gpd* promoter and *trpC* PCR products were amplified using pPTRI-gpd-trpC vector DNA (Cary et al. 2015) as template and specific primer pairs (TABLE S2.1). The *egfp* gene was amplified from plasmid pUC18-egfp-nmt1 (Rajasekaran et al. 2008) and mCherry was

amplified from plasmid pJES35-mCherry (a gift from N. Keller, University of Wisconsin) expressing the histone H2A-*mcherry* gene under the control of the *A. nidulans gpd* promoter. All fragment amplifications were performed using Q5 High Fidelity (New England BioLabs M0492). Linear cassettes of the three overlapping PCR products (gpd-GFP-trpC or gpd-mCherry-trpC) were generated using the overlap fusion PCR method of Szewczyk et al. (2008) and nested primers. The gpd-GFP-trpC or gpd-mCherry-trpC PCR products were co-transformed with the *ptrA* selectable marker PCR product into their respective *A. flavus* hosts. Fungal protoplasts for transformation were prepared as previously described (Chang 2008). Transformants were selected on Czapek–Dox Agar (CZA) (Becton Dickinson and Company, Sparks, MA, USA) supplemented with 0.1 µg/ml pyrithiamine. Regeneration plates were incubated at 30 C for 5 to 10 days. Selected isolates were then transferred to fresh CZA plates containing pyrithiamine.

For the sexual reproduction assay, 1534-eGFP (*MAT1-1*) was used as the source of conidia, while 1582-mCherry (*MAT1-2*) was the source of sclerotia. Initial interaction events from 0 to 72 hours were examined by overlaying sclerotia of 1582-mCherry strain over conidia of 1534-eGFP strain on very thin layer of CZA on cell imaging dishes (Eppendorf, Catalog No. 0030740017) and incubated at 30 C. Interaction events at 5 weeks were observed by crossing sclerotia of 1582-mCherry strain and conidia of 1534-eGFP strain in MCA plates as described above. The sclerotia of 1582-mCherry strain were then harvested, sectioned into half using a micro-scalpel, and glued to cell imaging dish using a spot of medical adhesive glue (Adapt 7730, Hollister, CA) to prevent from floating when water was added for imaging. Samples of conidia and sclerotia were imaged with Zeiss LSM 880 with Airyscan (Zeiss Inc, Germany) using wavelengths 488 and 561 nm for eGFP and mCherry, respectively. Captured images of the early phases of the interaction between

conidia and sclerotia and development of stromata during sexual reproduction in *A. flavus* were examined using Zen software (Blue Edition; Zeiss, Obercohen, Germany).

Sclerotia and stromata collection and initial fixation for scanning electron microscopy. – Stromata from reciprocal crosses between strains NRRL 21882 and NRRL 29507 and unmated sclerotia of NRRL 29507 were harvested as described above at the time of crossing (T_0), and at four subsequent time-points; 2 weeks (T_1), 4 weeks (T_2), 6 weeks (T_3), and 8 weeks (T_4) of incubation in the growth chamber at 30 C in continuous darkness. Manually sectioned stromata were first examined under the dissecting stereomicroscope for the presence of ascocarps. Sectioned sclerotia and stromata were then fixed in 3% glutaraldehyde + 0.1 M Na cacodylate buffer (pH 7.3) and stored at 4 C (Horn et al. 2009) until they were post-fixed as described below.

Scanning electron microscopy of sclerotia and stromata. – Sectioned stromata from the reciprocal crosses and sclerotia of unmated strain initially fixed at 3% glutaraldehyde + 0.1 M Na cacodylate buffer were pipetted to microporous capsules, processed with three washes of cold 0.1 M Na cacodylate buffer (pH 7.3) and followed by post-fixation for 1 hour in 2% OsO_4 in 0.1 M Na cacodylate buffer (pH 7.3) on ice and in the dark. Samples were then rinsed in three more changes of cold 0.1 M Na cacodylate buffer (pH 7.3), followed by dehydration in a graded ethanol series (30%, 50%, 70%, 95% and 100%) and warming to room temperature in 100% ethanol for 24 hours to complete the dehydration process. The latter involved two additional changes of 100% ethanol at room temperature, each for a 24 hour period. Dehydrated samples were critical-point dried in liquid carbon dioxide using a Samdri-795 Critical-Point Drier (Tousimis Research Corp., Rockville, MD). Samples were then mounted on microscope stubs using double stick tape and

small amounts of silver paint to provide conductivity and to ensure proper contact with the stub. Samples were sputter-coated with gold palladium using a Hummer 6.2 Sputter Coater (Anatech USA, Hayward, CA) based on manufacturer's instruction. Specimens were examined using a scanning electron microscope JEOL 5900LV SEM (JEOL USA, Peabody, MA) at an accelerating voltage of 15 kV.

RESULTS

Fertility of reciprocal crosses. – Fertility, defined as the presence of one or more ascospore-bearing ascocarps within the stromatal matrix (FIG. 2.1), varied between the sexually compatible strains used in this study (TABLE 2.1). In the cross where strain NRRL 29507 (*MAT1-1*) was used as the sclerotium-producing female parent and NRRL 21882 (*MAT1-2*) was used as the conidium-producing male parent, 247 of the 300 stromata examined had ascospore-bearing ascocarps. However, only 7 out of the 300 stromata examined had ascocarps in the reciprocal cross where strain NRRL 29507 was used as the male parent and NRRL 21882 as the female parent (TABLE 2.1). The proportion of fertilized stromata in the cross with NRRL 29507 as the female parent (82.3%) was significantly ($P < 0.05$) higher than the proportion of fertilized stromata in the cross with NRRL 29507 as the female parent (2.3%). Thus, the cross with NRRL 29507 as the female parent was designated as a high fertility cross, while the reciprocal cross with NRRL 21882 as the female parent was designated a low fertility cross. No ascocarps were observed in sclerotia of the unmated strain NRRL 29507 (TABLE 2.1).

Interaction between conidia and sclerotia using fluorescent strains. – A fluorescent-labeled conidium-producing strain of NRRL 21882, 1534-eGFP (FIG. 2.2A), and a fluorescent-labeled

sclerotium-producing strain of NRRL 29507, 1582-mCherry (FIG. 2.2B) were used to track and visualize the interaction between sexually compatible conidia and sclerotia during the early stage of sexual reproduction (FIG. 2.2). Conidia of 1534-eGFP germinated within 24 hours (FIG. 2.2C) producing hyphae that grew towards the base of the 1582-mCherry sclerotia within this period of time (FIG. 2.2D). During this same period of time, sclerotia of 1582-mCherry strain germinated producing hyphae that grew into the MCA medium**.** Hyphal growth of the two strains produced a distinct network of interlocking hyphal strands that were observed at the base of the 1582-mCherry sclerotia at 72 hours of incubation (FIG. 2.2E).

Well-defined ascocarps within the stromatal matrix were not observed when conidia from strain 1534-eGFP were used to fertilize sclerotia from strain 1582-mCherry. However, distinct cells with red fluorescence were observed within the stromatal matrix at 5 weeks of incubation (FIG. 2.2F–G). In addition, hyphal strands with green fluorescence were observed among the red fluorescence cells within the matrix of the stromata during this developmental period of the sclerotia (FIG. 2.2F).

Morphological changes in stromata and development of ascocarps. – Sclerotia from the high fertility cross, low fertility cross and the unmated strain were manually sectioned and examined using low magnification scanning microscopy to characterize changes in the morphology of sclerotia at the time of crossing (T_0) and morphological features in the stromata from T_1 (2 weeks) to T_4 (8 weeks) as influenced by the fertility of the cross (FIG. 2.3). Similarly, details depicting internal changes in the sclerotia and stromata were characterized using high magnification scanning microscopy during these time periods to determine how they are affected by the degree of sexual fertility (FIG. 2.4). At T_0, matrix of sclerotia from either the high fertility cross (FIG.

2.3A), low fertility cross (FIG. 2.3F) or sclerotia of the unmated strain NRRL 29507 (FIG. 2.3K), were mainly composed of compact hyphal cells. Similarly, the matrix of stromata from either the high fertility cross (FIG. 2.3B) or the low fertility cross (FIG. 2.3G) at T_1 were composed mainly of compact hyphal cells.

Openings (or channels) in some portions of the sclerotial and stromatal matrix were visible at T_0 or T_1 regardless of the fertility of the cross (FIG. 2.4A–B, H–I). Similar channels were also observed at T_1 in the matrix of the unmated sclerotia of NRRL 25907 (FIG. 2.4N). At T_2, ascocarp formation was detected at the center of stromatal matrix from the high fertility cross (FIG. 2.3C), but not in those from the low fertility cross (FIG. 2.3H) or in those of the unmated sclerotia (FIG. 3M). Formation of distinct ascocarps was progressively clear at T_3 (FIG. 2.3D) and T_4 (FIG. 2.3E) in the matrix of stromata from the high fertility cross. No formation of distinctive morphological features or differentiation of cells at the center of the matrix of stromata from the low fertility cross (FIG. 2.3J) or in the unmated sclerotia (FIG. 2.3O) were observed for any time-point within the study. Each observed ascocarp was enclosed and delineated from the stromatal matrix by its own wall (or peridium) (FIG. 2.5A) and the surface of the peridium was composed of irregularly flattened cells. Most of the fertile stromata examined in this study contained 1 to 3 ascocarps (FIG. 2.5B).

Ascus and ascospore formation. – At T_2, hyphae were observed inside ascocarps of the high fertility cross (FIG. 2.4C), but no similar structures were observed within the matrix of stromata from the low fertility cross (FIG. 2.4J) or sclerotia of the unmated strain NRRL 29507 (FIG. 2.4O). Formation of asci was initiated by the presence of hook-tipped croziers (FIG. 2.5E) and subsequent coiling and branching of the crozier chain (FIG. 2.5F) to form ascus mother cells. Distinct asci and

ascospores were observed inside the ascocarps at T_3 (FIG. 2.4D, F) and T_4 (FIG. 2.4E, G). Each ascocarp contained numerous asci, which in turn bore approximately eight ascospores per ascus (FIG. 2.5H). Asynchronous development of asci and ascospores was observed among (FIG. 2.5B–D) and within (FIG. 2.5G) ascocarps from the same stroma. For example, one of the ascocarp (c1) had already developed several asci (FIG. 2.5B–C), while the second ascocarp (c2) in the same stroma was still forming internal hyphae in preparation for differentiation and formation of an ascus (FIG. 2.5B, D). Further, asci within the same ascocarp grew asynchronously wherein young and relatively more mature asci were observed side by side in the same ascocarp (FIG. 2.5E). At maturity, starting at approximately T_3, the ascus was observed to breakdown as seen by the distinctive fissure in the ascus wall (FIG. 2.5I) to release ascospores. Each ascospore was ornamented with fine tuberculation and an equatorial ridge (FIG. 2.5J).

DISCUSSION

This study was undertaken to characterize morphological changes that occur within sclerotia and stromata during sexual reproduction in *A. flavus* and how differences in female fertility in crosses of compatible strains of the fungus influences these morphological features. Using an eGFP-labeled conidium-producing male parent and mCherry-labeled sclerotium-producing female parent, hyphae of the conidial strain were detected growing on the surface of the agar media towards the base of the sclerotium (i.e., region in contact with the agar surface) at 24 hours of incubation. A network of interlocking hyphal strands from both parental strains was observed at the base of the sclerotia at 72 hours of incubation. Differences in morphological changes between sclerotia and stromata due to female fertility were evident at 4 weeks of incubation with distinct ascocarps being observed in the stromatal matrix of the high fertility cross but not in the low

fertility cross or unmated strain. This study is the first to document interactions between conidia and sclerotia during the initial phases of sexual development in *A. flavus* and how female fertility influences morphological features and changes in stromata during sexual reproduction.

Information on the mechanism(s) of fertilization and the subsequent development of sclerotia, stromata and other sexual structures is limited in *A. flavus*. No receptor structures for fertilization have ever been reported on the surface of sclerotia of *A. flavus* (Horn et al. 2016). Further, it was unclear as to how conidia and sclerotia interact during the initial phases of sexual reproduction. In this study, we observed that the hyphae of the conidium-producing parental strain extends in growth towards the base of the sclerotium of the female parental strain immediately following incubation. This observation, which was similar irrespective of fertility of the cross, tends to suggest some element of chemotactic growth by the hyphae from conidia towards the sclerotia during this initial period. As with the chytridiomycete *Allomyces macrogynus*, male gametes are attracted to the pheromone sirenin produced by the female gametes and thus swarm towards the location of the female gametangia (Pommerville 1977; Carlile 1996). Similarly, no cognate receptors for sirenin have yet been identified (Lichius and Lord 2014). In *A. flavus*, besides serving as survival structures in adverse environmental conditions (Raper and Fennell 1965; Bennet 2010), sclerotia that are functionally female contain nutrients that are required for sexual reproduction (Bojović-Cvetić and Vujičić 1988; Willetts 1997). These nutrients alone or in combination with other bioactive compounds produced by the female parent may thus serve as stimuli for the directed growth of conidial hyphae towards the sclerotia.

Openings in the outer rind cells that can serve as entry points into the sclerotia by hyphae of a compatible strain have been observed in sclerotia of *Sclerotinia sclerotiorum* (Colotelo 1974). However, no openings or regions where fusion occurred on the surface of the sclerotia through

which hyphae from conidia could have gained entry into the sclerotium were observed in this study. Rather, a network of hyphal strands from the conidium-producing and sclerotium-producing parental strains was observed at the base of sclerotia at 72 hours of incubation. At 4 weeks of incubation, fungal cells expressing red fluorescence were observed to be interspersed with green fluorescent hyphal strands within the stromatal matrix. Thus, it is possible that this hyphal network of *A. flavus* observed at 72 hours of incubation could provide a means through which genetic information from the conidium-producing male parent is transferred into the sclerotium of the female parent. Additional studies are thus needed to determine whether or not interactions between the hyphae from the conidium- and sclerotium-producing strains that lead to the transformation of a sclerotium into a stroma occur on the exterior of the sclerotium.

A. flavus is one of four members of the genus *Petromyces* that is heterothallic (Kwon-Chung and Sugui 2009). Strains that are sexually compatible belong to opposite mating types and different vegetative compatibility groups (Horn et al. 2009; Horn et al. 2016). During the sexual cycle, the conidia or hyphal fragments of one strain fertilize the sclerotia of a compatible strain. These sclerotia are hardened, thick-walled, darkly pigmented and spherical structures that are known to survive adverse environmental conditions (Raper and Fennell 1965; Bennet 2010). The sclerotium transforms into a stroma by producing one or more spherical ascocarps in the stromatal matrix (Dyer and O'Gormann 2012), within which meiosis occurs. The ability to produce female organs in which meiosis occurs is a key component of sexual reproduction in fungi (Saleh et al. 2012). This ability, which is referred to as female fertility, is dependent on the parental strains used as the source of conidia and sclerotia. In this study, use of strain NRRL 29507 as the female parent resulted in a high fertility cross, while a reciprocal cross with NRRL 21882 as the female parent resulted in a low fertility cross. These results are similar to those reported in a study by Horn et al.

(2016) where one female-male combination in each reciprocal cross was highly fertile, while the reciprocal combination resulted in a very low frequency of ascocarps with ascospores. Further, Horn et al (2016) observed a wide variation in fertility in different but compatible male and female strains of *A. flavus*. Some pairs readily produced ascocarps and ascospores, while others show little or no evidence of sexual reproduction. The variation in levels of fertility has been attributed to female fertility factors in the strain producing the sclerotia or the degree of sexual compatibility between the paired strains (Horn et al. 2016). On the other hand, sexual incompatibility in *Aspergillus* can be due to accumulation of mutations in genes regulating different stages of development and may be responsible for the crosses that exhibit low fertility or those that do not produce viable progeny (Saleh et al. 2012).

One major objective of this study was to establish how the degree of female fertility influences morphological changes in stromata during sexual reproduction in *A. flavus*. Our results show that differences between stromata from high fertility cross versus low fertility cross and unmated strain became evident at 4 weeks after crossing. At this point, the matrix at the center of stroma started to differentiate to form ascocarps. However, similar changes were not apparent in stromata from the low fertility cross or in sclerotia of the unmated strain. Free mature ascospores from the high fertility cross were observed starting at 6 weeks of incubation after breakdown of the ascus wall. While this study used only a single set of compatible male and female parental strains, we recommend additional studies to examine a larger set of compatible strains to establish the consistency of our observations. Our observed timeline for the formation of ascocarps and ascospores was essentially similar to that reported by Horn et al (2014) where ascocarps were observed at 4 weeks of incubation. However free mature ascospores were observed in a relatively shorter time than that reported by Horn et al (2014), where free mature ascospores were observed

at 8 weeks of incubation. Ascocarps were globose and variable in size, consisting of ascogenous hyphae, asci, and ascospores, and surrounded by thin sheath-like peridia that are composed of single layers of irregular, flattened cells. Ascocarps that contained several asci at maturity had their entire cavity filled with free ascospores. As reported in other studies (Horn et al. 2009; Dyer and O'Gormann 2012), each ascus observed in this study contained approximately eight ascospores.

While distinct gametangia have been reported in several *Aspergillus* species such as *Eurotium repens* and *E. amstelodami* (Benjamin 1955), none were observed in this study and there are no reports of ascogonia or antheridia in members of *Aspergillus* section *Flavi*. As such, the mechanism of fertilization and development of sexual structures is still largely unknown. 'Channeling' within the matrix of the stromata just before the appearance of ascocarps has been thought to be involved with the initiation of the ascogenous phase during sexual reproduction in *A. alliaceus* (Fennell and Warcup 1959) and in *A. flavus* (Horn et al. 2016). In the current study, channeling was observed both in fertilized stromata and in unmated sclerotia in which no ascocarps were formed (FIG. 2.4), suggesting that channeling may not be associated exclusively with sexual reproduction in *A. flavus*. Although distinct ascocarps were not formed when fluorescent-labeled strains were crossed in this study, our observation of green-fluorescent intracellular hyphae within the stromatal matrix of the transformed female strain suggests that hyphae from the conidium-producing male parent may be involved in the formation of ascocarps in *A. flavus*, as suggested by Horn et al (2016). Given the lack of observed openings in the sclerotia of *A. flavus*, the presence of green fluorescence within the ascocarps suggests that genetic information from the male parent was transferred into the stroma possibly through anastomosis of hyphae originating from both conidia and sclerotia on the exterior of sclerotia.

As reported for many ascomycetes, asci formation within the ascocarps of *A. flavus* were initiated in a consecutive order (Wu and Kimbrough 1990), resulting in the asynchronized development and maturation of asci observed in this study. The ascus exhibited specialized determinate growth in contrast to unspecialized vegetative hyphae. Ascospore formation usually occurs as ascospore walls develop between double delimiting membranes derived from the plasma membrane of the ascus (Read and Beckett 1996). The ascospores of *A. flavus* observed in this study were oblate and finely tuberculate, resembling a double convex lens with a thin equatorial ridge as reported by Horn et al (2009). Mature ascospores are naturally released within the stromatal matrix after the breakdown of the ascus wall and peridium of the ascocarp (Horn et al. 2009; Dyer and O'Gorman 2012). Ascospores have thick cell walls and resistant to a range of environmental stressors including heat (Dijksterhuis 2007). These sexual spores also have a long incubation period for fruiting body development, which has been thought to be an evolutionary mechanism to withstand adverse environmental conditions (Dyer and O'Gorman 2012).

In summary, interactions between compatible male and female parental strains during sexual reproduction and development in *A. flavus* are initiated within a relatively short period of time when compatible strains come into close proximity. Understanding the influence of female fertility on morphological changes during the development of sclerotia and stromata will provide insights into the mechanism of sexual reproduction within *A. flavus* leading to a better understanding of the reproductive potential of individual strains and populations of the fungus. Such knowledge will enable better selection of non-aflatoxigenic strains of *A. flavus* for use in biocontrol of aflatoxin contamination of crops. The efficacy of biocontrol is largely dependent on the genetic structure of the native population of *A. flavus* in the soil (Molo et al. 2019). Thus, the use of highly fertile female strains of *A. flavus* that are non-aflatoxigenic may be preferred as

biocontrol agents since they will take full advantage of sexual reproduction to further decrease aflatoxin levels in field populations. Future work will examine differentially expressed genes associated with morphological changes during sexual reproduction in high and low fertility crosses, to identify marker genes for screening candidate biocontrol strains. This molecular characterization will be coupled with metabolomic analysis of compounds associated with specific developmental stages of the stroma, to rapidly identify candidate *A. flavus* biocontrol strains with high female fertility.

ACKNOWLEDGEMENTS

We thank Valerie Lapham at the NC State University Center of Electron Microscopy for providing technical assistance with scanning electron microscopy; Eva Johannes and Mariusz Zareba at the NC State University Cellular and Molecular Imaging Facility for their technical assistance with fluorescence microscopy; and Gregory O'Brian, Yaken Samah Ameen and Richard Gell for their input and assistance with laboratory experiments. The authors also thank David Geiser (Pennsylvania State University) for his comments and suggestions on an earlier draft of the manuscript.

FUNDING

This study was supported by a grant from Aflatoxin Mitigation Center for Excellence and the National Corn Growers Association Award No. 2016-0949, USDA National Institute of Food and Agriculture (NIFA) Hatch Funds for Project NC02432 and funds from USDA-ARS. This project was also supported by the Agriculture and Food Research Initiative Competitive Grants Program grant no. 2013-68004-20359 from the USDA NIFA.

LITERATURE CITED

Bayman P, Cotty PJ. 1991. Vegetative compatibility and genetic diversity in the *Aspergillus flavus* population of a single field. Canadian Journal of Botany 69: 1707-1711.

Benjamin CR. 1955. Ascocarps of *Aspergillus* and *Penicillium*. Mycologia 47: 669-687.

Bennett JW. 2010. An overview of the genus *Aspergillus*. In: Machida M, Gomi K, eds. *Aspergillus*: molecular biology and genomics. Portland: Caiser Academic Press. P. 1-17.

Bojović-Cvetić D, Vujičić R. 1988. Polysaccharide cytochemistry in maturing *Aspergillus flavus* sclerotia. Transaction of the British Mycological Society 91: 619-624.

Carlile MJ. 1996. The discovery of fungal sex hormones: I. sirenin. Mycologist 10: 3-6.

Cary JW, Han Z, Yin Y, Lohmar JM, Shantappa S, Harris-Coward PY, Mack BM, Ehrlich KC, Wei Q, Arroyo-Manzanares N, Uka V, Vanhaecke L, Bhatnagar D, Yu J, Nierman WC, Johns M, Sorensen D, Shen H, De Saeger S, Diana Di Mavungu J, Calvo AM. 2015. Transcriptome analysis of *Aspergillus flavus* reveals *veA*-dependent regulation of secondary metabolite gene clusters, including the novel aflavarin cluster. Eukaryotic Cell 14: 983-997.

CAST. 2003. Mycotoxins: risks in plant, animal, and human systems. Council for Agricultural Science and Technology. Ames, IA: Task Force Report. p. 1-199.

Chang PK, Horn BW, Abe K, Gomi K. 2014. *Aspergillus*. In: Batt CA, Tortorello ML, eds. Encyclopedia of food microbiology, Volume 1. Elsevier Ltd, Academic Press. p. 77-82.

Chang PK. 2008. A highly efficient gene-targeting system for *Aspergillus parasiticus*. Letters in Applied Microbiology 46: 587-592.

Colotelo N. 1974. A scanning electron microscope study of developing sclerotia of *Sclerotinia sclerotiorum*. Canadian Journal of Botany 52: 1127-1130.

Cotty PJ, Bayman P. 1993. Competitive exclusion of a toxigenic strain of *Aspergillus flavus* by an atoxigenic strain. Phytopathology 83: 1283-1287.

Damann KJ. 2015. Atoxigenic *Aspergillus flavus* biological control of aflatoxin contamination: what is the mechanism? World Mycotoxin Journal 8: 235-244.

Dijksterhuis J. 2007. Heat-resistant ascospores. In: Dijksterhuis J, Samson RA, eds. Food mycology: a multifaceted approach to fungi and food. Boca Raton, FL: CRC Press. p. 101-117.

Dorner JW. 2004. Biological control of aflatoxin contamination in crops. Journal of Toxicology Toxin Reviews 23: 425-450.

Dyer PS, O'Gorman CM. 2012. Sexual development and cryptic sexuality in fungi: insights from *Aspergillus* species. FEMS Microbiology Reviews 36: 165-192.

Ehrlich KC. 2014. Non-aflatoxigenic *Aspergillus flavus* to prevent aflatoxin contamination in crops: advantages and limitations. Frontiers in Microbiology 5: 50.

Fennell DI, Warcup JH. 1959. The ascocarps of *Aspergillus alliaceus*. Mycologia 51: 409-415.

Hedayati MT, Pasqualotto AC, Warn PA, Bowyer P, Denning DW. 2007. *Aspergillus flavus*: human pathogen, allergen and mycotoxin producer. Microbiology 153: 1677-1692.

Horn BW, Gell RM, Singh R, Sorensen RB, Carbone I. 2016. Sexual reproduction in *Aspergillus flavus* sclerotia: acquisition of novel alleles from soil populations and uniparental mitochondrial inheritance. PLoS One 11: e0146169.

Horn BW, Moore GG, Carbone I. 2009. Sexual reproduction in *Aspergillus flavus*. Mycologia 101: 423-429.

Horn BW, Ramirez-Prado JH, Carbone I. 2009. Sexual reproduction and recombination in the aflatoxin-producing fungus *Aspergillus parasiticus*. Fungal Genetics and Biology 46: 169-175.

Horn BW, Sorensen RB, Lamb MC, Sobolev VS, Olarte RA, Worthington CJ, Carbone I. 2014. Sexual reproduction in *Aspergillus flavus* sclerotia naturally produced in corn. Phytopathology 104: 75-85.

Horn BW, Greene RL. 1995. Vegetative compatibility within populations of *Aspergillus flavus*, *A. parasiticus*, and *A. tamarii* from a peanut field. Mycologia 87: 324-332.

Huang C, Jha A, Sweany R, De Robertis C, Damann KEJ. 2011. Intraspecific aflatoxin inhibition in *Aspergillus flavus* is thigmoregulated, independent of vegetative compatibility group and is strain dependent. PLoS One 6: e23470.

Khlangwiset P, Shephard GS, Wu F. 2011. Aflatoxins and growth impairment: a review. Critical Reviews in Toxicology 41:740-755.

Kwon-Chung KJ, Sugui JA. 2009. Sexual reproduction in *Aspergillus* species of medical or economical importance: why so fastidious? Trends in Microbiology 17: 481-487.

Lichius A, Lord KM. 2014. Chemoattractive mechanisms in filamentous fungi. The Open Mycology Journal 8: 28-57.

McAlpin CE, Wicklow DT. 2005. Culture media and sources of nitrogen promoting the formation of stromata and ascocarps in *Petromyces alliaceus* (*Aspergillus* section *Flavi*). Canadian Journal of Microbiology 51: 765-771.

Molo M, Heiniger R, Boerema L, Carbone I. 2019. Trial summary on the comparison of various non-toxigenic strains of *Aspergillus flavus* on mycotoxin levels and yield in maize. Agronomy Journal 111: 942-946.

Ojiambo PS, Battilani P, Cary JW, Blum BH, Carbone I. 2018. Cultural and genetic approaches to manage aflatoxin contamination: recent insights provide opportunities for improved control. Phytopathology 108: 1024-1037.

Olarte RA, Horn BW, Dorner JW, Monacell JT, Singh R, Stone EA, Carbone I. 2012. Effect of sexual recombination on population diversity in aflatoxin production by *Aspergillus flavus* and evidence for cryptic heterokaryosis. Molecular Ecology 21: 1453-1476.

Paulussen C, Hallsworth JE, Álvarez-Pérez S, Nierman WC, Hamill PG, Blain D, Rediers H, Lievens B. 2016. Ecology of aspergillosis: insights into the pathogenic potency of *Aspergillus fumigatus* and some other *Aspergillus* species. Microbial Biotechnology 10: 296-322.

Pommerville J. 1977. Chemotaxis of *Allomyces* gametes. Experimental Cell Research 109: 43-51.

Rajasekaran K, Cary JW, Cotty PJ, Cleveland TE. 2008. Development of a GFP-expressing *Aspergillus flavus* strain to study fungal invasion, colonization, and resistance in cottonseed. Mycopathologia 165:89-97.

Ramirez-Prado JH, Moore GG, Horn BW, Carbone I. 2008. Characterization and population analysis of the mating-type genes in *Aspergillus flavus* and *Aspergillus parasiticus*. Fungal Genetics and Biology 45: 1292-1299.

Raper KB, Fennell DI. 1965. The Genus *Aspergillus*. Baltimore: The Williams & Wilkins Co. p. 1-686.

Read N, Beckett A. 1996. Ascus and ascospore morphogenesis. Mycological Research 100: 1281-1314.

Saleh D, Milazzo J, Adreit H, Tharreau D, Fournier E. 2012. Asexual reproduction induces a rapid and permanent loss of sexual reproduction capacity in the rice fungal pathogen

Magnaporthe oryzae: results of in vitro experimental evolution assays. BMC Evolutionary Biology 12:42.

Saupe SJ. 2000. Molecular genetics of heterokaryon incompatibility in filamentous ascomycetes. Microbiology and Molecular Biology Reviews 64: 489-502.

Szewczyk E, Chiang YM, Oakley CE, Davidson AD, Wang CC, Oakley BR. 2008. Identification and characterization of the asperthecin gene cluster of *Aspergillus nidulans*. Applied and Environmental Microbiology 74: 7607-7612.

Wild CP, Miller JD, Groopman JD, eds. 2015. Mycotoxin control in low- and middle-income countries. IARC Working Group Reports, No. 9. Lyon, France.

Wild CP. 2007. Aflatoxin exposure in developing countries: the critical interface of agriculture and health. Food and Nutrition Bulletin 28: S380.

Willetts HJ. 1997. Morphology, development and evolution of stromata/sclerotia and macroconidia of the Sclerotiniaceae. Mycological Research 101: 939-952.

Wu C, Kimbrough JW. 1990. Ultrastructural studies on the cleistothecial development of *Emericellopsis microspora* (Eurotiales, Ascomycetes). Canadian Journal of Botany 68: 1877-1888.

Table 2.1. Fertility of crosses between fungal strains belonging to opposite mating types used to characterize morphological changes during sexual reproduction in *A. flavus*.

Sclerotium-producing strain[a]			Conidium-producing strain[a]			No. of sclerotia examined	No. of stromata fertilized[c]	Fertility (%)[d,e]	Fertility designation
MAT1-1[b]	*MAT1-2*[b]	VCG[c]	*MAT1-1*[b]	*MAT1-2*[b]	VCG[c]				
29507	–	33	–	21882	24	300	247 ± 13	82.3 ± 4.4	High
–	21882	24	29507	–	33	300	7 ± 2	2.3 ± 0.7	Low
29507	–	33	–	–	–	300	0	0	–

[a] NRRL strain number is from USDA Agricultural Research Service Culture Collection, Peoria, IL.

[b] Mating type is designated as described by Ramirez-Prado et al. (2008).

[c] Vegetative compatibility group.

[d] Values are means ± standard deviation based on three replications.

[e] Proportion of total number of sclerotia and stromata examined with ascospore-bearing ascocarps. A stroma was considered fertile if at least one ascospore-bearing ascocarp was present within its matrix.

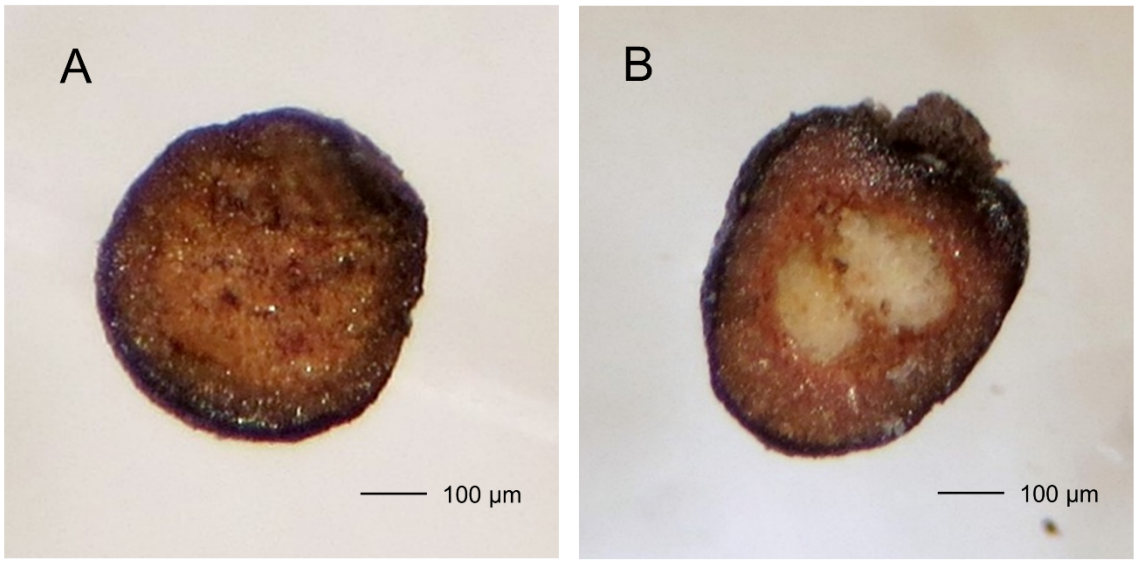

Figure 2.1. A. Unmated sclerotium of *A. flavus* strain NRRL 29507. B. Fertilized stroma of *A. flavus* strain NRRL 29507. Successful fertilization of a sclerotium by conidia from a strain of an opposite mating type is evidenced by the formation of ascocarp(s) within the stromal matrix. Image B shows two ascocarps as observed under a dissecting stereomicroscope (45X magnification). Scale bar = 100 µm.

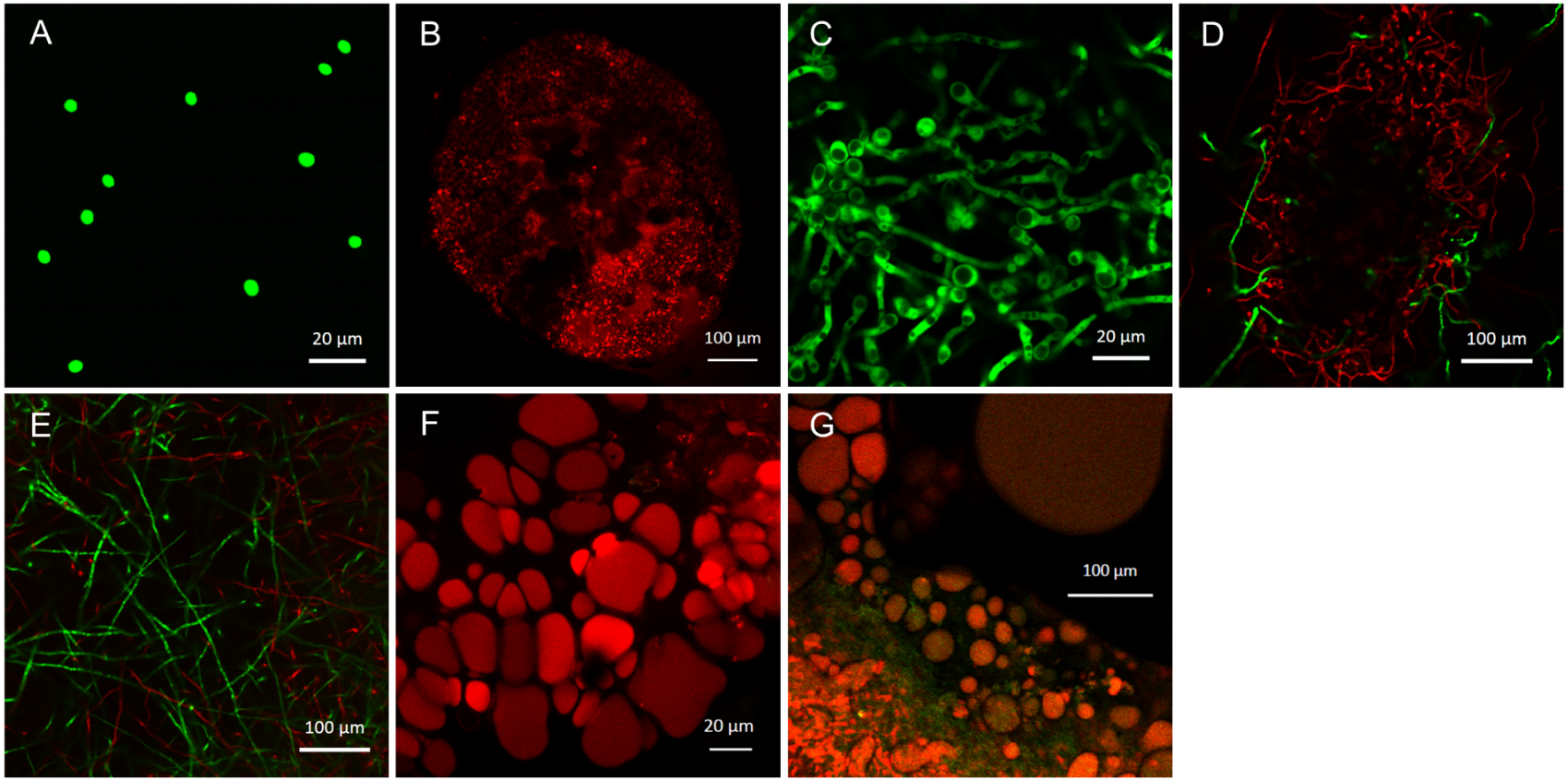

Figure 2.2. Confocal images (10X to 40X) showing the different phases of interaction between conidia (NRRL 21882) and sclerotia (NRRL 29507) of sexually compatible strains of *A. flavus*. A. Conidia of eGFP-labeled NRRL 21882 *(A. flavus* 1534-eGFP) at the time of crossing. B. Sclerotium of mCherry-labeled NRRL 29507 (*A. flavus* 1582-mCherry) at the time of crossing. C. Germinated conidia after overnight growth on agar media. D. After 24 hours of incubation, hyphae of the conidial strain were detected at the base and surface of the sclerotium. Hyphae that emerged from the sclerotium of the mCherry strain were also detected in the medium. E. Network of interlocking hyphal strands from both strains as seen at the base of a sclerotium at 72 hours of incubation. F-G: Cells with red fluorescence were observed within the stromal matrix at 5 weeks of incubation. Note the hyphal strands with green fluorescence interspaced within the mCherry stromal matrix in G. Scale bar: A, C, F = 20 µm; B, D-E, G = 100 µm.

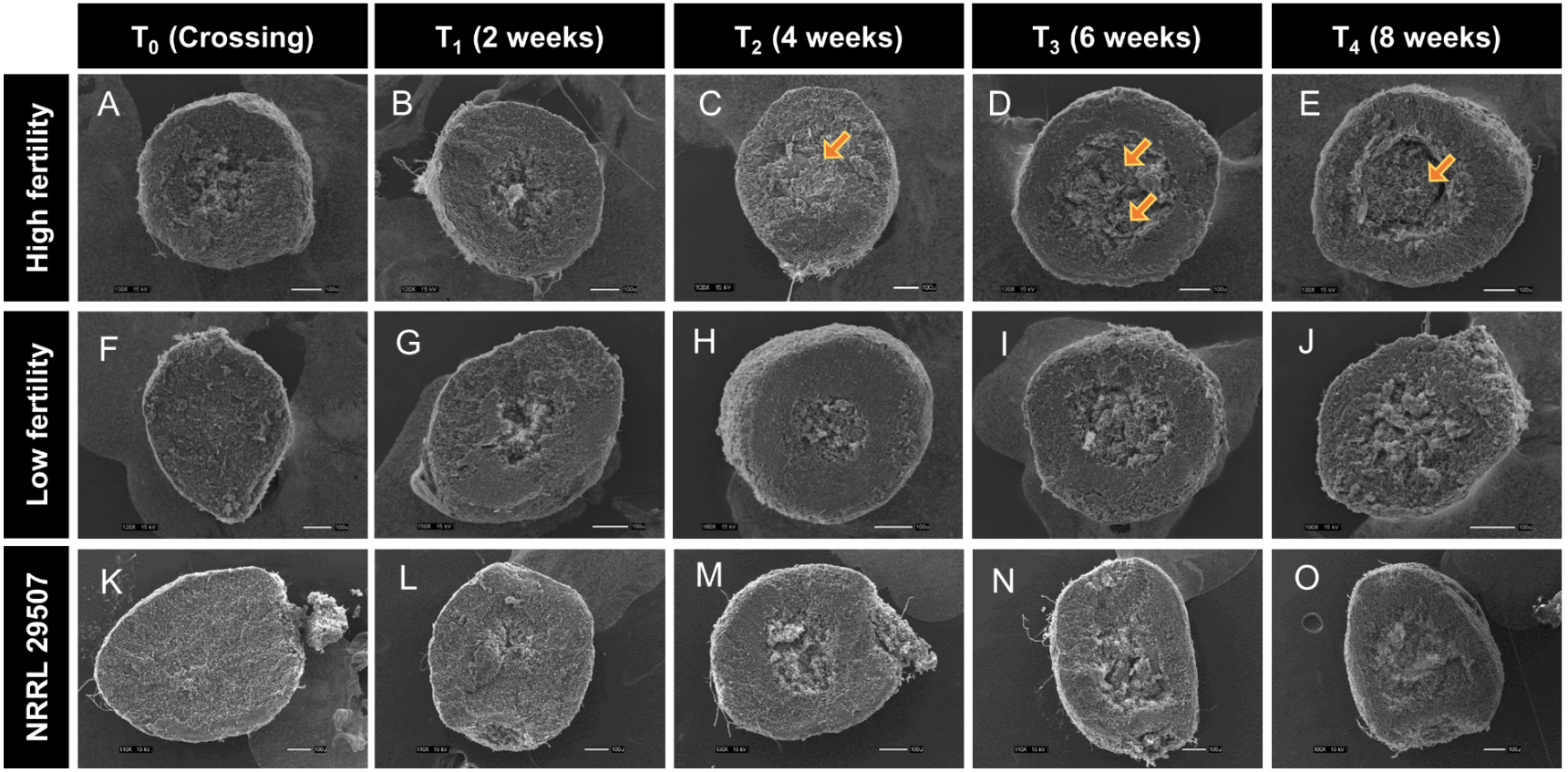

Figure 2.3. Low magnification (90X to 130X) scanning electron micrographs showing morphological changes in the development of fertilized stromata and unmated sclerotia of *A. flavus* strains NRRL 29507 and NRRL 21882 from time of crossing (T_0) until 8 weeks of incubation (T_4). Micrographs show stromata from a high fertility cross (A-E), a low fertility cross (F-J) and unmated sclerotia of NRRL 29507 (K-O). A-B, F-G, K-L. Sclerotial matrix was composed of compact hyphal cells. Some portions of the matrix exhibit loosening and channeling of cells, but no formation of visible sexual structures at the time of crossing until 2 weeks of incubation. C. Arrow shows an ascocarp that formed within the stromal matrix of the high fertility cross at 4 weeks of incubation. The ascocarp wall consists of compact layers of irregularly flattened cells that separates the ascocarp from the stromal matrix. D-E. Arrows point to numerous ascospore-bearing asci inside ascocarps of the high fertility cross at 6 and 8 weeks of incubation. H-J, M-O: Continued loosening and channeling of the sclerotial matrix but no formation of visible sexual structures for the low fertility cross and unmated strain at 4 to 8 weeks of incubation. Scale bar = 100 µm.

Figure 2.4. High magnification (500X to 8500X) scanning electron micrographs showing morphological changes in the development of fertilized stromata and unmated sclerotia of *A. flavus* strains NRRL 29507 and NRRL 21882 from time of crossing (T_0) until 8 weeks of incubation (T_4). Micrographs show stromata from a high fertility cross (A-G), low fertility cross (H-L) and unmated sclerotia of NRRL 29507 (M-Q). A-B, H-I, M-N. Sclerotial matrix was composed of compact hyphal cells. Some portions of the matrix exhibit loosening and channeling of cells, but no formation of visible sexual structures until 2 weeks of incubation. C. Arrows point to internal hyphae detected inside an ascocarp. Tips of these hyphae will later form croziers and develop into ascus mother cells. D-E. Mature asci containing approximately eight ascospores. Ascospores are identified by their characteristic tuberculate ornamentation and are protruding beneath the ascus wall. F-G. Free ascospores (arrows) that have emerged out of their asci. J-L, O-Q. Continued loosening and channeling within the matrix of stromata and sclerotia with no formation of visible sexual structures for the low fertility cross and unmated strain at 4 to 8 weeks of incubation. Scale bar: A-C, H-Q = 10 μm; D-G = 1 μm.

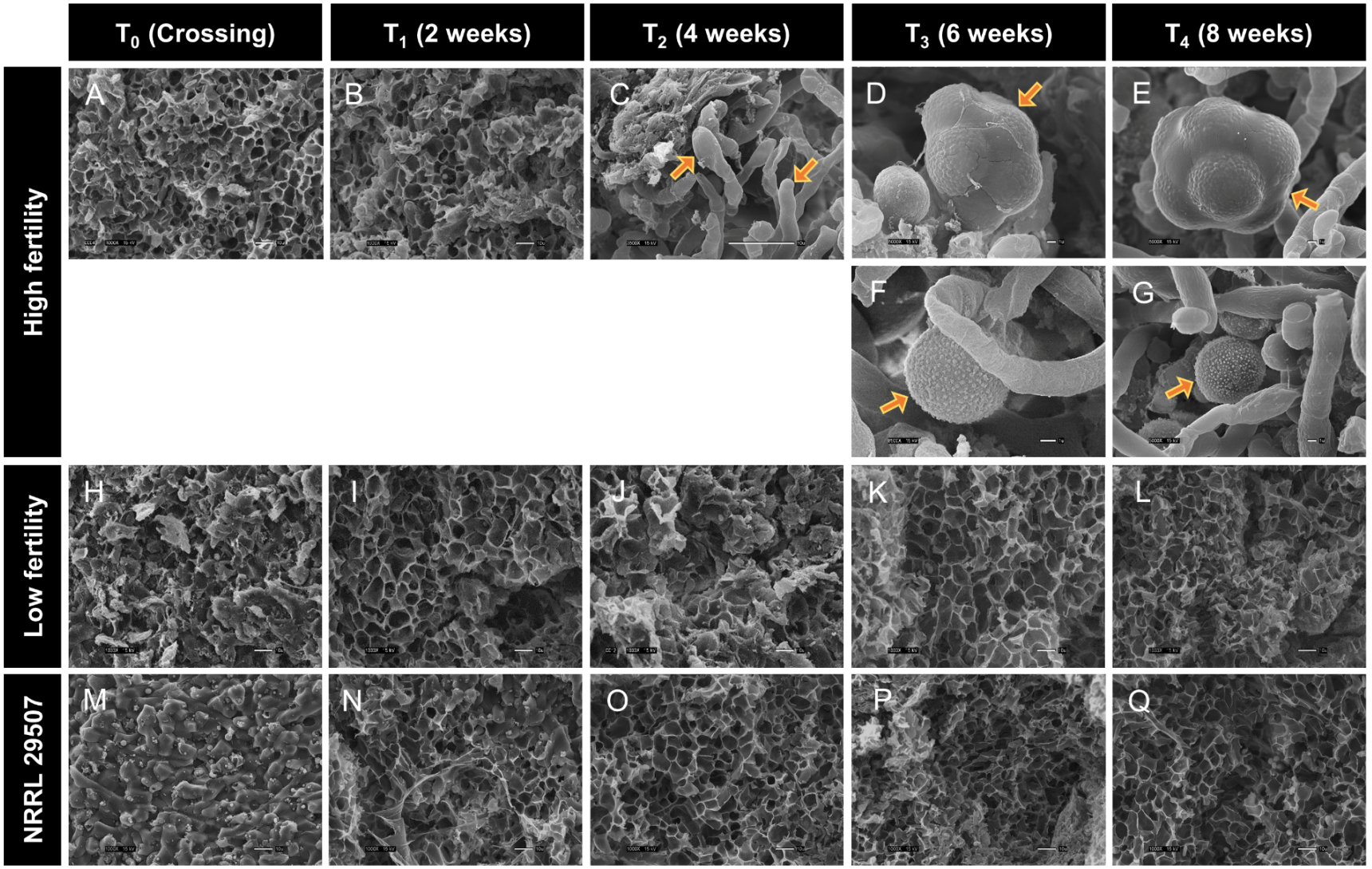
T0 (Crossing)
T1 (2 weeks)
T2 (4 weeks)
T3 (6 weeks)
T4 (8 weeks)
High fertility
Low fertility
NRRL 29507
A
B
C
D
E
F
G
H
I
J
K
L
M
N
O
P
Q

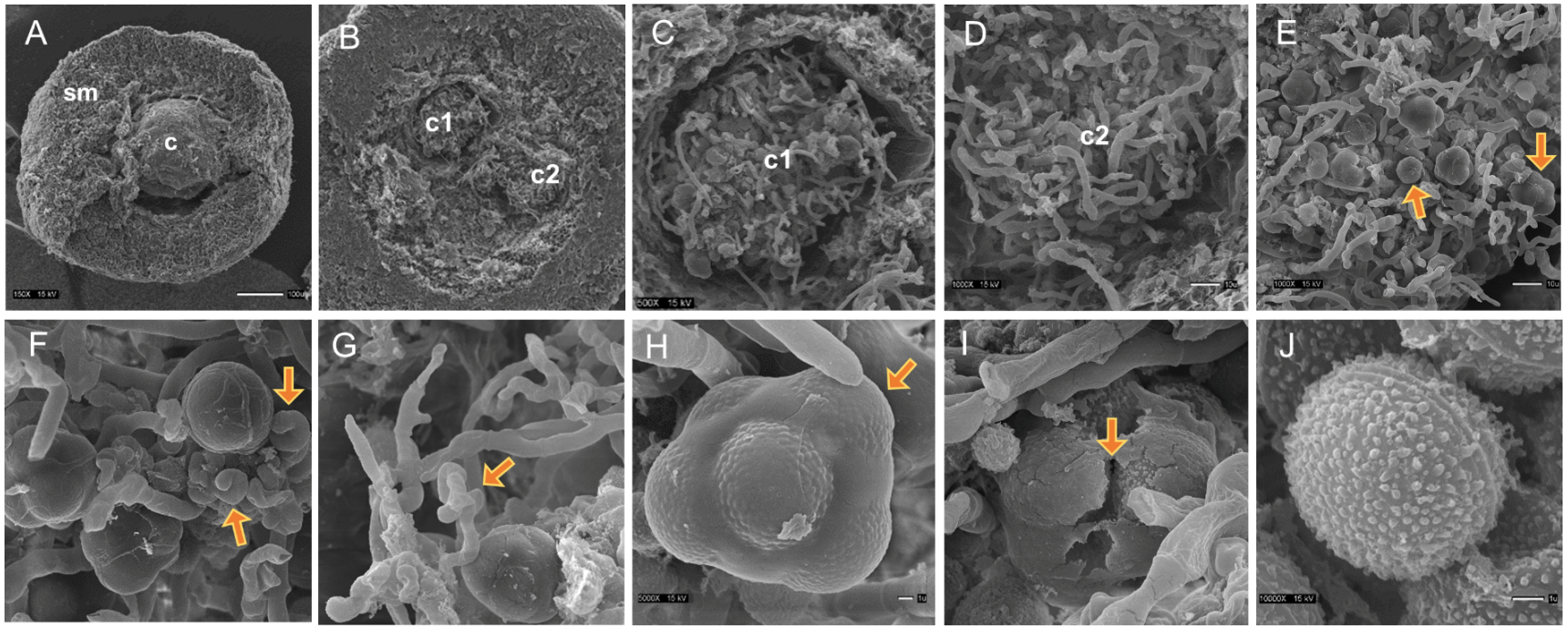

Figure 2.5. Scanning electron micrographs (1000X to 8500X) showing sexual reproductive structures within the stromata of *A. flavus*. A. Ascocarp (c) is enclosed by distinct walls and separated from the stromatal matrix (sm). B-D. Asynchronous development of sexual structures between two ascocarps (c1 and c2) that formed within the same stromatal matrix. Ascospore-bearing structures develop inside c1, while only internal hyphae are detected within c2. E. Asynchronous development of younger and more mature asci developing within the same ascus shown by arrows. F. Hook-tipped croziers shown by arrows. G. Coiling of crozier chains shown by arrow. H. Mature ascus containing approximately eight ascospores. The ascospores are identified by their characteristic finely tuberculate ornamentation (arrow) protruding beneath the ascus wall. I. Ascus wall breaking down to release ascospores. Arrow points to the fissures in the ascus wall where surface ornamentations of the ascospores peek out beneath the ascus wall. J: A mature ascospore with fine tuberculation and an equatorial ridge. Scale bar: A = 100 µm; D-E = 10 µm; H, J = 1 µm; B–C, F-G, I = image enlarged to show structures.

Table S2.1. Oligonucleotide primers used in the construction of the gpd-GFP-trpC, gpd-mCherry-trpC and *ptrA* resistance gene PCR products.

Primer designation	Oligonucleotide sequence (5′-3′)[a]
ptrA resistance gene	
ptrA-F	ACGGGATCCCATTGGTAAC
ptrA-R	GCCGCTCTTGCATCTTTG
gpd-GFP-trpC PCR	
gpd outside-F	CTTCCGGCTCGTATGTTGTGTGG
gpd (egfp)-R	gctcctcgcccttgctcaccatggtgCTGCTCAAGCGGGGTAGCTGTTA
egfp (gpd)-F	actaacagctaccccgcttgagcagCACCATGGTGAGCAAGGGCGAGG
egfp (trpC)-R	tgatttcagtaacgttaagtggatcGAGCTCGCTTTACTTGTACAGCTCGTC
trpC (egfp)-F	cgagctgtacaagtaaagcgagctcGATCCACTTAACGTTACTGAAATCATCAAACAG
trpC outside-R	GTTGGGTAACGCCAGGGTTTTCC
gpd nest-F	AGCTTGAATTCCCTTGTATCTCTACAC
trpC nest-R	ACCGTTACTAGGTTGCAGTCAATGC
gpd-mCherry-trpC PCR	
gpd-F2	CACTCATTAGGCACCCCAGG
gpd (mCherry)-R	cttcgcccttgctgaccatGCCTGCTCAAGCGGGGTAG
mCherry (gpd)-F	ctaccccgcttgagcaggcATGGTCAGCAAGGGCGAAG
mCherry (trpC)-R	tcagtaacgttaagtggatcTCACTTGTACAGCTCGTCCA
trpC (mCherry)-F	tggacgagctgtacaagtgaGATCCACTTAACGTTACTGA
trpC outside-R1	TGAATTCGAGCTCGGTACCG
gpd nest-F1	TCTTGCATCGTCCCAAAGCT
trpC nest-R	ACCGTTACTAGGTTGCAGTCA

[a] Lower case letters represent sequence overlaps with either the *gpd* promoter, reporter gene or *trpC* transcriptional terminator regions.

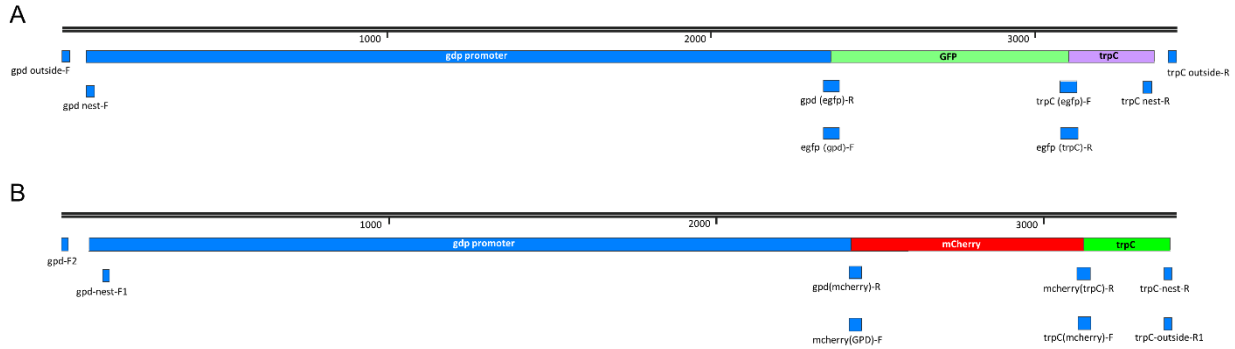

Figure S2.1. Physical map of *A. flavus* 1534-eGFP and *A. flavus* 1582-mCherry constructs.

CHAPTER 3

Female fertility influences metabolomic and transcriptomic profiles during sexual reproduction in *Aspergillus flavus*

To be submitted to *Fungal Genetics and Biology*

Jane Marian Luis[a], Ignazio Carbone[a], Gary A. Payne[a], Deepak Bhatnagar[b], Matthew D. Lebar[b], Jeffrey W. Cary[b], Geromy G. Moore[b], and Peter S. Ojiambo[a]

[a] Center for Integrated Fungal Research, Department of Entomology and Plant Pathology, North Carolina State University, Raleigh, NC 27695

[b] USDA-ARS Southern Regional Research Center, New Orleans, LA 70124

ABSTRACT

Female fertility, the capability of a strain to produce ascocarps in which meiosis occurs, influences morphological changes in the stromata during sexual reproduction in *Aspergillus flavus*. Although sclerotial morphogenesis has been genetically linked to biosynthesis of secondary metabolites (SMs), metabolomic and transcriptomic profiles that occur in the stromata during sexual development in *A. flavus* are not known. Reciprocal crosses with different (i.e., low vs. high) levels of female fertility and unmated sclerotia were grown in mixed cereal agar and incubated at 30°C in continuous dark. Samples were harvested immediately after crosses were made and every 2 weeks until 8 weeks of incubation then subjected to targeted metabolomics and transcriptomic analyses. Aflatoxin B_1 (AFB_1) exhibited reversed expression patterns between samples from the high fertility cross and unmated sclerotia, while AFB_1 consistently remained low in samples from the low fertility cross. Seventeen additional SMs were detected and principal component analysis distinguished these SMs based on female fertility and SM abundance at specific time-points during stromatal development. Hierarchical cluster analysis showed elevated abundance of hydroxyaflavazole, an indole diterpene isomer, and an aflavinine isomer in samples from the high fertility at 4 to 8 weeks of incubation, which coincided with formation of ascocarps, asci and ascospores in our previous study. Transcriptional analysis identified 5,485 genes that were differentially expressed between low and high fertility crosses in at least one time-point. Among these genes, those that are associated with catalytic activity, binding, transporter activity, cellular components, metabolic process, cellular process, localization, and biological regulation were upregulated in samples of the high fertility cross. The genes *brlA*, *chiB*, *gprD*, *ppoC*, and *rodA*, which are involved in the growth and development of *Aspergillus*, were upregulated in the high fertility cross at 4 or 6 weeks of incubation. Further, eight backbone genes that encoded core

biosynthetic enzymes in the 56 predicted *A. flavus* secondary metabolism gene clusters were upregulated at 4 or 6 weeks of incubation in samples from the high fertility cross. Results of this study broaden our knowledge of the biochemical processes that occur when sclerotia transforms to stromata and provide a foundation for further exploration of the biochemical mechanisms underlying sexual development in *A. flavus*.

Keywords: fertilization, metabolome, sexual development, sclerotia, stromata, transcriptome

1. Introduction

Aspergillus flavus (teleomorph: *Petromcyes flavus*) is a filamentous ascomycete found on a range of substrates and in diverse ecological habitats (Klich et al., 1992; Scheidegger and Payne, 2003). The fungus spends a large portion of its life cycle as a soil saprophyte where it decomposes dead or decaying organic matter (Abbas et al., 2009; Chang et al., 2014). Under conducive temperature and moisture conditions, *A. flavus* can become an opportunistic pathogen of important agricultural crops including maize (Payne and Widstrom, 1992; Taubenhaus, 1920), peanuts (Mahmoud, 2015; Pettit, 1984), cottonseed and cotton bolls (Goynes and Lee, 1989; Marsh et al., 1955), and tree nuts (Bayman et al., 2002), contaminating harvested produce with aflatoxins. Aflatoxins are hepatotoxic and immunosuppressive compounds and have been associated with adverse health risks following exposure to humans and livestock (Kumar et al., 2016). The fungus can also directly infect livestock (Seyedmousavi et al., 2015) and humans with compromised immune system (Hedayati et al., 2007). Aflatoxin contamination, thus, poses significant food safety and food security risk particularly in developing countries where these crops are important food crops and are also a major contributor to the economies of these developing countries (Ojiambo et al., 2018).

The fungus reproduces primarily asexually through repeated cycles of conidia production, germination, hyphal growth and conidiophore formation (Ojiambo et al., 2018). Adverse environmental conditions such as lack of adequate water or nutrients trigger many strains of *A. flavus* to produce specialized survival structures known as sclerotia (Chang et al., 2014). Sclerotia are compact, thick-walled aggregates of hyphal cells that assume globose to subglobose shapes when mature (Chang et al., 2002; Raper and Fennell, 1965). Upon germination, the sclerotia of *A. flavus* can give rise to aerial conidiophores and asexual conidia (Wicklow and Donahue, 1984).

However, the fungus can also reproduce sexually when sclerotia are fertilized by conidia of a strain belonging to the opposite mating type (i.e. *MAT1-1* sclerotia is fertilized by *MAT1-2* conidia, and vice versa) (Horn et al., 2016; Ojiambo et al., 2018). In *A. flavus*, the conidium and sclerotium perform parental functions during fertilization, whereby the conidium functions as male which fertilizes the sclerotium, while the sclerotium functions as female and provides nutrients and bears sexual reproductive structures (Horn et al., 2016). A successfully fertilized sclerotium transforms into a stroma and forms up to eight indehiscent ascospore-bearing ascocarps embedded within the stromatal matrix (Horn et al., 2009). In the presence of compatible strains, the degree of fertility or sterility is dictated by the parental source of conidium and sclerotium (Horn et al., 2016).

In silico analysis of the *A. flavus* genome predicts that the fungus contains 56 secondary metabolite (SM) gene clusters (Ehrlich and Mack, 2014; Georgianna et al., 2010). Each cluster contains core backbone genes embedded within the cluster that likely modify the final SM product. Many of these SMs remain uncharacterized and the fungus has the capacity to synthesize even a higher number of SMs (Amare and Keller, 2014). Indeed, *A. flavus* has been reported to produce a wide range of SMs during its growth and development (Georgianna et al., 2010; Vadlapudi et al., 2017). To date, 38 SMs, many of which are known to be toxins and include aflatoxins, are produced by *A. flavus* in culture (Cary et al., 2018). Secondary metabolites are small molecules that are chemically transformed during metabolism and provide a functional readout of the status of a cell (Bhatnagar, 2012; Cary et al., 2018). These SMs serve essential biological roles for the producing fungus, including insect attractants or deterrents, alleviation of abiotic stress, developmental regulators, and chemical signals for communication with other organisms (Cary et al., 2018). Thus, these metabolites serve as direct signatures of biochemical activity and can be correlated to a phenotype of interest since their levels are sensitive to changes in both metabolic

fluxes and enzyme activity (Chubukov et al., 2014). In this regard, mass-spectrometry (MS)-metabolite profiling (or metabolomics) provides a powerful approach to evaluate cellular physiology at any given period.

Sclerotia production and morphogenesis in *A. flavus* has been linked to changes in aflatoxin and various SM biosynthesis (Chang et al., 2002; Wu et al., 2014). The transition from sclerotia to stroma during sexual reproduction may, thus, affect the quantity and diversity of SMs produced by the fungus during this period. To the best of our knowledge, there is very limited information on production of SMs and transcriptional changes during fertilization in *A. flavus*. Further, in our recent study (Luis et al., 2017), the fertility of the sclerotium-producing female strain influenced morphological changes in the stroma following fertilization by conidia from a compatible strain. Thus, we hypothesize that female fertility will influence the metabolic and transcriptional profiles during sexual reproduction in *A. flavus*. In this case, targeted metabolomics can be used to explore the dynamics of metabolite changes during sexual development in *A. flavus*, while transcriptomic analysis can facilitate identification of associated genes. An understanding of these processes may provide a foundation for further exploration of the biochemical mechanism underlying sexual reproduction in *A. flavus*. In addition, results from such studies could be useful in identifying additional biological strategies to manage aflatoxigenic strains of *A. flavus* and/or design novel biocontrol strategies (Bhatnagar, 2012).

In this study, differential analyses of the *A. flavus* metabolome were combined with targeted gene expression analysis and transcriptional profiling to examine how differences in female fertility affect metabolomic processes that occur during sexual reproduction in *A. flavus*. Here, we characterized and established how female fertility affects SMs produced during sexual

reproduction in *A. flavus* and determine differential gene expression between reciprocal crosses of compatible strains that have different levels of female fertility.

2. Materials and Methods

2.1. Fungal strains and fertility of reciprocal crosses

Two *A. flavus* strains, NRRL 29507 and NRRL 21882, were used as parental strains in this study. Strain NRRL 29507, which was originally isolated from a peanut field in Georgia (Horn and Green, 1995), is aflatoxigenic and has the mating type *MAT1-1*. Strain NRRL 21882 which is the active ingredient in the biocontrol product Afla-Guard® (Dorner, 2004) was originally isolated from Georgia and has mating type *MAT1-2*. The vegetative compatibility group (VCG) of NRRL 29507 is VCG 33, while that of NRRL 21882 is VCG 24 (Horn and Green, 1995).

Conidia and sclerotia of these two strains were produced as described below and used in crosses to establish the degree of female fertility. In the first cross, strain NRRL 29507 was used as the sclerotium-producing female parent, while NRRL 21882 was used as the conidium-producing male parent. In a reciprocal cross, strain NRRL 21882 was used as the sclerotium-producing female parent, while NRRL 29507 was used as the sclerotium-producing male parent. Unmated sclerotia of NRRL 29507 were included as a control. Crosses were made by overlaying the sclerotia onto the surface of mixed cereal agar (MCA) plates containing the conidia of the opposite mating type and incubating the culture plates at 30°C under continuous darkness. After 8 weeks, sclerotia and stromata (n = 300) from the unmated strain and reciprocal crosses were manually sectioned in half with a micro-scalpel under a dissecting microscope and examined for the presence of ascocarps. Fertility was calculated as the proportion of stromata with visible ascocarps and expressing the result as a percentage.

2.2. Sclerotia production for omics analysis

Parental strains of NRRL 29507 and NRRL 21882 were separately grown in MCA (McAlpin and Wicklow, 2005) and incubated at 30°C in darkness for 14 days (Horn et al., 2016). Conidia and sclerotia from each culture of the parental strains were harvested individually. Dry conidia were suspended with 3 ml distilled water containing 0.01% Triton-X. The resultant conidial suspension was adjusted to 5×10^5 conidia/ml and 20 µl aliquots were spread onto new MCA plates. Sclerotia were carefully detached from the agar by adding distilled water containing 0.01% Triton-X and gently scraping the surface with a transfer loop. The sclerotia were transferred to 50 ml tubes, washed with distilled water (for SM extraction) or DEPC-treated water (for RNA extraction) through repeated vortexing and decanting to remove residual conidia then filtered through a Mira cloth. Crosses between the two strains were made by overlaying the sclerotia of the female strain onto the surface of MCA plates containing the conidia of the opposite mating type male strain. Sclerotia of unmated NRRL 29507 strain were transferred to new MCA plates but with no conidia of NRRL 21882. The culture plates were sealed with parafilm, enclosed in ziplock bags to prevent desiccation, and incubated at 30°C in darkness. Stromata from the two crosses and sclerotia from the unmated strain were subsequently harvested as described above at various time-points: at the time of crossing (T_0) and at 2 weeks (T_1), 4 weeks (T_2), 6 weeks (T_3), and 8 weeks (T_4) of incubation. Harvested stromata and sclerotia were flash frozen in liquid nitrogen then stored at -80°C until used for SM and RNA extractions as described below.

2.3. Extraction and analysis of secondary metabolites

Harvested stromata and sclerotia from the two crosses and unmated strain at each time-point were added with 1 ml Milli-Q water, frozen and lyophilized. Samples (i.e. sclerotia and

stromata) from a single culture plate were considered as a replicate and samples from three plates (n = 3) were processed individually at each time-point. Lyophilized samples were extracted with 1 ml ethyl acetate containing 0.1% formic acid for 24 h at room temperature on a shaker at 150 rpm. Extraction was performed two times and extracts were concentrated *in vacuo*. Filtered extracts were then combined and concentrated under nitrogen. Dried extracts were dissolved in methanol at 5 mg/ml and centrifuged at 14000 × g to remove insoluble material prior to analysis using ultra-performance liquid chromatography (UPLC) described below.

Analysis of SMs in the extracts was conducted on a Waters ACQUITY UPLC system using photo diode array (PDA) UV and QDA mass detection using the following conditions: 0.26 ml/min, solvent A (0.1% formic acid in water); solvent B (0.1% formic acid in acetonitrile); 5% B (0 - 2.5 min), gradient to 25% B (2.5 - 3.0 min), gradient to 100% B (3.0 - 10.0 min), 100% B (10.0 - 15.0 min), then column equilibration 5% B (15.1 - 20.1 min). To prepare the extract for analysis, 1 g of the extract was dissolved in 9 ml of 50:50 (v/v) acetonitrile/water. The resulting mixture was sonicated for 20 min and syringe filtered into an autosampler vial using a 0.2 μm PVDF filter. The flow rate of liquid chromatography for ACQUITY system was 0.8 ml/min. Resultant peaks were identified using authentic analytical standards. Aflatoxin B_1 (AFB_1), cyclopiazonic acid (CPA) and ergosterol standards were purchased from Sigma-Aldrich (St. Louis, MO, United States). Aflavinine, aflavarin, aflavazole, and aflatrem standards were kindly provided by Dr. James Gloer, University of Iowa, Iowa City, IA, United States. Empower 3 chromatography software was used for data acquisition and processing.

The abundance of the remaining SMs detected by the UPLC System in harvested samples was quantified by comparing the area of their peaks to standard calibration curves. Relative abundance values were subsequently obtained by normalizing raw peak area values based on yield

of lyophilized sclerotia or stromata (mg/ml) used for extraction of SMs. To reduce non-normality and large gaps among values, the relative abundance values were square-root transformed for further analysis. AFB_1 levels in samples from both crosses and unmated strain (i.e., treatments) were subjected to analysis of variance using PROC ANOVA in SAS 9.4 (SAS Institute, Cary, NC). Differences in AFB_1 levels within treatments at each time-point were estimated using Tukey's studentized range test at $\alpha = 0.05$. Further, multivariate statistical analysis was conducted using JMP Pro 14 (SAS Institute Inc.) by principal component analysis (PCA) on normalized peak values of all SMs except AFB_1 to visually demonstrate the variance of metabolic phenotypes based on fertility and sampling time-point. Hierarchical cluster analysis of SMs was also performed to reveal associations between replicate biological samples within a group based on the similarity of their relative abundance profiles.

2.4. RNA extraction, library construction and Illumina sequencing

Harvested samples from the low and high fertility crosses were homogenized to a powder using chilled mortar and pestle and extracted using RNeasy Plant Mini Kit (Qiagen, Hilden, Germany) according to the manufacturer's instruction. Illumina RNA library construction and sequencing were conducted by the North Carolina State Genomic Sciences Laboratory (Raleigh, NC, USA). Prior to library construction, RNA integrity, purity, and concentration were assessed using an Agilent 2100 Bioanalyzer with an RNA 6000 Nano Chip (Agilent Technologies, USA). Purification of messenger RNA (mRNA) was performed using the oligo-dT beads provided in the NEBNExt Poly(A) mRNA Magnetic Isolation Module (New England Biolabs, USA). Complementary DNA (cDNA) libraries for Illumina sequencing were constructed using the NEBNext Ultra Directional RNA Library Prep Kit (NEB) and NEBNext Multiplex Oligos for

Illumina (NEB) using the manufacturer-specified protocol. Briefly, the mRNA was chemically fragmented and primed with random oligos for first strand cDNA synthesis. Second strand cDNA synthesis was then carried out with dUTPs to preserve strand orientation information. Double-stranded cDNA was then purified, end repaired and "a-tailed" for adaptor ligation. Following ligation, the samples were selected for a final library size of 400-550 bp (including adapters) using sequential AMPure XP bead isolation (Beckman Coulter, USA). Library enrichment was performed and specific indices for each sample were added during the protocol-specified PCR amplification. The amplified library fragments were purified and checked for quality and final concentration using an Agilent 2200 Tapestation (Agilent Technologies, USA). The final quantified libraries were pooled in equimolar amounts for clustering and sequencing on an Illumina HiSeq 2500 DNA sequencer (5 lanes, 16 samples per lane), utilizing a 125 bp single end sequencing reagent kit (Illumina, USA). The software package Real Time Analysis (RTA) was used to generate raw BCL (base call files) which were then de-multiplexed by sample into FASTQ files.

2.5. Transcriptomic analysis

Raw sequencing reads for each sample were analyzed using the Cyberinfrastructure for Data Management and Analysis or Cyverse which was formerly known as iPlant Collaborative (Merchant et al., 2016). The quality of reads was checked using FastQC v0.2 (Andrews, 2010) and adapter sequences were removed using Trimmomatic v0.33 (Bolger et al., 2014). Filtered reads were aligned to the *A. flavus* NRRL 3357 genome (GCF_00006275_JCVI-afl1-v2.0) using Tophat2 v2.1.1 (Trapnell et al., 2012). Mapped reads were assembled into transcripts using Cufflinks2 v2.1.1 1 (Trapnell et al., 2012), merged using Cuffmerge2 v2.1.1 (Trapnell et al., 2012),

then gene expression levels between fertility levels and time-points were analyzed as time-series using Cuffdiff2 v2.2.1 (Trapnell et al. 2013). Transcript levels represented as fragments per kilobase of transcript per million mapped reads (FPKM) and *K*-means clustering were visualized using cummerbund v2.22 (Trapnell et al., 2014; Goff et al., 2018) in R v3.5.1 (R Core Team, 2013). *K*-means clustering assembles the list of sequences into clusters such that sequences in the same cluster share high similarity, while the resemblance among sequences in different clusters is low (Ajayan et al., 2015). A gene was considered differentially expressed when $\log_2$(fold_change) $\geq |1|$ with an adjusted *P*-value ≤ 0.05. Gene ontology (GO) terms for molecular function, cellular component and biological process for differentially expressed genes were generated using PANTHER 14.1 (http://www.pantherdb.org/) (Thomas et al., 2003). Since *A. flavus* is not listed as a reference organism in the PANTHER database, AFLA and XLOC gene annotations for *A. flavus* were first converted to CB gene annotations of *A. nidulans* (teleomorph: *Emericella nidulans*) using the BLASTp and BLASTx options in NCBI BLAST tool (http://blast.ncbi.nlm.nih.gov/Blast.cgi). The converted list of gene names were then entered in PANTHER and analyzed using *Emericella nidulans* as the selected organism. Venn diagram was created using Venny v2.1 (http://bioinfogp.cnb.csic.es/tools/venny/index.html) (Oliveros, 2015) to visualize genes that are unique and/or shared between the low and high fertility crosses.

3. Results

3.1. Fertility of reciprocal crosses

Fertility of the reciprocal crosses varied depending on the strain used as the female or male parent (Table 3.1). When strain NRRL 21882 was used as the sclerotium-producing female parent and NRRL 29507 was used as the conidium-producing male parent, 7 of the 300 stromata

examined were fertile. On the other hand, 247 of the 300 examined stromata were fertile when strain NRRL 29507 was used as the sclerotium-producing female parent and NRRL 21882 was used as the conidium-producing male parent (Table 3.1). The proportion of fertilized stromata when NRRL 29507 was used as the female parent (82.3%) was significantly ($P < 0.05$) higher than the proportion of fertilized stromata when NRRL 21882 was used as the female parent (2.3%). No ascocarp was detected from the sclerotia of the unmated strain (Table 3.1). The cross with NRRL 29507 as the female parent was designated as a high fertility cross, while the reciprocal cross with NRRL 21882 as the female parent was designated as a low fertility cross (Table 3.1).

3.2. Aflatoxin analysis

Aflatoxin content (AFB_1) in harvested samples varied between treatments and within and between time-points (Table 3.2; Fig. 3.2). High levels of AFB_1 were present in samples from the high fertility cross (mean = 26 ppm) and unmated strain (mean = 31 ppm) but low in samples from the low fertility cross (mean = 2 ppm) (Table 3.2). AFB_1 in samples from the high fertility cross was highest at T_0 (time of crossing) (58 ppm) but then decreased to significantly lower levels (17 to 19 ppm) that did not change from T_1 (2 weeks) to T_4 (8 weeks) (Fig. 3.2). In contrast, levels of AFB_1 in samples from the unmated strain were low at T_0 but increased progressively over time from T_1 (34 ppm) to T_4 (49 ppm). Levels of AFB_1 in samples from the low fertility cross were relatively low and increased marginally to 2-3 ppm between T_1 and T_4 (Fig. 3.2). At the end of the sampling period (T_4), levels of AFB_1 were significantly higher ($P < 0.05$) in samples from the unmated strain than from either of the low or high fertility cross (Table 3.2).

3.3. Other secondary metabolites detected

Besides AFB_1, 17 other SMs were detected in sclerotia and stromata sampled during this study (Table 3.3). Aflavarin, hydroxyaflavinine, aflatrem isomers 1 and 2, and IDT-Z were the most abundant SMs, while aflatrem isomer 3, hydroxyaflavazole and sterol analog were the least abundant (Table 3.3). Significant ($P < 0.05$) differences in the relative abundance of most of these SMs were also observed among stromata from reciprocal crosses and unmated sclerotia except for aflavarin, aflatrem isomer 1 and 2, and ergosterol (Table 3.3).

Six SMs namely aflavarin, hydroxyaflavinine, aflavazole, aflatrem isomer 1, aflatrem isomer 2, and ergosterol, were detected in stromata from both crosses and in unmated sclerotia (Table 3.3). The SMs aflatrem isomer 3, aflavinine, cyclopiazonic acid (CPA), and IDT-Z were detected only in samples from the high fertility cross and unmated strain, while aflavarin isomer and sterol analog were detected only in samples from both low and high fertility (Table 3.3). The SMs leporin and kotanin A were only detected in samples from the low fertility cross, while hydroxyaflavazole, IDT-C, and an aflavarin isomer were detected only in the high fertility cross (Table 3.3).

3.4. Multivariate analysis of secondary metabolites

Principal component analysis revealed clear discrimination and clustering of SMs based on either a combination of female fertility and time-point (Fig. 3.2A), their relative abundance in test samples (Fig. 3.2B), or level of female fertility (Fig. 3.2C). Limited discrimination was observed when SMs were grouped based on time-point alone (Fig. 3.2D). In this first case, the PCA score plot accounted for 74% of the total variability and clustered the samples in three distinct groups (Fig. 3.2A), where Component 1 accounted for 52% of the total variance and Component

2 accounted for 22%. The group of samples from the high fertility cross was clearly discriminated from those of either unmated sclerotia or low fertility cross at all time-points (Fig. 3.2A). The PCA score plot generated based on the relative abundance of the 17 SMs accounted for 74% of the total variability (Fig. 3.2B). Clustering of SMs were observed, with one group comprising of SMs that were present in samples from the low fertility cross (leporin and kotanin A), and those present only in samples from the high fertility cross (hydroxyaflavazole, IDT-C, aflavinine isomer) (Fig. 3.2B). When the SMs were analyzed based on the fertility of samples, the PCA score plot accounted for 96.6% of the total variance with two distinct groups of SMs consisting of low fertility cross samples and of high fertility cross and unmated strain samples (Fig. 3.2C).

Hierarchical cluster analysis grouped abundance of SMs into two main groups; the low fertility cross group, and group of high fertility cross and unmated strain (Fig. 3.3). Aflavarin was the most abundant SM across all treatments and time-points especially in samples from the low fertility cross, while IDT-Z was the most abundant in samples from the high fertility cross and unmated strain (Fig. 3.3). Leporin and kotanin A were only produced in samples from the low fertility cross. On the other hand, hydroxyaflavazole, IDT-C and aflavinine isomer were only produced in samples from the high fertility cross and exhibited continued upregulation over time (Fig. 3.3).

3.5. Transcriptomic analysis of differentially expressed genes

A total of 1.23×10^{12} filtered quality reads were generated from 80 libraries composed of eight samples for each of low and high fertility crosses per time-point. Of these, 83% were mapped to the *A. flavus* genome with an average of 12.8×10^{6} filtered quality reads per sample and 102.38×10^{6} reads per time-point. Among the 13,487 genes comprising the *A. flavus* genome, 13,261

genes were detected in the dataset. A global view of 5,485 genes showing differential expression [$\log_2$(fold_change) ≥ |1| and adjusted *P*-value ≤ 0.05] between the low and high fertility crosses in at least one time-point is shown in Fig. 3.4. The dendrogram in the horizontal axis displayed separation of samples into two major clusters corresponding to female fertility levels. Further, there was distinct clustering of samples from the high fertility cross harvested at T_3 and T_4 (Fig. 3.4). An increasing number of differentially expressed genes (DEGs) between low and high fertility crosses were observed over time (Fig. 3.5A). At each time-point, more genes were upregulated than downregulated in the high fertility cross (Fig. 3.5A). The highest number of upregulated genes was observed between T_2 and T_3 in the high fertility cross (Fig. 3.5B), while there was a continuous decrease in the number of upregulated genes in the low fertility cross over time (Fig. 3.5C).

3.6. Gene ontology of differentially expressed genes

Mapping of the *A. flavus* gene annotations to the *A. nidulans* genome yielded 1,476 significant hits that were used for functional analysis in the PANTHER database. Functional categories were defined by Gene ontology (GO) terms, which identified genes as associated with specific molecular function, cellular component, and biological process. Distribution of GO-terms among up- and downregulated DEGs is shown in Fig. 3.6. Significantly enriched DEGs in the high fertility cross were mainly involved in catalytic activity (GO:0003824), binding (GO:0005488), and transporter activity (GO:0005215) (Fig. 3.6). Cellular component GO terms associated with cell (GO:0005623), membrane (GO:0016020), organelle (GO:0043226), and protein-containing complex (GO:0032991) were also highly enriched in the high fertility cross. Close observation of these GO terms revealed that most of the DEGs were upregulated in the high fertility cross at T_3

(Fig. 3.6). Finally, biological process GO terms associated with metabolic process (GO:0008152), cellular process (GO:0009987), localization (GO:0051179), and biological regulation (GO:0065007) were highly enriched in the high fertility cross. Two proteins associated with reproduction (GO:0000003), namely AFLA_093580 (membrane oxidoreductase *tmpA*, putative) and AFLA_056870 (uncharacterized protein), were also upregulated in the high fertility cross at T_3 (Fig. 3.6).

3.7. K-means clustering

The expression patterns of DEGs between samples from the low and high fertility crosses were classified into 10 clusters (Fig. 3.7A-B). In both fertility crosses, cluster 9 depicted an initial plateau of gene expression at T_0 and T_1, followed by elevated expression at T_2, then slight changes at T_3 and T_4. Among the compared genes, 18 were uniquely expressed in the high fertility cross (Fig. 3.7C). These were composed of ten genes (AFLA_023510, AFLA_110040, AFLA_009110, AFLA_085880, AFLA_089770, AFLA_017220, AFLA_101780, AFLA_007210, AFLA_023520, AFLA_139670) that encode previously characterized proteins in *A. flavus*, and eight genes (AFLA_009870, AFLA_009880, AFLA_089640, AFLA_013600, AFLA_089640, AFLA_099050, AFLA_101380, and XLOC_010320) that encode proteins which are yet to be characterized (Table 3.4).

3.8. Genes involved in development and secondary metabolism gene clusters

The differential expression of 81 previously identified genes involved in the growth and development of *Aspergillus* (Dyer and O'Gorman, 2012; Krijgsheld et al., 2013; Wu et al., 2014) was examined in this study. Among these, five genes consisting of *ppoC* (AFLA_030430), *brlA*

(AFLA_082850), *rodA* (AFLA_098380), *chiB* (AFLA_104680) and *gprD* (AFLA_135680) were upregulated in the high fertility cross but not in the low fertility cross during the later time-points. *GprD* and *ppoC* showed upregulated expression in the high fertility cross at T_2, while *brlA*, *chiB* and *rodA* showed upregulated expression in the high fertility cross at T_3 (Table 3.5).

The differetial expression of 80 previously reported backbone genes involved in 56 secondary metabolite gene clusters predicted in *A. flavus* (Ehrlich and Mack 2014; Georgianna et al 2010) during the progression of sexual reproduction was also examined. Backbone genes for clusters 2 (AFLA_004300) and 7 (AFLA_009140) showed upregulated expression in the high fertility cross at T_2, while backbone genes for clusters 13 (AFLA_038600), 14 (AFLA_041050), 17 (AFLA_053870), 25 (AFLA_070920), 46 (AFLA_118960), and 47 (AFLA_119110) showed upregulated expression at T_3 (Table 3.6).

4. Discussion

Sexual reproduction and development in *A. flavus* is initiated when sclerotia of a female strain is fertilized by conidia of a compatible conidium-producing male strain leading to the formation of stromata. We recently documented morphological changes that occur in sclerotia and stromata during this period and how female fertility influences this process (Luis et al., 2017). However, there is limited information on how metabolomic and transcriptomic properties are associated with development of sclerotia and/or stromata in *A. flavus.* This study extended our observations on morphological changes in stromata to establish metabolomic and transcriptional changes that occur during sexual development in *A. flavus*. Distinct metabolomic profiles were detected among samples from low and high fertility crosses and unmated strain. Specifically, the SMs hydroxyaflavazole, IDT-C, and aflavinine isomer detected or increased in expression at 4 to

8 weeks incubation of samples from the high fertility cross could be involved in the formation of ascocarps within the stromatal matrix. Further, transcriptomic analyses identified genes that were uniquely expressed in the high fertility cross during later time-points. This study is the first to document how female fertility influences metabolomic and transcriptional profiles in stromata during sexual reproduction and development in *A. flavus*.

Secondary metabolism has been shown to be genetically linked to morphological development in *Aspergillus* species (Calvo and Cary, 2015; Calvo et al., 2002). The close association between these two biological processes provides a window to explore how genetic factors can potentially influence metabolomic and transcriptional properties associated with the development of stromata during sexual reproduction in *A. flavus*. Of the 38 SMs identified to be produced by *A. flavus* in culture (Cary et al., 2018), 18 were detected in the study. Further, distinct SM profiles were observed among samples from the low and high fertility crosses and unmated strain, and the abundance of SMs generally increased with incubation time except for AFB_1 and CPA for samples from the high fertility cross. Although the exact roles of AFB_1 and CPA are not yet established, they have been postulated to provide some benefits to *A. flavus*. Some of the roles of AFB_1 include feeding deterrents against arthropods for resource competition or fungivory (Drott et al., 2018) and remediation from oxidative stress (Fountain et al., 2016; Grintzalis et al., 2014). CPA was shown to be an excellent chelator of iron and suggested to be involved in rapid fungal growth during niche occupation in saprophytic environments (Chang et al. 2009). These benefits partly explain the progressive increase in AFB_1 and CPA in the unmated sclerotia. Accordingly, the unmated sclerotia are probably producing increasing amounts of AFB_1 and CPA over time to function as a defensive mechanism against potential predators and/or alleviate stress in response to nutrient depletion in its environment.

The formation of sexual structures in *Aspergillus* species exerts energy during sexual reproduction (Kwon-Chung and Sugui, 2009). When fertilized, the stroma may be diverting its energy from AFB_1 or CPA production to formation of sexual structures and other SMs necessary to support and maintain fertilization. This partly explains the decrease in the production of AFB_1 and CPA over time observed in samples from the high fertility cross. A similar trade-off between aflatoxin production and morphological development via competition for acetate in the development of ascocarps has been proposed in *A. parasiticus* (Chang et al., 2001). The decreased production of AFB_1 in samples from the high fertility cross with NRRL 29507 (aflatoxigenic) and NRRL 21882 (non-aflatoxigenic) as the parental strains further supports previous reports that a non-aflatoxigenic strain of *A. flavus* has the potential to reduce AFB_1 when crossed with an aflatoxigenic strain through sexual reproduction (Olarte et al., 2012).

AFB_1 production in samples from the low fertility cross was relatively low and only increased marginally to 2-3 ppm between T_1 and T_4. Given that the non-aflatoxigenic NRRL 21882 strain was used as the sclerotium-producing parent in the low fertility cross, the trace amounts of AFB_1 likely originated from the hyphae of the aflatoxigenic conidium-producing parental strain that remained attached to the sclerotia during the washing procedure.

Besides AFB_1, the 17 additional SMs detected in the samples examined in this study also showed different expression profiles according to fertility of crosses. Multivariate analysis showed that 52% of the variation is accounted by the level of fertility with a clear separation between samples from the high fertility cross and unmated strain from those of the low fertility cross. The clustering of SMs in samples from the high fertility cross with those from the unmated strain is primarily due to the source of sclerotium-producing parent that was similar between these two treatments. The nine SMs that were produced either uniquely or in highest concentrations in the

samples from high fertility cross or unmated strain all belonged to the class indole diterpenes (IDTs). IDTs encompass a structurally diverse group of SMs composed of a common cyclic diterpene backbone and an indole group that is most likely derived from indole-3-glycerol phosphate (Saikia et al., 2008) and they seem to be confined to a few ascomycetes including *Aspergillus*, *Claviceps*, *Penicillium* and *Epichloe* (Parker and Scott, 2004). The ability to synthesize IDTs in *Aspergillus* is commonly associated with species that form sclerotia (Parker and Scott, 2004; Frisvad et al., 2019). These IDTs have anti-feedant biological activities against fungivorous insects, and thus they are produced primarily to protect sclerotia from consumption or damage caused by fungivorous insects (Gloer et al. 1988; TePaske et al. 1990; TePaske et al. 1992; Saikia et al. 2008).

One of the major goals of this study was to determine whether production of specific SMs can be linked to the level of female fertility in *A. flavus*. Hydroxyaflavazole, IDT-Z, and aflavinine isomer were uniquely detected in samples from the high fertility cross and only developed or increased in concentration at 4 or 6 weeks of incubation. In our previous study (Luis et al., 2017), morphological differences between unmated sclerotia and stromata became apparent at 4 weeks of incubation during which ascocarps started to develop. Thus, the appearance of these three SMs especially hydroxyaflavazole and aflavinine isomer in samples from the high fertility cross during the later time-points may be associated with the formation of sexual structures in *A. flavus*. While these three SMs are known to exhibit anti-insect activity, the role they could potentially play in the formation of sexual structure is not clear. It is highly possible that this increase in the abundance of these SMs which coincides with formation of sexual structures is simply an evolutionary response designed to enhance the protection of fertilized stromata from damage caused by fungivorous insects thereby ensuring successful dissemination of ascospores into the surrounding

environment. Additional studies are recommended to systematically establish any potential role that hydroxyaflavazole or aflavinine may play in formation of sexual structures in *A. flavus*. Such studies should also utilize different but compatible strains of *A. flavus* to establish consistency of the results reported in this study.

Seven SMs namely, aflavarin, aflatrem isomer 1, leporin, kotanin A, ergesterol, aflavarin isomer, and sterol analog, were either only produced or were most abundant in samples from the low fertility cross. Aflavarin, aflatrem isomer 1, and ergesterol were detected in highest quantities in samples from the low fertility cross but also present in the high fertility cross and unmated strain. Aflavarin and aflatrem isomers have been reported to have anti-insect activity against the fungivorous beetle *Carpophilus hemipterus* (TePaske et al., 1992), while ergosterol is a major component of fungal membranes that is essential for numerous biological functions, including membrane fluidity regulation, activity and distribution of integral proteins and control of the cellular cycle (Alcazar-Fuolia et al., 2008). The aflavarin isomer and sterol analog were detected in samples from both the low and high fertility crosses, while leporin and kotanin A were detected only in samples from the low fertility cross. Leporin and kotanin A have also been detected in other Aspergilli such as *A. leporis* (TePaske et al., 1991), *A. glaucus* (Buechi et al., 1971) and *A. niger* (Hüttel and Müller, 2007). In this study, these two SMs were detected in *A. flavus* NRRL 21882 but not in NRRL 29507. Differences in the profiles of SMs produced by different strains of *Aspergillus* species have been previously reported (Gloer, 1995) and could be related to the natural diversity of complex cocktails of SMs found in different strains of *Aspergillus* species or could be related to differences in aflatoxigenicity between these two strains.

RNA-sequencing is a powerful tool that has been successfully used to interrogate the transcriptomes of numerous fungi (Wang et al., 2015). Here, this technique was used to identify

genes that could be associated with different levels of female fertility in *A. flavus*. A total of 5,485 genes were shown to be differential expressed between samples of the high and fertility crosses in at least one of the five time-points, wherein the number of DEGs between low and high fertility levels increased over time. Further analysis showed that a high number of genes in samples from the high fertility cross were upregulated at T_2 (158 genes) and T_3 (306 genes), suggesting active genetic changes corresponding to morphological changes during these time-points. Among these genes are *cetA* and *calA* involved in conidial germination, hyphal branching and cell wall morphogenesis in *A. nidulans* (Belaish et al., 2008; Greenstein et al., 2005), *tmpA* (function described below), *cdc25* involved in conidiation and regulation of cell size in *Beauveria bassiana* (Qiu et al., 2014), and *sepA* required for septation and actin ring formation in *A. nidulans* (Sharpless and Harris, 2002). In contrast, the number of upregulated genes in samples from the low fertility cross gradually dropped over time.

In silico functional analysis revealed high enrichment of GO terms associated with molecular functions (catalytic activity, binding, and transporter activity), cellular components (cell, membrane, organelle, and protein-containing complex), and biological processes (metabolic process, cellular process, localization, and biological regulation) in samples from the high fertility cross compared to the low fertility cross. Among the biological processes, two proteins associated with the GO term reproduction (AFLA_093580 = membrane oxidoreductase *tmpA*, putative; and, AFLA_056870 = uncharacterized protein) were upregulated at T_3 in samples from the high fertility cross only. *TmpA* has been shown to be involved in regulation of conidiation in *A. nidulans* (Soid-Raggi et al., 2006) and regulation of asexual and sexual development in *A. flavus* (Gilbert et al., 2016). In addition, *K*-means cluster analysis of gene expression patterns revealed 18 genes uniquely expressed in samples from the high fertility cross that exhibited an initial plateau of gene

expression at T_0 and T_1, followed by elevated expression at T_2, then slight changes at T_3 and T_4. This expression pattern mirrors the morphological development of sexual structures within the stromata where no structures were visible within the stromatal matrix at T_0 and T_1, followed by formation of ascocarps at T_2, and development of asci and ascospores at T_3 and T_4 (Luis et al., 2017). Additional studies on these abovementioned genes, especially those encoding uncharacterized proteins, are needed to establish their roles as candidate markers of high fertility and/or indicator of successful fertilization in *A. flavus*.

Five genes previously identified to be involved in growth and development in different *Aspergillus* species, namely *gprD*, *ppoC*, *brlA*, *chiB* and *rodA*, were upregulated in samples from the high fertility cross at T_2 or T_3 but not in the low fertility cross. *GprD* acts as site receptors for active cell wall or cell membrane synthesis and is an essential regulator of hyphal morphogenesis in *A. fumigatus* (Gehrke et al., 2010). *PpoC* encodes putative fatty acid oxygenases involved in the production of oleic and linoleic acid derived oxylipins (*psiBβ*) that regulates asexual and sexual development in *A. nidulans* (Krijgsheld et al., 2013). *BrlA* is a C_2H_2-type zinc finger transcription factor involved in the regulation of conidiophore development (Krijgsheld et al., 2013). It mediates the expression of *rodA*, a hydrophobin involved in the formation of rodlet layer during conidiophore development in *A. fumigatus* (Krijgsheld et al., 2013). *ChiB* is an endochitinase that plays a major role in autolysis or enzymatic self-degradation of cells in *A. nidulans* (Shin et al., 2009). Upregulation of these genes at T_2 or T_3 points towards their potential role in the formation of sexual structures in *A. flavus*.

The synthesis of secondary metabolites by filamentous fungi usually involves a group of clustered genes. Within these cluster of genes is one or more genes referred to as the backbone gene(s) of the cluster that generally encode for a biosynthetic enzyme (Ehrlich and Mack, 2014;

Gilbert et al., 2016). In this study, backbone genes for clusters 2 (AFLA_004300), 7 (AFLA_009140), 13 (AFLA_038600), 14 (AFLA_041050), 17 (AFLA_053870), 25 (AFLA_070920), 46 (AFLA_118960), and 47 (AFLA_119110) were observed to be upregulated at later time-points in samples from the high fertility cross. In *A. flavus*, AFLA_004300 encodes a putative dimethylallyl tryptophan synthase, AFLA_053870 and AFLA_118960 encode putative polyketide synthases (PKS), AFLA_009140 encodes a putative PKS-like enzyme, AFLA_038600 encodes a putative nonribosomal peptide synthase (NRPS), AFLA_070920 and AFLA_119110 encode putative NRPS-like enzymes, while AFLA_041050 encodes a putative enterobactin esterase IroE-like enzyme. Among the 56 predicted secondary metabolism gene clusters, the upregulation of the abovementioned backbone genes suggest the possible role of these clusters in the formation of sexual structures in *A. flavus*.

In summary, we investigated metabolomic and transcriptomic profiles that occur during sexual reproduction in *A. flavus*. Our results showed the presence of distinct metabolomic profiles of SMs based on the fertility level of crosses between compatible strains of the fungus. The elevated abundance of hydroxyaflavazole, IDT-C, and aflavinine isomer in time-points that coincide with morphogenesis of ascocarps in the high fertility cross suggests that these SMs could play a potential role in the formation of sexual structures in *A. flavus*. Secondary metabolites are final downstream products of gene expression and as such, they can be critical mediators that link changes in stromatal matrix to morphological adaptation. Similarly, upregulation of *gprD*, *ppoC*, *brlA*, *chiB* and *rodA* and the backbone genes for clusters 2, 7, 13, 14, 17, 25, 46, and 47 at later time-points in samples from the high fertility cross but not in the low fertility cross may be associated in the formation of sexual structures in *A. flavus*. Additional studies involving more sets of fertility crosses are needed to confirm whether the unique genes expressed in the samples from

the high fertility cross identified in this study are specific to strains that exhibit high fertility and/or play important roles during sexual reproduction in *A. flavus*. Integration of metabolomic and transcriptomic analysis has contributed to a comprehensive biological understanding of previously observed phenotypic differences due to fertility (Luis et al., 2017) that gene expression studies alone would otherwise be unable to achieve. These results also provide a foundation for further exploration of the biochemical mechanism underlying sexual development in *A. flavus*.

Acknowledgements

We thank David Baltzegar and Erin Young at the NC State University Genomic Sciences Laboratory for guidance in sample processing and RNA-sequencing; Greg O'Brian and Yaken Samah Ameen for their assistance during the crossing experiments; and Elizabeth Scholl, Allison Dickey and Roslyn Noar for assistance in transcriptomic analysis. This study was supported by a grant from Aflatoxin Mitigation Center for Excellence and the National Corn Growers Association Award No. 2016-0949, USDA NIFA Hatch Funds for Project NC02432 and funds from USDA-ARS.

References

Abbas, H.K., Wilkinson, J.R., Zablotowicz, R.M., Accinelli, C., Abel, C.A., Bruns, H.A., Weaver, M.A., 2009. Ecology of *Aspergillus flavus*, regulation of aflatoxin production, and management strategies to reduce aflatoxin contamination of corn. Toxin Rev. 28, 142-153.

Ajayan, T., Sony, P., Panicker, J.R., Shailesh, S., 2015. Clustering DNA sequences of *Aspergillus fumigatus* using incremental multiple medoids. Fifth International Conference on Advances in Computing and Communications (ICACC), pp. 342-345.

Alcazar-Fuolia, L., Mellado, E., Garcia-Efron, G., Lopez, J.F., Grimalt, J.O., Cuenca-Estrella, J.M., Rodriguez-Tudela, J.L., 2008. Ergosterol biosynthesis pathway in *Aspergillus fumigatus*. Steroids 73, 339-347.

Amare, M.G., Keller, N.P., 2014. Molecular mechanisms of *Aspergillus flavus* secondary metabolism and development. Fungal Genet. Biol. 66, 11-18.

Andrews, S., 2010. FastQC: A quality control tool for high throughput sequence data. Retrieved December 20, 2018. From https://www.bioinformatics.babraham.ac.uk/projects/fastqc/.

Bayman, P., Baker, J.L., Mahoney, N.E., 2002. *Aspergillus* on tree nuts: incidence and associations. Mycopathologia 155, 161-169.

Bauer, A.J., Rayment, I., Frey, P.A., Holden, H.M., 1992. The molecular structure of UDP-galactose 4-epimerase from *Escherichia coli* determined at 2.5 Å resolution. Proteins 12, 372-381.

Belaish, R., Sharon, H., Levdansky, E., Greenstein, S., Shadkchan, Y., Osherov, N., 2008. The *Aspergillus nidulans cetA* and *calA* genes are involved in conidial germination and cell wall morphogenesis. Fungal Genet. Biol. 45, 232-242.

Bhatnagar, D., 2012. The 'omics' approach for solving the pre-harvest aflatoxin contamination problem: understanding the genomics and metabolomics of the fungus and proteomics of the affected corn crop, in Fernández-Luqueño, F., López-Valdez, F., Luzano-Muñiz, S. (Eds.), Proceedings of Biotechnology Summit 2012, Yucatán, Mexico, pp. 192-196.

Bolger, A.M., Lohse, M., Usadel, B., 2014. Trimmomatic: a flexible trimmer for illumina sequence data. Bioinformatics (Oxford, England) 30, 2114-2120.

Buechi, G., Klaubert, D.H., Shank, R.C., Weinreb, S.M., Wogan, G.N., 1971. Structure and synthesis of kotanin and desmethylkotanin, metabolites of *Aspergillus glaucus*. J. Org. Chem. 36, 1143-1147.

Calvo, A.M., Cary, J.W., 2015. Association of fungal secondary metabolism and sclerotial biology. Front. Microbiol. 16, 62. doi: 10.3389/fmicb.2015.00062.

Calvo, A.M., Wilson, R.A., Bok, J.W., Keller, N.P., 2002. Relationship between secondary metabolism and fungal development. Microbiol. Mol. Biol. Rev. 66, 447-459.

Cary, J.W., Gilbert, M.K., Lebar, M.D., Majumdar, R., Calvo, A.M., 2018. *Aspergillus flavus* secondary metabolites: more than just aflatoxins. Food Safety 6, 7-32.

Chang, P.K., Horn, B.W., Abe, K., Gomi, K., 2014. *Aspergillus*, in Batt, C.A., Tortorello, M.L. (Eds.), Encyclopedia of Food Microbiology 2nd Edition. Elsevier Ltd, Academic Press, New York, pp. 77-82.

Chang, P.K., Ehrlich, K.C., Fujii, I., 2009. Cyclopiazonic acid biosynthesis of *Aspergillus flavus* and *Aspergillus oryzae*. Toxins 1, 74-99.

Chang, P.K., Bennett, J.W., Cotty, P.J., 2001. Association of aflatoxin biosynthesis and sclerotial development in *Aspergillus parasiticus*. Mycopathologia 153, 41-48.

Chubukov, V., Gerosa, L., Kochanowski, K., Sauer, U., 2014. Coordination of microbial metabolism. Nat. Rev. Microbiol. 12, 327-340.

Cristalli, G., Costanzi, S., Lambertucci, C., Lupidi, G., Vittori, S., Volpini, R. Camaioni, E., 2001. Adenosine deaminase: functional implications and different classes of inhibitors. Med. Res. Rev. 21, 105-128.

De Vries, R., Kester, H., Poulsen, C., Benen, J., Visser, J., 2000. Synergy between accessory enzymes from *Aspergillus* in the degradation of plant cell wall polysaccharides. J. Carbohydr. Res. 327, 401-410.

Dorner, J.W., 2004. Biological control of aflatoxin contamination in crops. J. Toxicol. Toxin Rev. 23, 425-450.

Drott, M.T., Lazzaro, B.P., Brown, D.L., Carbone, I., Milgroom, M.G., 2018. Balancing selection for aflatoxin in *Aspergillus flavus* is maintained through interference competition with, and fungivory by insects. Proc. Biol. Sci. 284, 20172408. doi: 10.1098/rspb.2017.2408.

Dyer, P.S., O'Gorman, C.M., 2012. Sexual development and cryptic sexuality in fungi: insights from *Aspergillus* species. FEMS Microbiol. Rev. 36, 165-192.

Dunwell, J.M., Culham, A., Carter, C.E., Sosa-Aguirre, C.R., Goodenough, P.W., 2001. Evolution of functional diversity in the cupin superfamily. Trends Biochem. Sci. 26, 740-746.

Ehrlich, K.C., Mack, B.M., 2014. Comparison of expression of secondary metabolite biosynthesis cluster genes in *Aspergillus flavus*, *A. parasiticus*, and *A. oryzae*. Toxins 6, 1916-1928.

Elahian, F., Sepehrizadeh, Z., Moghimi, B., Mirzaei, S.A., 2014. Human cytochrome b5 reductase: structure, function, and potential applications. Crit Rev Biotechnol. 34, 134-143.

Etchegaray, A., Silva-Stenico, M.E., Moon, D.H., Tsai, S.M., 2004. In silico analysis of nonribosomal peptide synthetases of *Xanthomonas axonopodis* pv. *citri*: identification of putative siderophore and lipopeptide biosynthetic genes. Microbiol. Res. 159, 425-437.

Fountain, J.C., Bajaj, P., Nayak, S.N., Yang, L., Pandey, M.K., Kumar, V., Jayale, A.S., Chitikineni, A., Lee, R.D., Kemerait, R.C., Varshney, R.K., Guo, B., 2016. Responses of *Aspergillus flavus* to oxidative stress are related to fungal development regulator, antioxidant enzyme, and secondary metabolite biosynthetic gene expression. Front. Microbiol. 7, 2048. doi: 10.3389/fmicb.2016.02048.

Frisvad, J.C., Hubka, V., Ezekiel, C.N., Hong, S.B., Novakova, A., Chen, A.J., Arzanlou, M., Larsen, T.O., Sklenar, F., Mahakarnchanakul, W., Samson, R.A., Houbraken, J., 2019. Taxonomy of *Aspergillus* section *Flavi* and their production of aflatoxins, ochratoxins and other mycotoxins. Stud. Mycol. 93, 1-63.

Furge, K.A., Cheng, Q., Jwa, M., Shin, S., Song, K., Albright, C.F., 1999. Regions of Byr4, a regulator of septation in fission yeast, that bind Spg1 or Cdc16 and form a two-component GTPase-activating protein with Cdc16. J. Biol. Chem. 274, 11339-11343.

Georgianna, D.R., Fedorova N.D., Burroughs J.L., Dolezal A.L., Bok J.W. Horowitz-Brown S., Woloshuk C.P., Yu J., Keller N.P., Payne G.A., 2010. Beyond aflatoxin: four distinct expression patterns and functional roles associated with *Aspergillus flavus* secondary metabolism gene clusters. Mol. Plant Pathol. 11, 213-226.

Gehrke, A., Heinekamp, T.J., Ilse, D., Brakhage, A.A., 2010. Heptahelical receptors gprC and gprD of *Aspergillus fumigatus* are essential regulators of colony growth, hyphal morphogenesis, and virulence. Am. Soc. Microbiol. J. 76, 3989-3998.

Gilbert, M.K., Mack, B.M., Wei, Q., Bland, J.M., Bhatnagar, D., Cary, J.W., 2016. RNA sequencing of an *nsdC* mutant reveals global regulation of secondary metabolic gene clusters in *Aspergillus flavus*. Microbiol. Res. 182, 150-161.

Gloer, J.B., 1995. Antiinsectan natural products from fungal sclerotia. Acc. Chem. Res. 28, 343-350.

Gloer, J.B., TePaske, M.R., Sima, J.S., Wicklow, D.T., Dowd, P.F., 1988. Antiinsectan aflavinine derivatives from the sclerotia of *Aspergillus flavus*. J. Org. Chem. 53, 5457-5460.

Goff, L., Trapnell, C., Kelley, D., 2018. CummeRbund: analysis, exploration, manipulation, and visualization of Cufflinks high-throughput sequencing data. R package version 2.24.0.

Goynes, W.R., Lee, L.S., 1989. *Aspergillus flavus* infection of developing cottonseed: microscopical determination of mycelial progression and associated aflatoxin formation. Arch. Environ. Contam. Toxicol. 18, 421-428.

Greenstein, S., Shadkchan, Y., Jadoun, J., Sharon, C., Marckovich, S., Osherov, N., 2005. Analysis of the *Aspergillus nidulans* thaumatin-like *cetA* gene and evidence for transcriptional repression of *pyr4* expression in the *cetA*-disrupted strain. Fungal Biol. Genet. 43, 42-53.

Grintzalis, K., Vernardis, S.I., Klapa, M.I., Georgiou, C.D., 2014. Role of oxidative stress in sclerotial differentiation and aflatoxin B1 biosynthesis in *Aspergillus flavus*. Appl. Environ. Microbiol. 80, 5561-5571.

Hedayati, M.T., Pasqualotto, A.C., Warn, P.A., Bowyer, P., Denning, D.W., 2007. *Aspergillus flavus*: human pathogen, allergen and mycotoxin producer. Microbiology 153, 1677-1692.

Horn, B.W., Gell, R.M., Singh, R., Sorensen, R.B., Carbone, I. 2016. Sexual reproduction in *Aspergillus flavus* sclerotia: acquisition of novel alleles from soil populations and

uniparental mitochondrial inheritance. PloS One 11, e0146169. doi: 10.1371/journal.pone.0146169.

Horn, B.W., Sorensen, R.B., Lamb, M.C., Sobolev, V.S., Olarte, R.A., Worthington, C.J., Carbone, I., 2014. Sexual reproduction in *Aspergillus flavus* sclerotia naturally produced in corn. Phytopathology 104, 75-85.

Horn, B.W., Moore, G.G., Carbone, I., 2009. Sexual reproduction in *Aspergillus flavus*. Mycologia 101, 423-429.

Horn, B.W., Greene, R.L., 1995. Vegetative compatibility within populations of *Aspergillus flavus, A. parasiticus*, and *A. tamarii* from a peanut field. Mycologia 87, 324-332.

Hüttel, W., Müller, M., 2007. Regio- and stereoselective intermolecular oxidative phenol coupling in kotanin biosynthesis by A*spergillus niger.* Chembiochem. 8, 521-529.

Jwa, M., Song, K., 1998. Byr4, a dosage-dependent regulator of cytokinesis in *S. pombe*, interacts with a possible small GTPase pathway including Spg1 and Cdc16. Mol. Cells 8, 240-245.

Klich, M.A., Tiffany, L.H., Knaphus, G., 1992. Ecology of the aspergilli of soils and litter, in Bennett, J.W., Klich, M.A. (Eds.), *Aspergillus*: Biology and Industrial Applications, Butterworth-Heinemann, Boston, pp. 329-353.

Krijgsheld, P., Bleichrodt, R., van Veluw, G.J., Wang, F., Muller, W.H., Dijksterhuis, J., Wosten, H.A.B., 2013. Development in *Aspergillus*. Stud. Mycol. 74, 1-29.

Kumar, P., Mahato, D.K., Kamle, M., Mohanta, T.K., Kang, S.G., 2016. Aflatoxins: a global concern for food safety, human health and their management. Front. Microbiol. 7, 2170. doi: PMC5240007.

Kwon-Chung, K.J., Sugui, J.A., 2009. Sexual reproduction in *Aspergillus* species of medical or economical importance: why so fastidious? Trends Microbiol. 17, 481-487.

Luis, J.M., Carbone, I., Payne, G.A., Bhatnagar, D., Cary, J., Lebar, M., Moore, G.G., Ojiambo, P.S., 2017. Morphological, metabolic and transcriptional characterization of sexual fertilization in *Aspergillus flavus*. Phytopathology 107, S5.135.

Mahmoud, M.A., 2015. Detection of *Aspergillus flavus* in stored peanuts using real-time PCR and the expression of aflatoxin genes in toxigenic and atoxigenic *A. flavus* isolates. Foodborne Pathog. Dis. 12, 289-296.

Marsh, P.B., Bollenbacher, K., San Antonio, J.P., Merola, G.V., 1955. Observations on certain fluorescent spots in raw cotton associated with growth of microorganisms. Textile Res. J. 25, 1007-1016.

McAlpin, C.E., Wicklow, D.T., 2005. Culture media and sources of nitrogen promoting the formation of stromata and ascocarps in *Petromyces alliaceus* (*Aspergillus* section *Flavi*). Can. J. Microbiol. 51, 765-771.

Merchant, N., Lyons, E., Goff, S., Vaughn, M., Ware, D., Micklos, D., Antin, P., 2016. The iPlant collaborative: cyberinfrastructure for enabling data to discovery for the life sciences. PLOS Biol. 14, e1002342. doi: 10.1371/journal.pbio.1002342.

Ojiambo, P.S., Battilani, P., Cary, J.W., Blum, B.H., Carbone, I., 2018. Cultural and genetic approaches to manage aflatoxin contamination: recent insights provide opportunities for improved control. Phytopathology 108, 1024-1037.

Olarte, R.O., Horn, B.W., Dorner, J.W., Monacell, J.T., Singh, R., Stone, E.A., Carbone, I. 2012. Effect of sexual recombination on population diversity in aflatoxin production by *Aspergillus flavus* and evidence for cryptic heterokaryosis. Mol. Ecol. 21:1453-1476.

Oliveros, J.C., 2007-2015. Venny. An interactive tool for comparing lists with Venn's diagrams. From http://bioinfogp.cnb.csic.es/tools/venny/index.html.

Parker, E.J., Scott, B., 2004. Indole-diterpene biosynthesis in ascomycetous fungi, in An, Z. (Ed), Handbook of Industrial Mycology. Marcel Dekker, New York, pp. 405-426.

Payne, G.A., Widstrom, N.W., 1992. Aflatoxin in maize. Crit. Rev. Plant Sci. 10, 423-440.

Pettit, R.E., 1984. Yellow mold and aflatoxin, in Porter, D.M., Smith, D.H., Rodriguez-Kabana, R. (Eds), Compendium of Peanut Diseases. The American Phytopathological Society, St. Paul, MN, pp. 35-36.

Qiu, L., Wang, J., Ying, S., Feng, M., 2015. *Wee1* and *Cdc25* control morphogenesis, virulence and multistress tolerance of *Beauveria bassiana* by balancing cell cycle-required cyclin-dependent kinase 1 activity. Environ. Microbiol. 17, 1119-1133.

R Core Team. 2013. R: a language and environment for statistical computing. R Foundation for Statistical Computing, Vienna, Austria.

Raper, K.B., Fennell, D.I., 1965. The Genus *Aspergillus*, The Williams & Wilkins Company, Baltimore, MD, pp. 1-686.

Saikia, S., Nicholson, M.J., Young, C., Parker, E.J., Scott, B., 2008. The genetic basis for indole-diterpene chemical diversity in filamentous fungi. Mycol. Res. 112, 184-199.

Scheidegger, K.A., Payne, G.A., 2003. Unlocking the secrets behind secondary metabolism: a review of *Aspergillus flavus* from pathogenicity to functional genomics. J. Toxicol. Toxin. Rev. 22, 423-459.

Seyedmousavi, S., Guillot, J., Arne, P., de Hoog, G.S., Mouton, J.W., Melchers, W.J.G., Verweij, P.E., 2015. *Aspergillus* and aspergilloses in wild and domestic animals: a global health concern with parallels to human disease. Med. Mycol. 53, 765-797.

Sharpless, K.E., Harris, S.D., 2002. Functional characterization and localization of the *Aspergillus nidulans* formin SEPA. Mol. Biol. Cell. 13: 469-479.

Shin, K., Kwon, N., Kim, Y.H., Park, H., Kwon, G., Yu, J., 2009. Differential roles of the chiB chitinase in autolysis and cell death of *Aspergillus nidulans*. Am. Soc. Microbiol. J. 8, 738-746.

Smith, D.M., Thomas N.R., Gani, D., 1991. A comparison of pyridoxal 5'-phosphate dependent decarboxylase and transaminase enzymes at a molecular level. Experientia 47, 1104-1118.

Soil-Raggi, G., Sanchez, O., Aguirre J., 2006. TmpA, a member of a novel family of putative membrane flavoproteins, regulates asexual development in *Aspergillus nidulans*. Mol. Microbiol. 59, 854-869.

Stogios, P.J., Downs, G.S., Jauhal, J.J., Nandra, S.K., Privé, G.G., 2005. Sequence and structural analysis of BTB domain proteins. Genome Biol. 6, R82. doi: 10.1186/gb-2005-6-10-r82.

Taubenhaus, J.L., 1920. A study of the black and yellow molds of ear-corn. Texas Agric. Exp. Sta. Bull. 270.

TePaske, M.R., Gloer, J.B., Wicklow, D.T., Dowd, P.F., 1992. Aflavarin and ß-aflatrem: new anti-insectan metabolites from the sclerotia of *Aspergillus flavus*. J. Nat. Prod. 55, 1080-1086.

TePaske, M.R., Gloer, J.B., Wicklow, D.T., Dowd, P.F., 1991. Leporin A: an antiinsectan N-alkoxypyridone from the sclerotia of *Aspergillus leporis*. Tetrahedron Lett. 32, 5687-5690.

TePaske, M.R., Gloer, J.B., Wicklow, D.T., Dowd, P.F., 1990. Aflavazole: a new antiinsectan carbazole metabolite from the sclerotia of *Aspergillus flavus*. J. Org. Chem. 55, 5299-5301.

Thomas, P.D., Campbell, M.J., Kejariwal, A., Mi, H., Karlak, B., Daverman, R., Diemer, K., Muruganujan, A., Narechania, A., 2003. PANTHER: a library of protein families and subfamilies indexed by function. Genome Res. 13: 129-2141.

Trapnell, C., Roberts, A., Goff, L., Pertea, G., Kim, D., Kelley, D.R., Pimentel, H., Salzberg, S.L., Rinn, J.L., Pachter, L., 2012. Differential gene and transcript expression analysis of RNA-seq experiments with TopHat and cufflinks. Nat. Protoc. 7, 562-578.

Trapnell, C., Hendrickson, D.G., Sauvageau, M., Goff, L., Rinn, J.L., Pachter, L., 2013. Differential analysis of gene regulation at transcript resolution with RNA-seq. Nature Biotechnol. 31, 46-53.

Trapnell, C., Roberts, A., Goff, L., Pertea, G., Kim, D., Kelley, D.R., Pimentel, H., Salzberg, S.L., Rinn, J.L., Pachter, L., 2012. Differential gene and transcript expression analysis of RNA-seq experiments with TopHat and Cufflinks. Nat. Protoc. 7, 562-578.

Vadlapudi, V., Borah, N., Yellusani, K.R., Gade, S., Reddy, P., Rajamanikyam, M., Narasimha, L., Vempati, S., Gubbala, S.P., Chopra, P., Upadhyayula, S.M., Amanchy, R., 2017. *Aspergillus* secondary metabolite database, a resource to understand the secondary metabolome of *Aspergillus* genus. Sci. Rep. 7, 7325. doi: 10.1038/s41598-017-07436-w.

Wang, H., Lei, Y., Yan, L., Cheng, K., Dai, X., Wan, L., Guo, W., Cheng L., Liao, B., 2015. Deep sequencing analysis of transcriptomes in *Aspergillus flavus* in response to resveratrol. BMC Microbiol 15, 182. doi: 10.1186/s12866-015-0513-6.

Wicklow, D.T., Donahue, J.E., 1984. Sporogenic germination of sclerotia in *Aspergillus flavus* and *A. parasiticus*. Trans. Br. Mycol. Soc. 82, 621-624.

Wu, X., Zhou, B., Yin, C., Guo, Y., Lin, Y., Pan, L., Wang, B., 2014. Characterization of natural antisense transcript, sclerotia development and secondary metabolism by strand-specific RNA sequencing of *Aspergillus flavus*. PLoS One 9, e97814. doi: 10.1371/journal.pone.0097814.

Yang, Y.S., Strittmatter, S.M., 2007. The reticulons: a family of proteins with diverse functions. Genome Biol. 8, 234. doi:10.1186/gb-2007-8-12-234.

Table 3.1.
Fertility of stromata generated from reciprocal crosses involving two compatible parental strains of *A. flavus*.

Cross (sclerotium × conidium)[a]	Number of stromata		Fertility (%)[b]	Fertility designation
	Examined	Fertile[b]		
NRRL 29507 × NRRL 21882	300	247 a	82.3 a	High
NRRL 21882 × NRRL 29507	300	7 b	2.3 b	Low
NRRL 29507 (unmated sclerotia)	300	0 b	0.0 b	–

[a] Crosses are between sclerotium-producing and conidium-producing parents. NRRL strain number is from USDA Agricultural Research Service Culture Collection, Peoria, IL. NRRL 29507 is *MAT1-1* and NRRL 21882 is *MAT1-2*.

[b] A stroma was considered fertile when at least one ascospore-bearing ascocarp was detected within the stromatal matrix. Results were calculated from the mean of three replicate plates per cross or strain. Fertility is calculated by dividing the number of fertile stromata by the number of total stromata or sclerotia examined and multiplied by 100%. Values followed by the same letter are not significantly different at $\alpha = 0.05$.

Table 3.2.
Aflatoxin B_1 (AFB_1) production in stromata from high and low fertility crosses and in sclerotia from an unmated strain of *A. flavus*.

Fertility of cross[a]	AFB_1 content (ppm) at different time-point[b]					Mean
	T_0	T_1	T_2	T_3	T_4	
High	58 ± 17 a	19 ± 2 a	18 ± 3 ab	19 ± 3 a	17 ± 2 b	26 ± 2 b
Low	0 ± 0 b	2 ± 1 b	3 ± 1 b	2 ± 0 b	2 ± 1 c	2 ± 1 c
Unmated	34 ± 4 a	27 ± 6 a	45 ± 12 a	41 ± 10 a	49 ± 11 a	39 ± 1 a

[a] Fertility designations are described in Table 3.1 and the unmated sclerotia are for strain NRRL 29507.

[b] Time-points are designated as follows: T_0 = time of crossing, while T_1, T_2, T_3, and T_4 refer to 2, 4, 6 and 8 weeks of incubation, respectively. Values of AFB_1 are means ± standard error. Within each time-point, values with the same letter are not significantly different at $\alpha = 0.05$.

Table 3.3.
Normalized abundance (absorbance per arbitrary units, AU) of 17 secondary metabolites detected in stromata from high and low fertility crosses or sclerotia from unmated strain of *A. flavus*.

Peak	Metabolite ID	AU per mg of lyophilized stromata or sclerotia[a]						*P*-value[b]
		High fertility		Low fertility		Unmated		
		Mean	S.E.	Mean	S.E.	Mean	S.E.	
1	Aflavarin	6938	1304	12637	2159	5971	1149	ns
2	Hydroxyaflavinine	1407	33	1888	329	2893	213	0.0052
3	Cyclopiazonic acid	749	76	0	–	2786	723	0.0001
4	Aflavazole	1045	25	333	54	1214	115	0.0001
5a	Aflatrem-1	2455	126	3155	213	2829	268	ns
5b	Aflatrem-2	1231	54	1308	95	1423	119	ns
5c	Aflatrem-3	253	18	0	–	282	73	0.0001
6	Aflavinine	1506	113	0	–	1511	88	0.0001
7	Leporin	0	0	588	95	0	–	0.0001
8	Kotanin A	0	0	988	149	0	–	0.0001
9	Ergosterol	1831	208	2135	278	1537	193	ns
A	Aflavarin isomer	638	173	1158	211	0	–	0.0001
B	Hydroxyaflavazole	91	45	0	–	0	–	0.0408
C	IDT-C	253	73	0	–	0	–	0.0001
D	Aflavinine isomer	1001	360	0	–	0	–	0.0005
E	Sterol analog	16	6	155	35	0	–	0.0001
Z	IDT-Z	11246	407	0	–	12039	955	0.0001

[a] Values are mean relative abundance of secondary metabolites in stromata or sclerotia sampled at all time-points; S.E. is the standard error of the mean.

[b] *P*-value is for testing for significant differences in AU values between stromata from high fertility cross, low fertility cross and unmated strain; ns = non-significant.

Table 3.4.
Genes involved in sexual reproduction in *A. flavus* as identified from gene ontology (GO) functional and *K*-means cluster analyses.

Gene ID	Protein name	Function
AFLA_007210	Cytokinesis regulator (Byr4), putative	Mitotic cell cycle, karyokinesis, and septation in *Schizosaccharomyces pombe* (Jwa and Song, 1998)
AFLA_009110	Reticulon-like protein	Endoplasmic reticulum-Golgi trafficking, vesicle formation, membrane morphogenesis, apoptosis (Yang and Strittmatter, 2007)
AFLA_017220	Pyridoxal-dependent decarboxylase domain protein	Decarboxylation of L-amino acid substrates with retention of configuration at C^{α} (Smith et al., 1991)
AFLA_023510	UDP-galactose 4-epimerase (GALE), putative	Conversion of UDP-galactose to UDP-glucose (Bauer et al., 1992)
AFLA_023520	Adenosine deaminase (ADA), putative	Deamination of adenosine to inosine, deoxyadenosine to deoxyinosine (Cristalli et al., 2001)
AFLA_085880	BTB domain transcription factor, putative	Transcriptional regulation, cytoskeleton dynamics (Stogios et al., 2005)
AFLA_089770	Alpha-L-arabinofuranosidase A (abfA), putative	Hydrolysis of terminal non-reducing α-L-arabinofuranosidic bonds in hemicelluloses (De Vries et al., 2000)
AFLA_093580	Membrane oxidoreductase (tmpA), putative	Conidiation in *A. nidulans* (Soid-Raggi et al., 2006); asexual/sexual development in *A. flavus* (Gilbert et al., 2016)
AFLA_101780	NADH-cytochrome B5 reductase, putative	Catalyze electron reduction of ferricytochrome b5 to ferrocytochrome b5 (Elahain et al., 2014)
AFLA_110040	Cupin domain protein	Cell wall modification (Dunwell et al., 2001)
AFLA_139670	Nonribosomal peptide synthase, putative	Biosynthesis of microbial toxins, specifically nonribosomal peptides (Smith et al., 1991)
AFLA_009870	Uncharacterized protein	–
AFLA_009880	Uncharacterized protein	–
AFLA_013600	Uncharacterized protein	–
AFLA_056870	Uncharacterized protein	–
AFLA_089640	Uncharacterized protein	–
AFLA_089640	Uncharacterized protein	–
AFLA_099050	Uncharacterized protein	–
AFLA_101380	Uncharacterized protein	–
XLOC_010320	Uncharacterized protein	–

Table 3.5.
Differential expression of genes involved in growth and development in *Aspergillus* species as identified in stromata from the high fertility cross.

Gene	Gene ID	Differential gene expression between time-points[a]							
		HiT_0_HiT_1		HiT_1_HiT_2		HiT_2_HiT_3		HiT_3_HiT_4	
		log_2FC[b]	q_value[c]	log_2FC	q_value	log_2FC	q_value	log_2FC	q_value
brlA	AFLA_082850	2.4317	0.0002	0.3073	0.2507	1.4785	0.0002	0.2059	0.2795
chiB	AFLA_104680	1.5567	0.0002	-0.2495	0.1296	1.0377	0.0002	-0.5993	0.0019
gprD	AFLA_135680	0.6800	0.0058	2.4835	0.0002	-1.2610	0.0002	-0.8016	0.0002
ppoC	AFLA_030430	0.2514	0.0987	1.5251	0.0002	-1.038	0.0002	-0.4104	0.0046
rodA	AFLA_098380	1.0846	0.0002	-2.9995	0.0002	2.1832	0.0002	-0.4324	0.0298

[a] Time-points are designated as follows: T_0 = time of crossing, while T_1, T_2, T_3, and T_4 refer to 2, 4, 6 and 8 weeks of incubation, respectively.

[b] log_2FC = log_2(fold_change), defined as the log_2 change in the second time-point as compared to the earlier time-point. Log_2(fold_change) ≥ |1| indicates a 2-fold upregulation or downregulation of gene expression. Positive values indicate upregulated gene expression, while negative values indicate downregulated gene expression.

[c] q-value = adjusted *P*-value. Only genes with log_2(fold_change) ≥ |1| and adjusted *P*-value ≤ 0.05 are considered differentially expressed.

Table 3.6.
Differential expression of backbone genes encoding the *A. flavus* secondary metabolism gene clusters as identified in stromata from the high fertility cross.

Cluster	Gene ID	Differential gene expression between time-points[a]							
		HiT_0_HiT_1		HiT_1_HiT_2		HiT_2_HiT_3		HiT_3_HiT_4	
		log_2FC[b]	q_value[c]	log_2FC	q_value	log_2FC	q_value	log_2FC	q_value
2	AFLA_004300	2.9343	1.0000	0.4980	1.0000	1.4812	0.0065	0.0485	0.9141
7	AFLA_009140	-0.3501	0.3445	-0.6871	0.0942	1.4610	0.0004	-0.3852	0.2625
13	AFLA_038600	-0.0085	1.0000	1.0497	0.0002	-0.2117	0.3250	-0.0385	0.8793
14	AFLA_041050	1.3612	1.000	2.8400	1.0000	3.9761	0.002	-0.2753	0.3896
17	AFLA_053870	0.6026	0.0002	2.2719	0.0002	0.0000	1.0000	0.0000	1.0000
25	AFLA_070920	1.5305	1.0000	-1.2125	1.0000	2.3462	0.0002	0.4009	0.1417
46	AFLA_118960	1.4417	1.0000	0.3160	1.0000	1.5693	0.0002	-0.0832	0.6788
47	AFLA_119110	0.2857	1.0000	0.5839	1.0000	2.5921	0.0002	0.3117	0.0829

[a] Time-points are designated as follows: T_0 = time of crossing, while T_1, T_2, T_3, and T_4 refer to 2, 4, 6 and 8 weeks of incubation, respectively.

[b] log_2FC = log_2(fold_change), defined as the log_2 change in the second time-point as compared to the earlier time-point. Log_2(fold_change) $\geq |1|$ indicates a 2-fold upregulation or downregulation of gene expression. Positive values indicate upregulated gene expression, while negative values indicate downregulated gene expression.

[c] q-value = adjusted *P*-value. Only genes with log_2(fold_change) $\geq |1|$ and adjusted *P*-value ≤ 0.05 are considered differentially expressed.

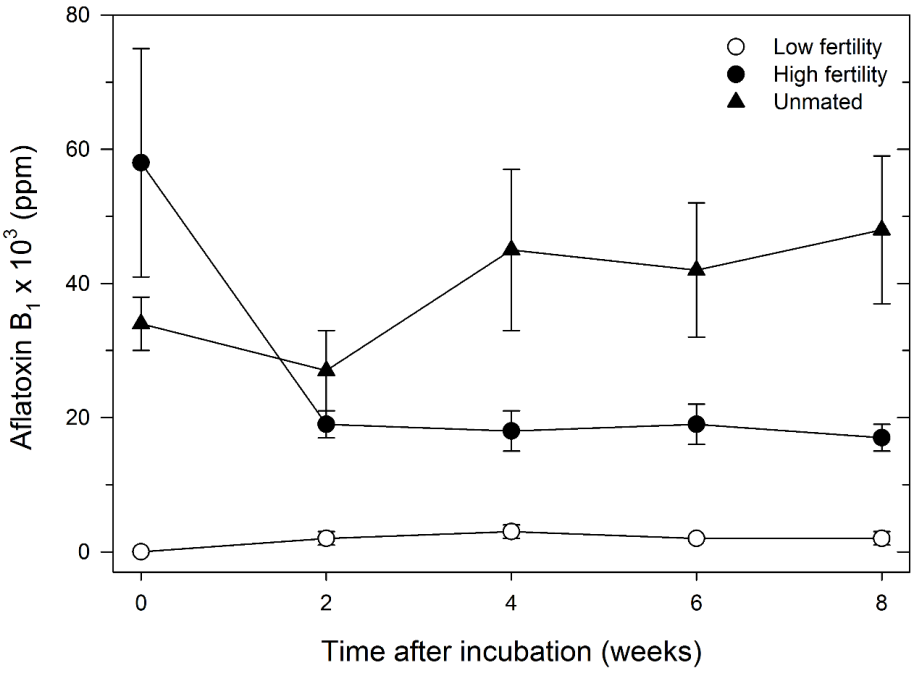

Fig. 3.1. Aflatoxin B_1 (AFB_1) content produced over time in stromata from low and high fertility crosses and in sclerotia from an unmated strain of *A. flavus*. Lipophilic extracts of sclerotia (three replicate plates for each treatment per time-point) were analyzed for AFB_1 content on ultra-performance liquid chromatography with photodiode array and mass spectrometry using fluorescence detection (excitation = 365 nm, emission = 440 nm) and compared to AFB_1 standard (Sigma Aldrich, St. Louis, MO). Data points represent means and whiskers are standard errors. Low fertility cross: NRRL 21882 sclerotia × NRRL 29507 conidia; high fertility cross: NRRL 29507 sclerotia × NRRL 21882 conidia; unmated strain: sclerotia from NRRL 29507. Time-points correspond to time at crossing (time = 0), and 2, 4, 6 and 8 weeks of incubation in a growth chamber in continuous darkness at 30°C.

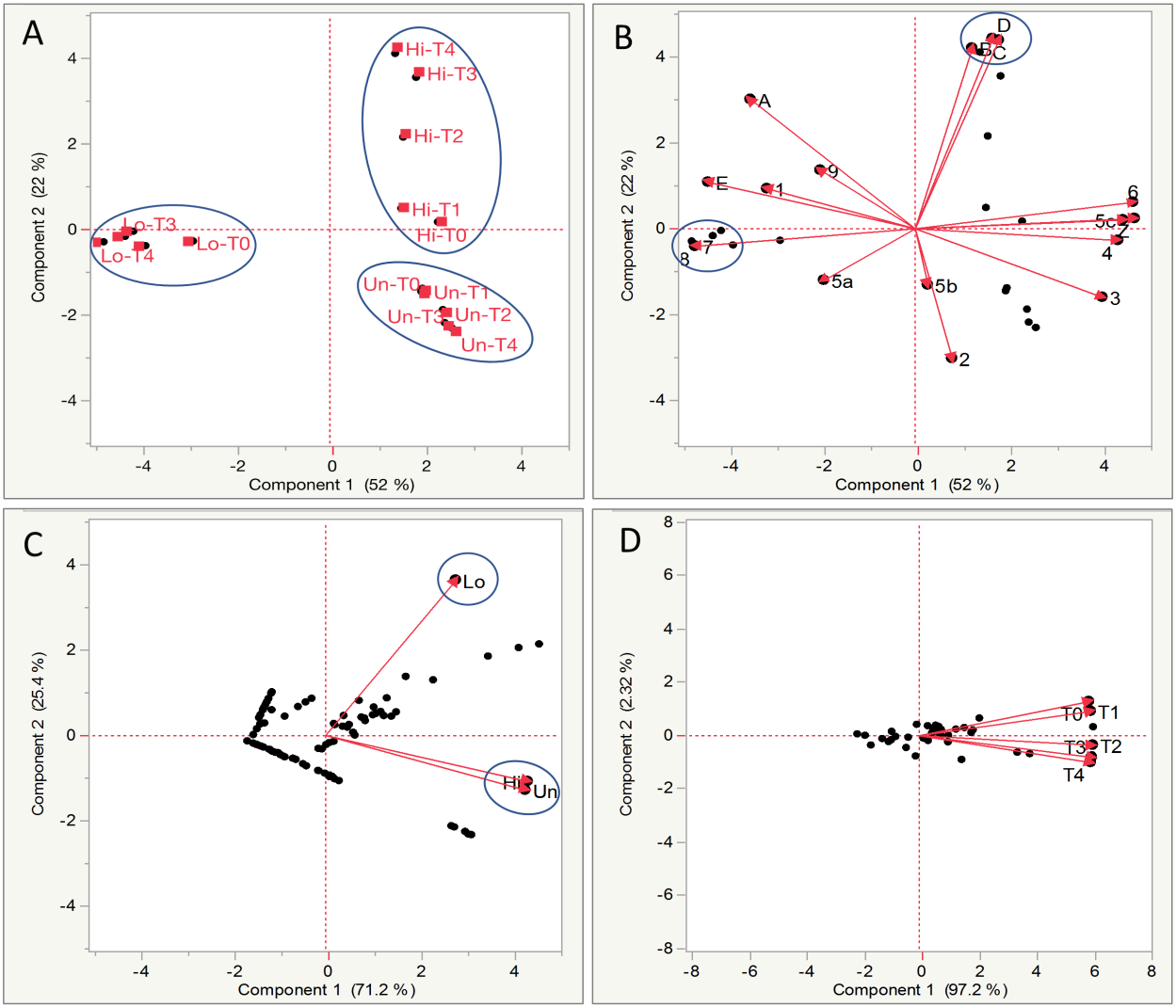

Fig. 3.2. Multivariate analysis of secondary metabolites detected in stromata from low and high fertility crosses and in sclerotia from an unmated strain of *A. flavus*. A) Principal Component Analysis (PCA) score plot showing clustering of secondary metabolites (SMs) based on female fertility and sampling time-point. B) PCA biplot showing the clustering of all SMs detected across entire study. Numbers or letters within the graph refer to SMs as described in Table 3.2. C) PCA biplot depicting clustering of SMs based on female fertility. D) PCA biplot showing clustering of SMs based on sampling time-point. Fertility: Lo and Hi = low and high fertility cross, respectively, while Un = unmated strain. Time-point: T_0 = time of crossing, while T_1, T_2, T_3 and T_4 refer to 2, 4, 6 and 8 weeks of incubation in a growth chamber in continuous darkness at 30°C.

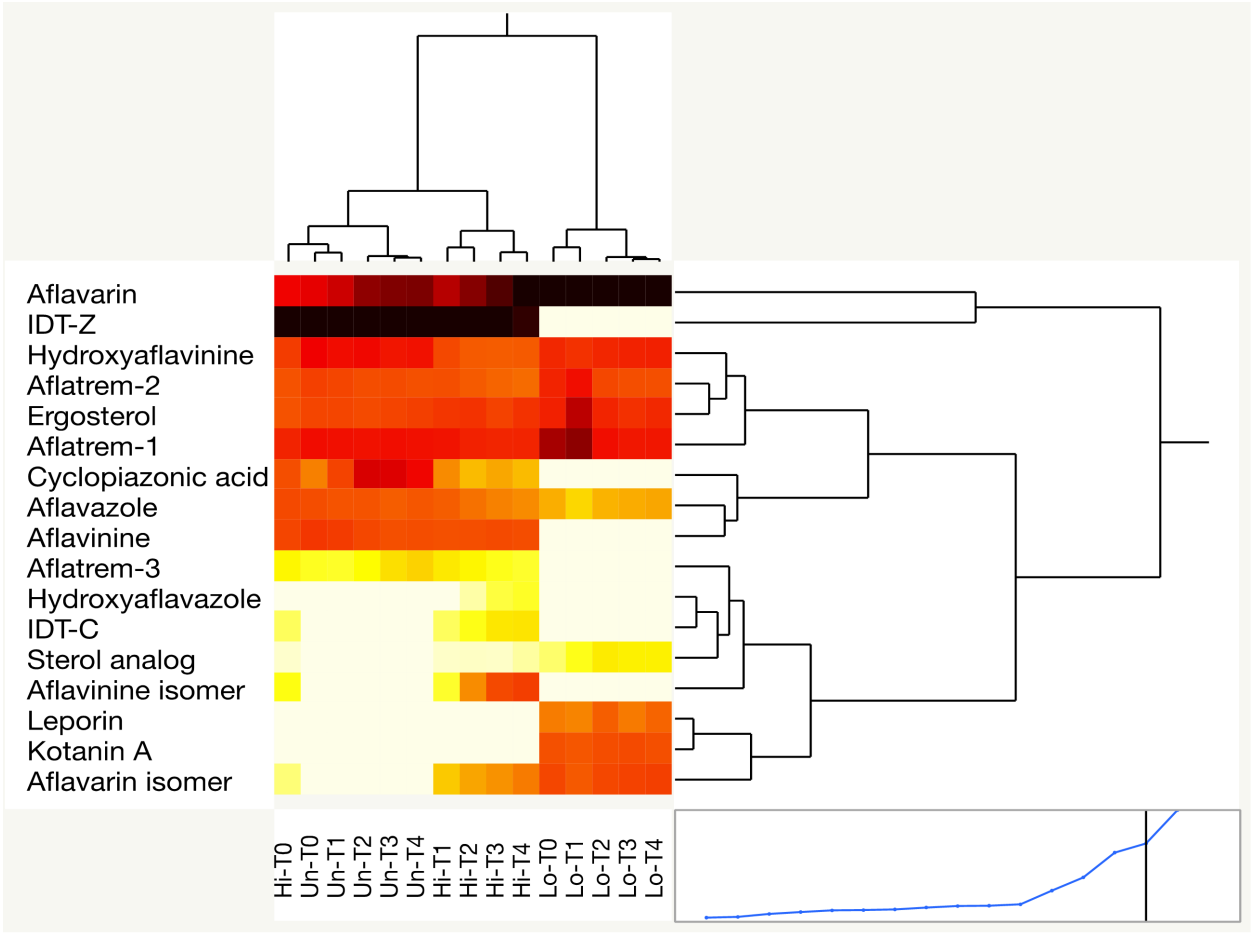

Fig. 3.3. Hierarchical cluster analysis of secondary metabolites detected in stromata from low or high fertility crosses and in sclerotia of an unmated strain of *A. flavus*. Figure depicts secondary metabolites (SMs) that are differentially expressed among stromata from low and high fertility crosses and sclerotia from unmated strain harvested at different time-points during the study. Lighter colors in the heat map show a decrease in the concentration of SMs, while darker colors show an increase in the concentration of SMs. Fertility: Lo and Hi = low and high fertility cross, respectively, while Un = unmated strain. Time-point: T_0 = time of crossing, while T_1, T_2, T_3 and T_4 refer to 2, 4, 6 and 8 weeks of incubation in a growth chamber in continuous darkness at 30°C.

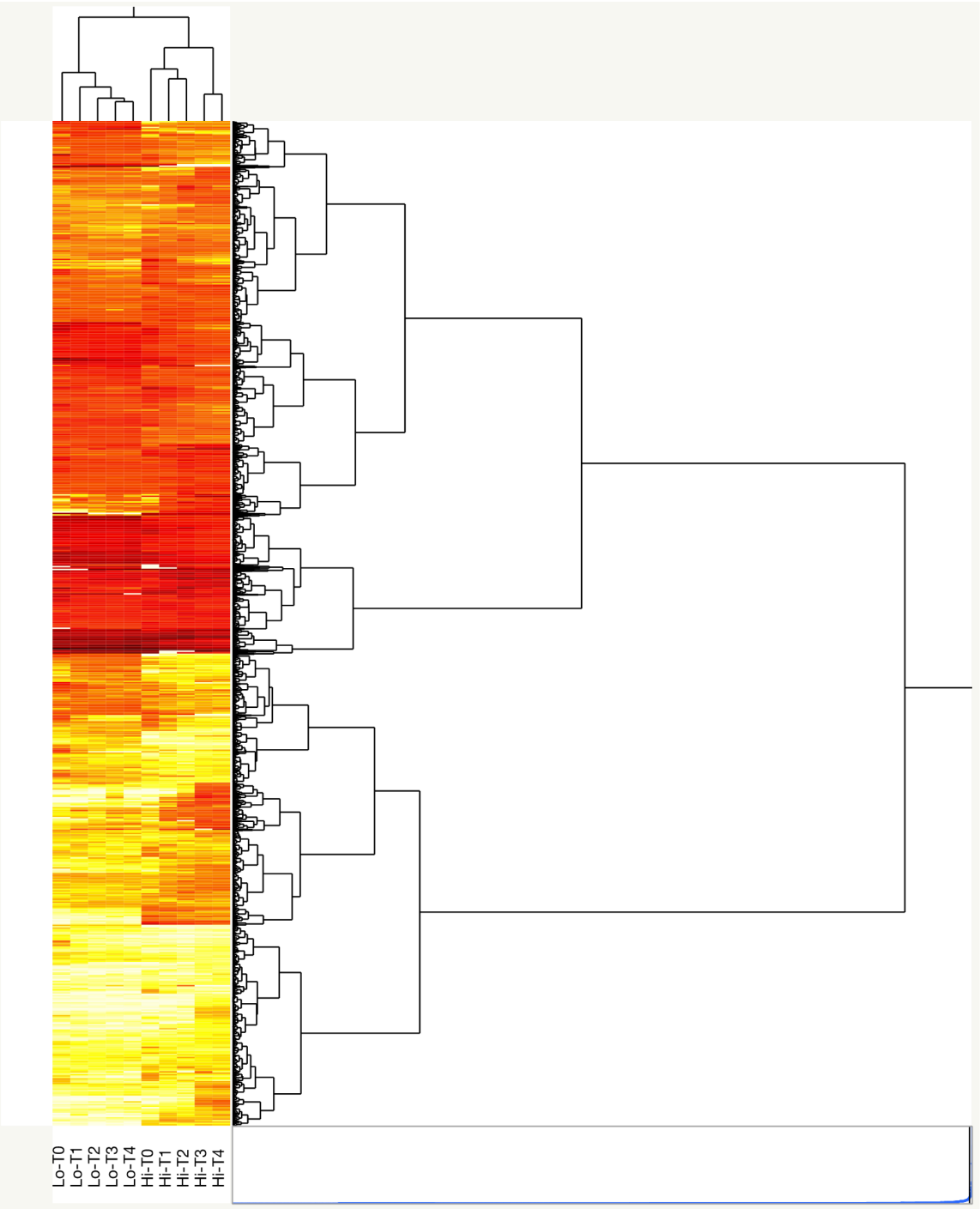

Fig. 3.4. Two-way hierarchical clustering of differential gene expression over time. The analysis includes 5,485 genes that are differentially expressed between samples from low and high fertility crosses in at least one time-point. Lighter colors in the heat map shows lower gene expression, while darker colors indicate higher gene expression. Genes with $\log_2$(fold_change) ≥ |1| and an adjusted *P*-value ≤ 0.05 are considered differentially expressed. Values were scaled using a normalization of $\log_{10}$(FPKM+1). Fertility: Lo and Hi = low and high fertility cross, respectively. Time-point: T_0 = time of crossing, while T_1, T_2, T_3 and T_4 refer to 2, 4, 6 and 8 weeks of incubation in a growth chamber in continuous darkness at 30°C.

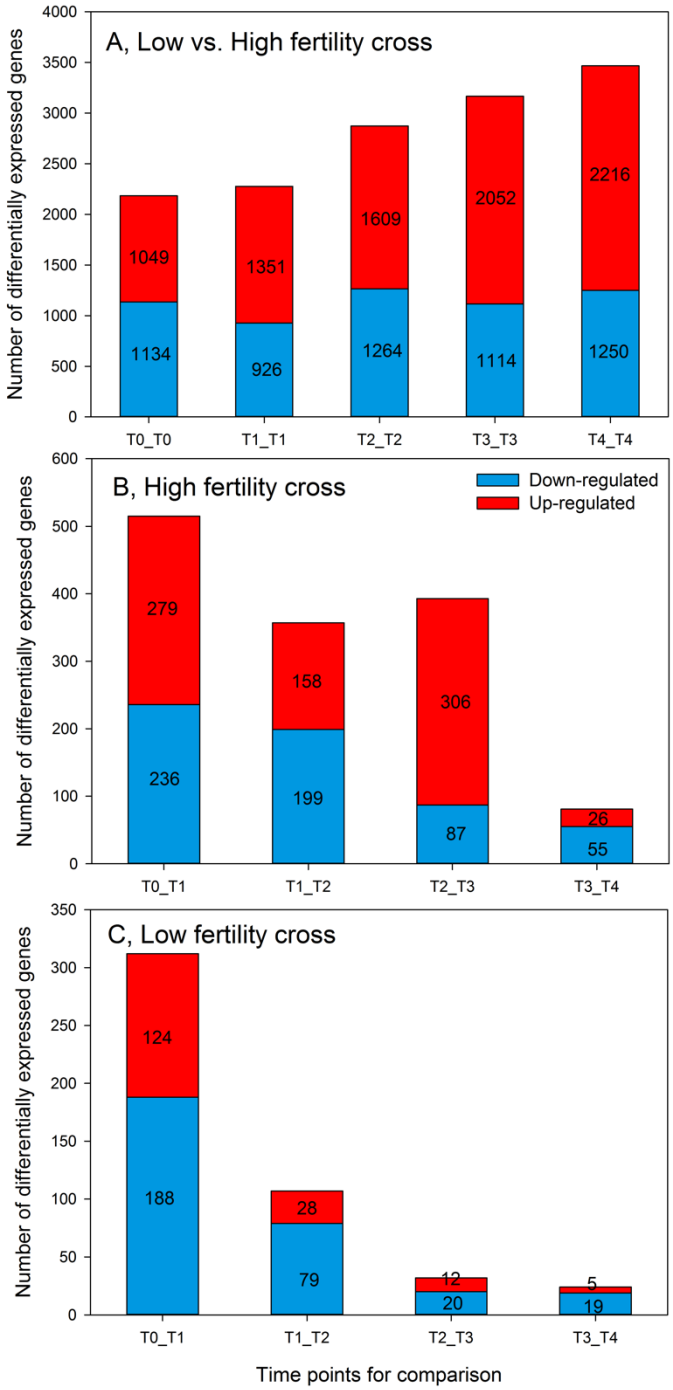

Fig. 3.5. Number of differentially expressed genes (DEGs). A) DEGS between samples from low and high fertility crosses at each time-point. B) DEGs between time-points of the high fertility cross. C) DEGs between time-points of the low fertility cross. Genes with $\log_2$(fold_change) ≥ |1| and an adjusted *P*-value ≤ 0.05 are considered differentially expressed. Fertility: Lo and Hi = low and high fertility cross, respectively. Time-point: T_0 = time of crossing, while T_1, T_2, T_3 and T_4 refer to 2, 4, 6 and 8 weeks of incubation in a growth chamber in continuous darkness at 30°C.

Fig. 3.6. Functional annotation of differentially expressed genes (DEGs) between stromata from the low and high fertility crosses over time. Gene ontology (GO) terms for molecular functions, cellular components, and biological processes for DEGs were generated using PANTHER 14.1 and *Emericella nidulans* as the selected organism.

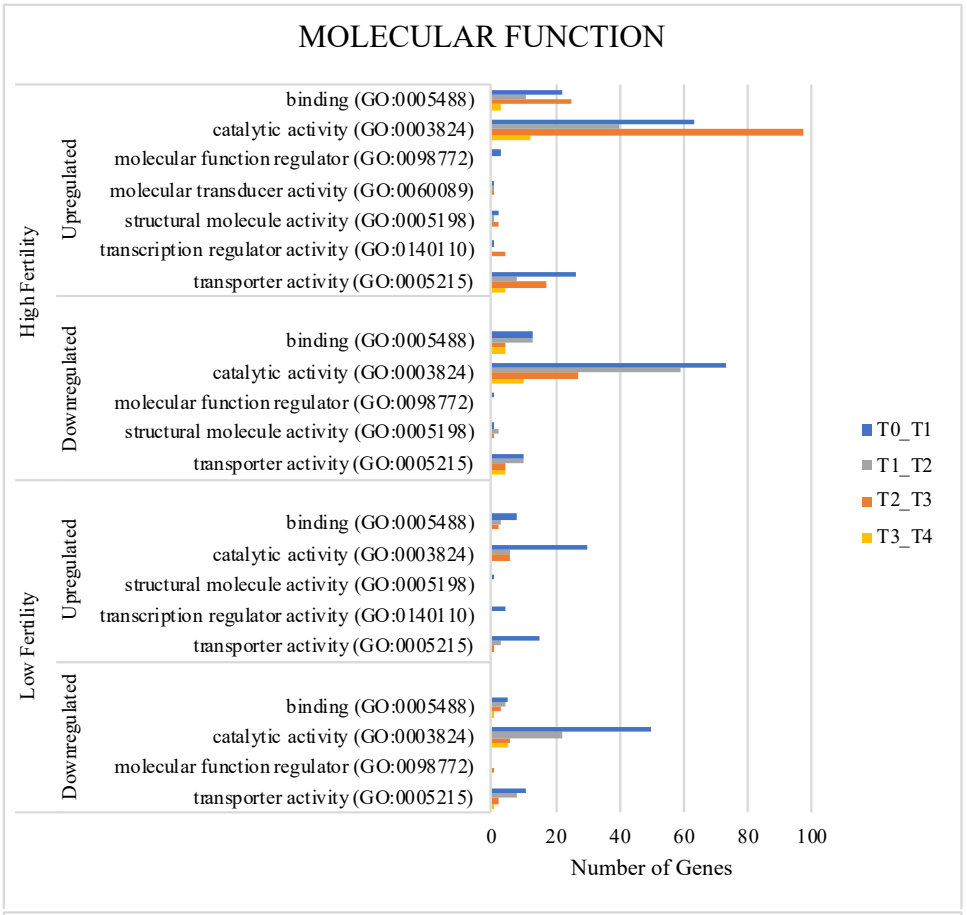
MOLECULAR FUNCTION
High Fertility
Upregulated
binding (GO:0005488)
catalytic activity (GO:0003824)
molecular function regulator (GO:0098772)
molecular transducer activity (GO:0060089)
structural molecule activity (GO:0005198)
transcription regulator activity (GO:0140110)
transporter activity (GO:0005215)
Downregulated
binding (GO:0005488)
catalytic activity (GO:0003824)
molecular function regulator (GO:0098772)
structural molecule activity (GO:0005198)
transporter activity (GO:0005215)
Low Fertility
Upregulated
binding (GO:0005488)
catalytic activity (GO:0003824)
structural molecule activity (GO:0005198)
transcription regulator activity (GO:0140110)
transporter activity (GO:0005215)
Downregulated
binding (GO:0005488)
catalytic activity (GO:0003824)
molecular function regulator (GO:0098772)
transporter activity (GO:0005215)
0
20
40
60
80
100
Number of Genes
T0_T1
T1_T2
T2_T3
T3_T4

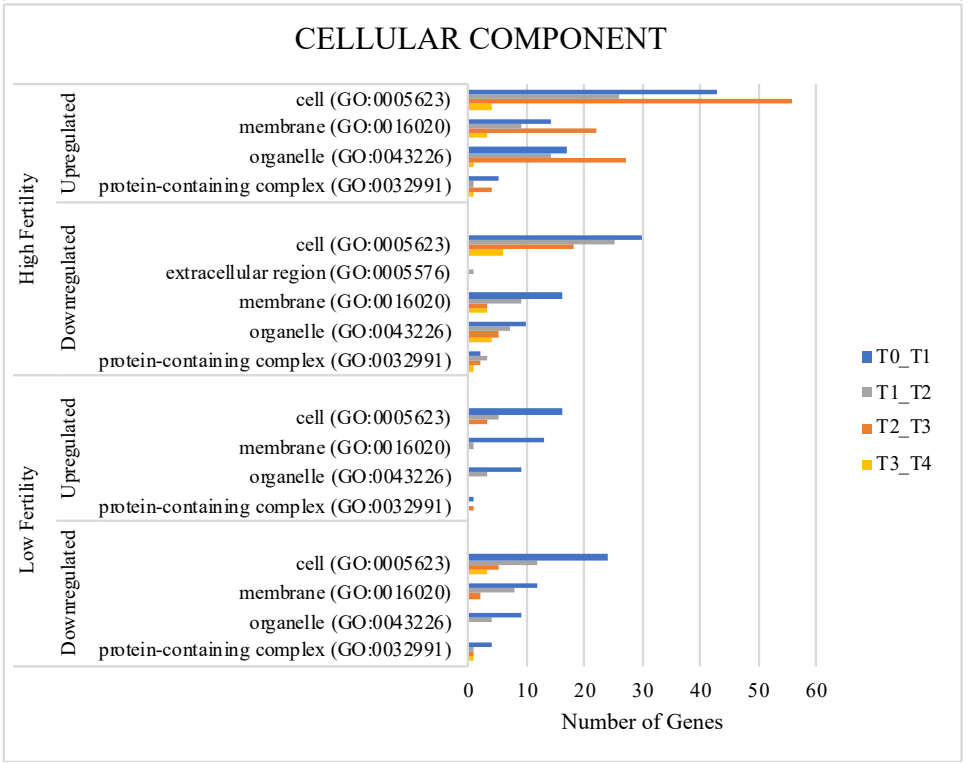
CELLULAR COMPONENT
High Fertility
Upregulated
cell (GO:0005623)
membrane (GO:0016020)
organelle (GO:0043226)
protein-containing complex (GO:0032991)
Downregulated
cell (GO:0005623)
extracellular region (GO:0005576)
membrane (GO:0016020)
organelle (GO:0043226)
protein-containing complex (GO:0032991)
Low Fertility
Upregulated
cell (GO:0005623)
membrane (GO:0016020)
organelle (GO:0043226)
protein-containing complex (GO:0032991)
Downregulated
cell (GO:0005623)
membrane (GO:0016020)
organelle (GO:0043226)
protein-containing complex (GO:0032991)
0
10
20
30
40
50
60
Number of Genes
T0_T1
T1_T2
T2_T3
T3_T4

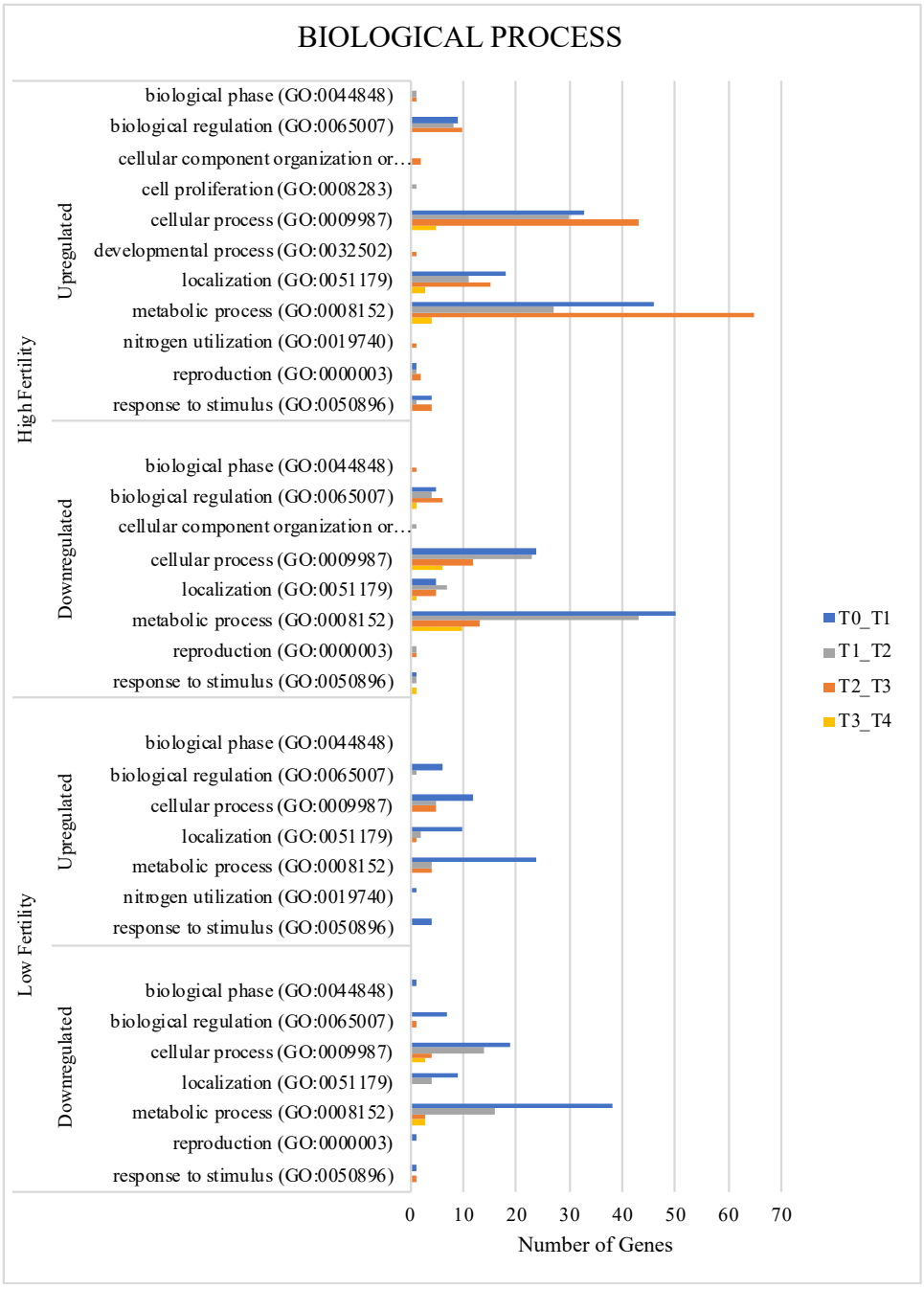
BIOLOGICAL PROCESS
High Fertility
Upregulated
biological phase (GO:0044848)
biological regulation (GO:0065007)
cellular component organization or…
cell proliferation (GO:0008283)
cellular process (GO:0009987)
developmental process (GO:0032502)
localization (GO:0051179)
metabolic process (GO:0008152)
nitrogen utilization (GO:0019740)
reproduction (GO:0000003)
response to stimulus (GO:0050896)
Downregulated
biological phase (GO:0044848)
biological regulation (GO:0065007)
cellular component organization or…
cellular process (GO:0009987)
localization (GO:0051179)
metabolic process (GO:0008152)
reproduction (GO:0000003)
response to stimulus (GO:0050896)
Low Fertility
Upregulated
biological phase (GO:0044848)
biological regulation (GO:0065007)
cellular process (GO:0009987)
localization (GO:0051179)
metabolic process (GO:0008152)
nitrogen utilization (GO:0019740)
response to stimulus (GO:0050896)
Downregulated
biological phase (GO:0044848)
biological regulation (GO:0065007)
cellular process (GO:0009987)
localization (GO:0051179)
metabolic process (GO:0008152)
reproduction (GO:0000003)
response to stimulus (GO:0050896)
0
10
20
30
40
50
60
70
Number of Genes
T0_T1
T1_T2
T2_T3
T3_T4

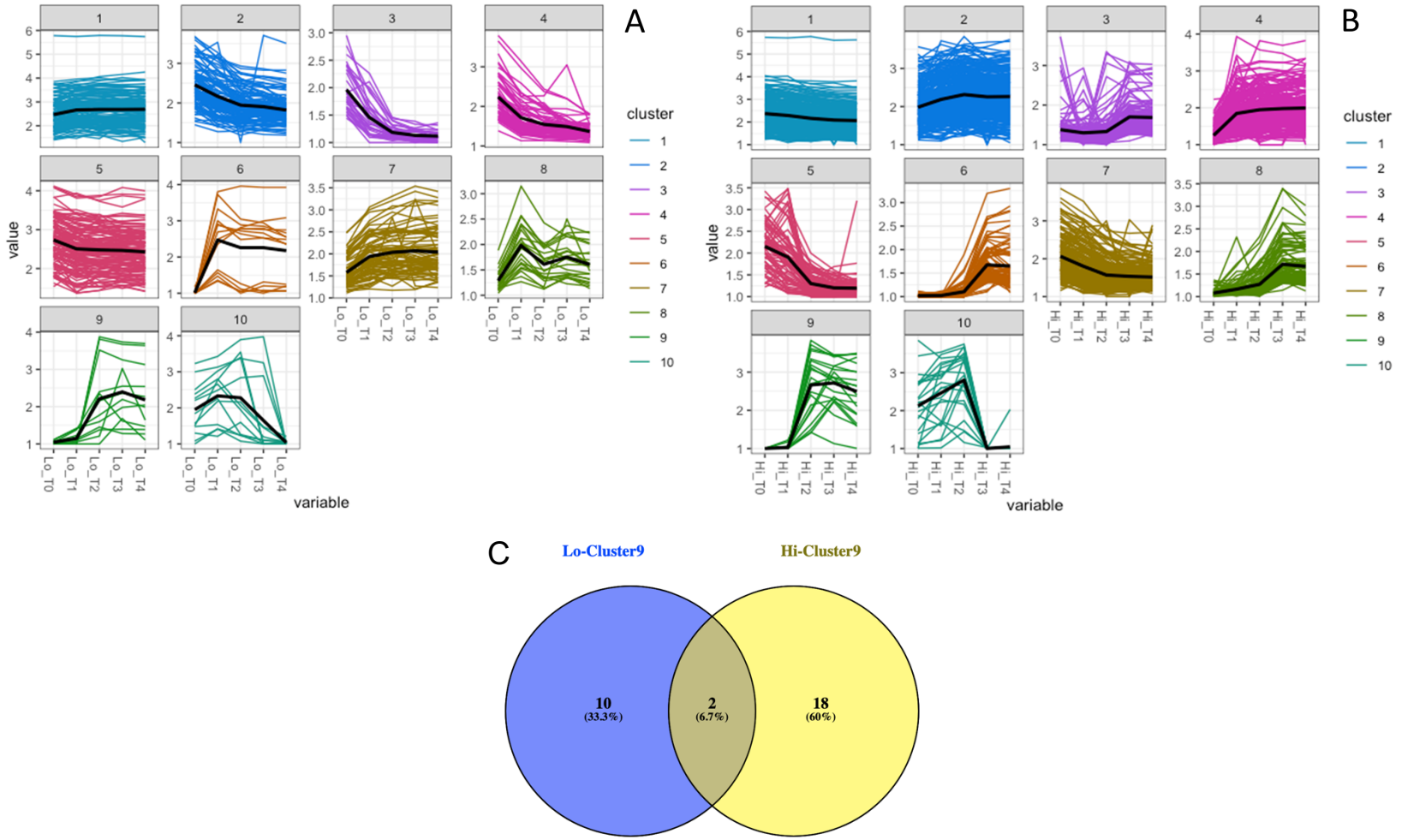

Fig. 3.7. Diagrams of *K*-means cluster analysis of gene expression between stromata from low (A) and high fertility (B) crosses over time. A-B) Genes were classified into ten categories (1-10) depending on changes in expression patterns. The x-axis and y-axis correspond to expression level and time-point, respectively. Fertility: Lo and Hi = low and high fertility cross. Time-point: T0 = time of crossing, while T_1, T_2, T_3 and T_4 refer to 2, 4, 6 and 8 weeks of incubation in a growth chamber in continuous darkness at 30°C. C) Venn diagram depicting differentially expressed genes between cluster 9 of the low and high fertility crosses. Cluster 9 in both crosses show initial plateau of gene expression at T_0 and T_1, followed by elevated expression at T_2, then slight changes at T_3 and T_4.

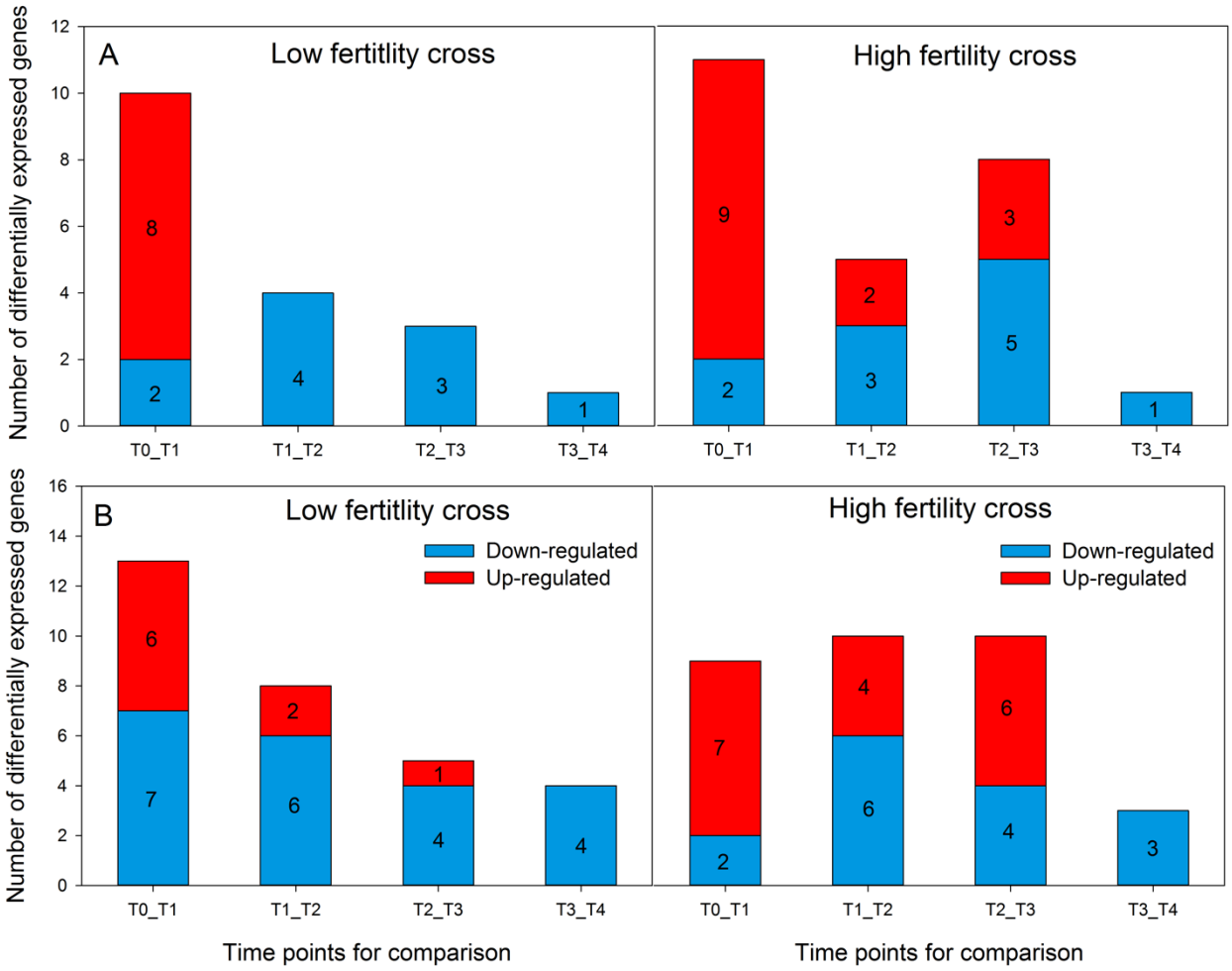

Fig. 3.8. Time-series analysis of differentially expressed genes in stromata from low and high fertility crosses. A) Number of differentially expressed genes (DEGs) related to growth and developmental stages of *Aspergillus*. C) Number of DEGs related to backbone genes encoding the *A. flavus* secondary metabolism gene clusters. Genes with $\log_2$(fold_change) ≥ |1| and an adjusted *P*-value ≤ 0.05 are considered differentially expressed. Fertility: Lo and Hi = low and high fertility cross, respectively. Time-point: T_0 = time of crossing, while T_1, T_2, T_3 and T_4 refer to 2, 4, 6 and 8 weeks of incubation in a growth chamber in continuous darkness at 30°C.

CHAPTER 4

Impact of RMb10 on the population dynamics of *Aspergillus flavus* in southern United States

To be submitted to *Applied and Environmental Microbiology*

Jane Marian Luis[a], Ignazio Carbone[a], Vicki Cornish[a], Ron Heiniger[b], Mark A. Weaver[c], Hamed K. Abbas[c], Tom W. Allen[d], Thomas S. Isakeit[e], Kira L. Bowen[f], and Peter S. Ojiambo[a]

[a] Center for Integrated Fungal Research, Department of Entomology and Plant Pathology, North Carolina State University, Raleigh, NC, USA

[b] Department of Crop Science, North Carolina State University, Plymouth, NC, USA

[c] USDA-ARS, Biological Control of Pests Research Unit, Stoneville, MS, USA

[d] Department of Biochemistry, Molecular Biology, Entomology, and Plant Pathology, Mississippi State University, Stoneville, MS, USA

[e] Department of Plant Pathology and Microbiology, Texas A&M University, College Station, TX, USA

[f] Department of Entomology and Plant Pathology, Auburn University, Auburn, AL, USA.

ABSTRACT

A large acreage of maize grown in the southern United States is chronically at risk of aflatoxin contamination caused by *Aspergillus flavus*. Biocontrol treatments using non-aflatoxigenic strains of *A. flavus* have been reported to reduce contamination by up to 98%. Two commercial biocontrol products, Afla-Guard® and AF36, are currently available in the United States. The *A. flavus* strains used in these products are of the mating type *MAT1-2* and are applied annually for effective performance. Currently, there is interest in the discovery of novel biocontrol strains and development of biocontrol approaches for sustainable reduction of aflatoxin contamination. We examined the efficacy of RMb10, a candidate biocontrol strain of the *MAT1-1* type, in replicated large-scale field trials in Alabama, Mississippi, North Carolina, and Texas in 2016 and 2017. Isolates (n = 780) collected from soil samples in these trials were screened for colony morphology, sclerotia production (+/-), mating type (*MAT1-1* or *MAT1-2*), and aflatoxin cluster type (full, partial or missing). Selected isolates were then subjected to next generation multi-locus sequence typing (NGMLST) using five loci (*amdS, aflM, aflW, mfs,* and *trpC*) in the *A. flavus* genome. A total of 23 multi-locus haplotypes (MLHs) were inferred from 311 *A. flavus* isolates using NGMLST. The frequency of *A. flavus* individuals belonging to the same MLH as RMb10 and Afla-Guard® increased at harvest as compared to pre-application of biocontrol treatments. Non-significant ($P > 0.05$) differences in the frequency of individuals with *MAT1-1* and *MAT1-2* genes suggests that the populations in this study are undergoing sexual reproduction. Patristic distance analysis also revealed phylogenetic incongruency among single locus phylogenies, supporting ongoing genetic exchange and recombination. Aflatoxin contamination was very low or below detectable limits except in Texas in 2016, where aflatoxin levels were lower in grain treated with RMb10 and Afla-Guard® as compared to the untreated plots. Results of this

study will be useful in developing additional biocontrol products and future biocontrol strategies for managing aflatoxin contamination in maize.

KEYWORDS: biocontrol, mating type, lineage, population structure

INTRODUCTION

Maize (*Zea mays* L.) was ranked as the highest produced grain in the world in 2018 and was cultivated on about 180 million hectares of land with a total production of 1.1 billion metric tons (Statista 2018a; Statista 2018b; USDA-FAS 2018). The United States with a production of about 377 million metric tons was the highest producer of maize globally, with more than half of its total production emanating from the Midwestern states of Iowa, Illinois, Nebraska and Minnesota. China with a production of about 216 million metric tons and Brazil with a production of 95 million metric tons rank second and third, respectively (NCGA 2018; USDA-NASS 2018). The average price of maize in the United States is around $3.25 per bushel (NCGA 2018), but the price received by maize growers and suppliers from food and feed companies is greatly influenced by the quality and safety of the grain. Contamination with mycotoxins, particularly aflatoxin, can lower the price or even lead to the rejection of contaminated maize lots (Mitchell et al. 2016).

Aflatoxins are hepatotoxic, carcinogenic and immunosuppressive secondary metabolites produced mainly by *A. flavus* and *A. parasiticus* (CAST 2003; Diener et al. 1987), with the former being the predominant species responsible for contamination in crops (Cotty et al. 1994). Continuous consumption of food or feed products with high aflatoxin levels has been associated with high mortality of avian flocks, reduced milk production in cattle, lesser egg yield in poultry, stunted growth in children, and hepatocellular carcinoma in elder adults (CAST 2003; Wild 2007). Hence, there is a need to continue to explore and develop management strategies that either prevent or limit mycotoxin contamination thereby resulting in grain that is safe for use as food or feed.

Several management strategies ranging from pre-harvest to storage options have been suggested to prevent or minimize the possibility of aflatoxin contamination. Some pre-harvest strategies include biological control, host resistance, plant density, and good agricultural practices

such as crop rotation, pesticide application, soil amendment, and moisture management (Ojiambo et al. 2018). Among these, biological control, which involves application of non-aflatoxigenic strains of *A. flavus* to competitively outcompete aflatoxigenic strains, is the most promising strategy to reduce aflatoxin contamination (Bandyopadhyay et al. 2016; Ehrlich 2014; Ojiambo et al. 2018). The other pre-harvest strategies are either still in their early stage of development, do not significantly reduce the risk of *A. flavus* invasion and resultant aflatoxin contamination relative to the regulatory limits, or may not be practical in areas where resources are limited (Ojiambo et al. 2018). Biocontrol is implemented by applying high densities of wheat or barley kernels that are coated with high concentrations of non-aflatoxigenic *A. flavus* strains to the plant canopy or soil surface. The treated grain absorbs moisture and allows the non-aflatoxigenic strain to sporulate profusely. The spores disperse to the developing crop prior to the occupation by toxigenic strains. This physically displaces and excludes toxigenic strains from infecting the target kernels and producing aflatoxin (Chang et al. 2014; Damann 2015; Mehl et al. 2012). Aflatoxin production may also be inhibited when appropriate aflatoxigenic and non-aflatoxigenic strains, with certain specificities, come in contact with each other in the first day of growth. This interaction initiates an unknown signaling pathway that prevents or down regulates the biosynthesis of aflatoxin that usually starts after three days of fungal growth (Huang et al. 2011).

Despite the reported success of utilizing biocontrol, only two commercial products namely AF36 and Afla-Guard® are registered to manage aflatoxin contamination in the United States. Furthermore, AF36 is registered for use only in the states of Arizona and Texas (EPA 2015). This leaves Afla-Guard® (EPA 2013) as the only product for use by farmers in other states. *A. flavus* strain NRRL 18543, used as the active ingredient in AF36, was isolated from an upland cotton in Arizona (Cotty 1989). Despite having a full aflatoxin gene cluster, it does not produce aflatoxin

due to a point mutation in its polyketide synthase gene that introduces a premature stop codon to prevent formation of norsolorinic acid and aflatoxin accumulation (Ehrlich and Cotty 2004). However, NRRL 18543 produces cyclopiazonic acid (CPA), a mycotoxin that can cause hepatic and splenic necrosis, and inflammation in chicken (Dorner et al. 1983). *A. flavus* strain NRRL 21882, the active ingredient in Afla-Guard®, was isolated from peanut in Georgia (Dorner 2005). This strain does not produce aflatoxin and CPA due to the complete deletion of its entire aflatoxin and CPA gene clusters (Chang et al. 2005; King et al. 2011). With the limited number of available biocontrol products, there is an increasing interest to identify additional biocontrol strains and develop sustainable biocontrol approaches that can mitigate aflatoxin contamination. Additional biocontrol strains are essential because the underlying population genetic structure of *A. flavus* largely determines its aflatoxin-producing potential, and thus the response of native populations to the application of different biocontrol strains is expected to be variable (Abbas 2011; Probst et al. 2011). The use and development of new biocontrol products must take into consideration the short- and long-term effects of the application of the strains in the field. Specifically, there is a need to better understand the potential of the biocontrol strain to recombine with existing local aflatoxigenic strains of *A. flavus* and assess the impact of biocontrol strains on the genetic structure of local populations of *A. flavus* in the field (Ehrlich 2014; Ehrlich 2015).

A. flavus is heterothallic, and hence each individual contains either one of the two mating type idiomorphs *MAT1-1* or *MAT1*-2 (Ramirez-Prado et al. 2008). The observation that all available biocontrol strains including NRRL 18543, NRRL 21882 and K49 in the United States have the *MAT1-2* phenotype (Chang et al. 2012) has led to the hypothesis that the mechanism of biocontrol is not simply displacement of toxigenic strains but is rather an active process (Ehrlich et al. 2015). Secondary metabolite production and development in *A. nidulans* is controlled partly

by metabolites at the cell surface (Lo et al. 2012). Thus, it is possible that signaling molecules or protein factors that are controlled by the mating type locus genes may actively prevent aflatoxin production in strains of the opposite mating type (Ehrlich et al. 2015). In this study, we build upon this hypothesis by examining the impact of a candidate biocontrol strain, RMb10, on the longitudinal population dynamics of *A. flavus* in the southern United States. Unlike the available biocontrol strains, RMb10 has the *MAT1-1* mating type. This strain was isolated from a maize field in Rocky Mount, North Carolina in 2012. It is non-aflatoxigenic and does not produce CPA because of the full deletion of its aflatoxin and CPA gene clusters. Further, RMb10 is in the IB lineage that is comprised of non-aflatoxigenic or low aflatoxin-producing L isolates of *A. flavus* and *A. oryzae* (Geiser et al. 2000). Preliminary competition trials with *A. flavus* aflatoxigenic strain NRRL 3357 in greenhouse and field trials showed that RMb10 reduced mean aflatoxin contamination by 90% (Table 4.1). This level of efficacy was comparable to that of Afla-Guard® which reduced mean aflatoxin contamination by 91% in these preliminary trials (Table 4.1). Here, we further examined the efficacy of RMb10 in replicated large-scale field trials on a regional scale in Alabama, Mississippi, North Carolina, and Texas in the southern United States with the following objectives: 1) determine the impact of RMb10 on the population dynamics of *A. flavus* in southern United States, and 2) assess the efficacy of RMb10 in mitigating aflatoxin contamination in maize grown in southern United States. Recent work has shown that shift towards lower aflatoxin levels can be greater if biocontrol products include strains of compatible mating type (Molo et al. 2019). Thus, it is conceivable that a biocontrol strain with a *MAT1-1* or *MAT1-2* mating type may be preferred for use in a specific environment based on the prevailing genetic structure of the native populations of *A. flavus*. Further, incorporating a complementary *MAT1-1* strain from lineage IB in a *MAT1-2* biocontrol formulation could also improve the efficacy

including long term effectiveness of biocontrol product, particularly in fields that harbor highly fertile strains of both mating types (Molo et al. 2019).

MATERIALS AND METHODS

Description of field sites. Field experiments were conducted in Alabama, Mississippi, North Carolina, and Texas in southern United States during the maize growing seasons in 2016 and 2017. Field experiment in Alabama was conducted only in 2017 while two field experiments were conducted in Mississippi in the same year. Field plots measuring at least 18 m long x 12 m wide with 9 m borders were adopted at all field sites in both years. In Alabama, experiments were conducted near Macon using the hybrid Pioneer 1197R that was planted in late April. Field experiments in Mississippi were conducted at Holocomb using the hybrid Augusta 7768 in 2016, and at Inverness (Mississippi_1) and Louise (Mississippi_2) using the hybrid DKC70-27 in 2017. Field plots in Mississippi were all planted in mid-April. In North Carolina, experiments were conducted at the Upper Coastal Plain Research Station in Rocky Mount using the maize hybrid NK-N78-3111 which was planted around mid-April in both years. In Texas, experiments were conducted at Backfield using the hybrid Integra 9673R in 2016 and DK62-05 in 2017. Plots were planted in late February and early March in respective years. Fertilization and weed control practices at each field site were performed according to standard management practices for maize production.

Weather data at each experimental site at the course of the study were obtained from the nearest state weather station or from the national weather database at the North Carolina State Climate Office in Raleigh, NC (http://www.nc-climate.ncsu.edu/cronos).

Treatments and experimental design. Three biocontrol treatments were evaluated in the study: (a) RMb10, a candidate biocontrol strain isolated from a maize field in Rocky Mount, North Carolina in 2012, (b) Afla-Guard® (Syngenta, United States), a commercial biocontrol agent labeled to reduce aflatoxin contamination in maize, and (c) sterilized wheat kernels which served as the untreated control. Treatments in Alabama were applied in early June in 2017. In Mississippi, treatments were applied in early June in 2016 and mid-June in 2017. In North Carolina, treatments were applied in late June in 2016 and mid-June in 2017. In Texas, treatments were applied in mid-April in 2016 and early May in 2017. Treatments were applied mechanically or manually by broadcasting the biocontrol product according to the recommended label rate of 10 lb/acre on top of the plant canopy. All field experiments were laid out in randomized complete block design with three to five replications.

Soil sample collection and preparation. Soil samples (approximately 100 g) were collected from 20 georeferenced points at approximately equal distances along two diagonals of each field site to assess densities of *A. flavus*. Soil samples were collected twice per growing season: (a) prior to the application of biocontrol treatments; and (b) at harvest. Soil samples were scraped from the top 10 cm layer of soil using sterile plastic scoops, placed in doubled-layered paper bags then transported to the laboratory for further processing. The first soil collection was generally conducted immediately before the application of biocontrol treatments, while the second collection was conducted immediately before harvest. The field experiment conducted in Alabama in 2017 was harvested in mid-October. In Mississippi, plots were harvested in mid-September in 2016 and mid-October in 2017. In North Carolina, plots were harvested in early September in both years. In Texas, plots were harvested in Mid-July in 2016 and late July in 2017. Soil samples

collected from Alabama, Mississippi, and Texas were refrigerated at 4°C until ready for shipment to North Carolina for processing.

Identification of *A. flavus* isolates and determination of colony forming units. Collected soil samples were air dried on a laboratory bench (25°C) for about 1 week until powder dry. Each sample was manually mixed and shaken for 1 min to homogenize soil contents. A subsample of 33 g was taken from different sections of the sample bag and added to 100 ml of 0.2% water agar. The soil-water agar suspension was shaken for 1 min and then plated on modified Dichloran Rose Bengal (mDRB) media as described by Horn and Dorner (1998). Aliquots of 200 µl of the soil-water agar suspension were evenly spread on the surface of mDRB media in 15-mm diameter Petri dishes (5 plates for each sample) using a sterile glass rod. The plates were incubated at 37°C for 3 days and then visually inspected for the growth of *Aspergillus* colonies. *A. flavus* colonies were identified based on colony morphology as described by Klich (2002) and Raper and Fennell (1965). Representative colonies were isolated onto 15-mm Petri dishes containing mDRB medium, incubated at 37°C for 5 days, and re-plated as needed to obtain pure cultures. Conidia from pure cultures were harvested using distilled water with 0.05% Triton-X and stored at -80°C for subsequent processing.

In addition, a subsample of 3 g soil from each bag was oven-dried at 65°C for 48 hours and then re-weighed to determine the amount of moisture loss. The resultant weights were used to calculate the soil moisture content and soil moisture correction factor to determine the number of *A. flavus* colony forming units (CFUs) per gram of dry soil.

DNA extraction, mating type identification and aflatoxin gene cluster type. Genomic DNA of *A. flavus* isolates was extracted using the DNeasy UltraClean Microbial Kit (Qiagen, Hilden, Germany) with some modifications to the manufacturer's protocol. These modifications

were: adding 4 µl RNAse A (10 ng/µl) during cell pellet suspension in 300 µl PowerBead solution for the removal of RNA; two rounds o of spore cell disruption by vortexing in MOBIO Vortex Adapter and Disruptor Genie (5 min each) then incubation at 60ºC for 10-20 min; and elution of DNA in 105 µl PCR-quality water. Final DNA concentration was measured using Qubit 2.0 Fluorometer (Invitrogen, Life Technologies, Singapore).

The mating type of each isolate was determined via multiplex PCR using *MAT1-1* and *MAT1-2* primers (Ramirez-Prado et al. 2008). PCR amplification was performed in 25 µl reactions containing 12.5 µl OneTaq® 2X MM with Standard Buffer (New England BioLabs Inc.), 0.5 µl each of forward and reverse primers, 10.5 µl PCR-quality water and 1 µl DNA (2 ng/µl). Reactions were run in a T100 Thermal Cycler (BIO-Rad T100, Singapore) with a thermal profile of 4 min at 94ºC for initial denaturation, followed by 30 cycles of 30 sec at 94ºC, 60 sec at 58ºC, 30 sec at 68ºC, and a final extension of 5 min at 68ºC. PCR products (5 µl + 1 µl loading dye) were analyzed using 1% agarose gels stained with 5% ethidium bromide in 1X TAE buffer. Isolates were designated as *MAT1-1* (396 bp) or *MAT1-2* (270 bp) using a 100 bp DNA ladder (Fisher Scientific International Inc.) as a size standard.

The aflatoxin gene cluster type of isolates was identified via multiplex PCR using three loci (*aflC, aflM* and *aflW*) located on chromosome 3 of the *A. flavus* genome (Moore et al. 2009). PCR amplification was performed in 25 µl reactions composed of 10 µl 2.0X Taq RED Master Mix (Apex Bioresearch Products), 1 µl each of forward and reverse primers, 12 µl PCR-quality water and 1 µl DNA (2 ng/ µl). These were run with a thermal profile of 95ºC for 5 min, followed by 30 cycles of 95ºC for 30 sec, 62ºC for 30 sec, 72ºC for 1 min, and a final extension of 72ºC for 3 min. PCR products (2 µl) were run in 1.5% agarose gels stained with 5% ethidium bromide in

1X TAE buffer. Isolates showing the presence of 0, 1-2, or 3 of the above loci were designated as having missing, partial, or full aflatoxin gene clusters, respectively.

Next generation multi-locus sequence typing (NGMLST). A total of 311 isolates of *A. flavus* were subjected to NGMLST to track the spread of the applied biocontrol strains of RMb10 and Afla-Guard®, and to detect changes in the population of native *A. flavus* in the field. Isolates were selected from different years, state, field site, and sampling date and further screened based on differences in colony color, sclerotia production (+/–), mating type (*MAT1-1* or *MAT1-2*), and aflatoxin gene cluster type (missing, partial, or full).

NGMLST was performed using a two-step PCR protocol to generate amplicons from the genomic DNA samples. The regions of interest (i.e., amplicon) were amplified in the first PCR (PCR1) using five locus-specific forward and reverse primers labeled with barcoded adaptors, resulting in an amplicon with overhang adaptor attached at the 5' end. In the second PCR (PCR2), 48 forward and primer reverse primers labeled with multiplexing index adaptors were added, resulting in an amplicon with multiplexing identifiers at both ends.

Barcoded primers used in PCR1 consists of three non-aflatoxin cluster loci (acetamidase *amdS* on chromosome 6, major facilitator superfamily *mfs* gene on chromosome 3, and tryptophan synthase *trpC* gene on chromosome 4) and two aflatoxin cluster loci (*aflM* and *aflW* on chromosome 3). Multiplex PCR1 was performed using KAPA HiFi HotStart PCR Kit (Kapa Biosystems, South Africa) in a 25 µl final volume composed of 0.5 µl Kapa DNA polymerase, 5 µl Kapa HiFi buffer, 0.75 µl dNTP mix (10 µM), 0.75 µl primer mix (10 µM), 8 µl PCR-quality water and 10 µl DNA (2 ng/µl). Thermal profiles comprised of 3 min at 95°C for initial denaturation, followed by 40 cycles of 20 sec at 98°C, 15 sec at 51°C, 15 sec at 72°C, and a final extension of 1 min at 72°C. Equal amounts of PCR1 products were combined by index and

suspended in PCR-quality water amounting to 1:10 dilution. One microliter of diluted PCR1 products were used as the template DNA for PCR2. PCR2 was performed using the same kit as PCR1 in a 50 µl final volume composed of 1 µl Kapa DNA polymerase, 10 µl Kapa HiFi buffer, 1.5 µl dNTP mix (10 mM), 2 µl forward primer (10 µM), 2 µl reverse primer (10 µM), and 32.5 µl PCR-quality water. Thermal profiles consisted of 3 min at 95°C for initial denaturation, followed by 10 cycles of 30 sec at 98°C, 20 sec at 68°C, 30 sec at 72°C, and a final extension of 5 min at 72°C. PCR2 products were cleaned using AxyPrep Mag™ PCR Clean-up Kit (Axygen BioSciences, Big Flats, NY) following the manufacturer's recommendations. Subsamples of 5 µl for each PCR2 product were submitted to North Carolina State University Genomic Sciences Laboratory (NCSU GSL) in Raleigh, North Carolina for TapeStation DNA analysis (Agilent 2200 TapeStation, D1000 Tapes) to check DNA integrity and quantify the amount of nucleic acids. Results of the TapeStation analysis were used to calculate the molarity of each indexed DNA sample. Lastly, 5 µl of each indexed sample (10 nM) were combined into a single Eppendorf tube and submitted to NCSU GSL for sequencing using MiSeq v.2 250 PE NANO flow cell.

Bioinformatics and sequencing analysis. DNA sequences obtained from NCSU GSL were processed using the DeCIFR Portal (https://decifr.hpc.ncsu.edu), a comprehensive web-based analysis portal of biodiversity informatics pipelines and visualization tools deployed at NCSU. Raw FASTQ files (96 forward and reverse read files) were converted into FASTA files using the NGMLST DeCIFR tool which implements DADA2 (Callahan et al. 2016) to identify the unique amplicon sequence variants (ASVs) for each sample. ASVs of the five loci for each isolate were linked together using the Concatenate Several Loci DeCIFR tool.

Population summary statistics for *aflM*, *aflW*, *amdS*, *mfs* and *trpC* were generated to infer different genetic aspects of *A. flavus* populations in the study. Nucleotide diversity (π) estimates,

population scaled mean mutation rate (θ), and neutrality tests based on Tajima's *D* (Tajima 1989) and Fu's *Fs* (Fu and Li 1993) were implemented in NeutralityTest (Li and Fu 2003). The maximum likelihood phylogenies of the isolates at different sampling periods, states and years were analyzed using Randomized Axelerated Maximum Likelihood (RAxML) (Stamatakis et al. 2008) and visualized using Tree-Based Alignment Selector (T-BAS) v.2.1. toolkit (Carbone et al. 2017; Carbone et al. 2019). Confidence limits of branches in the phylogenies were estimated from 1,000 rapid bootstrap replicates and branches having at least 70% bootstrap support were considered as monophyletic groups. Pairwise evolutionary distances or patristic distances from RMb10 and Afla-Guard® were calculated using DendroPy (Sukumaran and Holder 2010) to inspect probable recombination between the applied biocontrol and native strains. Patristic distances for *amdS*, *mfs* and *trpC* were individually displayed as a heat map via T-BAS v.2.1. in outer rings that surround the phylogenetic tree. For each locus phylogeny, a matrix of patristic distances that was normalized to a maximum value of 1 was generated for all pairs of sequences that represent individual isolates. The patristic distances calculated for the three loci were compared to identify incongruences in tree topologies which suggest genetic exchange and recombination. In contrast, congruent distances across tree topologies indicate clonal transmission and adaptation (Lewis et al. 2019).

Mating type distribution. The number of individuals containing *MAT1-1* and *MAT1-2* genes were counted per sampling period in each state and year. Individuals containing both mating types were counted twice as *MAT1-1* and *MAT1-2*. Isolates were clone corrected using *amdS*, *mfs*, *trpC*, *aflM*, and *aflW* to eliminate accidental sampling of the same individuals (Moore et al. 2013) and avoid overrepresentation of an isolate compared to the actual frequencies in the soil community (Islam et al. 2018).

Clone correction was implemented by counting the total number of unique haplotypes in each *MAT1-1* and *MAT1-2* category. The frequency of uncorrected and clone-corrected *MAT1-1* and *MAT1-2* isolates at each sampling period in each state per year was then tested for equal distribution using a two-tailed binomial test using PROC FREQ in SAS version 9.4 (SAS Institute, Cary, NC). Results showing a significant difference in the frequency of the two mating types in the uncorrected samples but not after clone correction suggests a population that is primarily undergoing sexual reproduction (Linde et al. 2003). A lack of a significant difference for both uncorrected and clone-corrected samples also suggests sexual reproduction, while a significant difference in mating type frequency before and after clone-correction suggests that the population is predominantly undergoing asexual reproduction (Leslie and Klein 1996; Linde et al. 2003).

Aflatoxin levels in harvested grain. Subsamples of 2.5 kg kernels from each field plot were dried to 15 to 17% moisture content. Dried kernels were homogenized using a Waring blender for 1 min, thoroughly mixed in a collection bag, then further subsampled for aflatoxin quantification. The aflatoxin content of maize kernels harvested in Alabama were measured using the Veratox Aflatoxin Kit (Neogen Corporation, Lansing, Michigan) with a detection limit of 2 ppb. Kernels in North Carolina were tested using QuickTox Kit for QuickScan Aflatoxin (Envirologix, Portland, Maine) and aflatoxin was quantified using the ACC 131 QuickScan System with a detection limit of 2.5 ppb. High performance liquid chromatography (HPLC) was used to quantify aflatoxin content for maize samples harvested in Mississippi and Texas.

Statistical analysis of soil population densities and aflatoxin contamination. Data for colony forming units (CFU) per gram of soil were collected for each sampling period, state and year. Mean CFUs were calculated and used to determine the difference in abundance of CFUs before treatment application and at harvest. Aflatoxin contents (ppb) in harvested grains were

analyzed for each field site at each state per year. Means of aflatoxin contents from treatment plots were subjected to analysis of variance using the PROC GLM of SAS. Differences between the mean aflatoxin contents of treatments were determined using Fisher's least significant differences (LSD) test.

RESULTS

Weather conditions. Daily air temperatures recorded at the field sites ranged from 12 to 34^{o}C in April to July of 2016 and 2017 (Table 4.2). The lowest temperature was recorded in North Carolina in 2016, while the highest temperature was recorded in Texas in both years. Daily mean temperatures during the maize planting months of April to May ranged from 18 to 22^{o}C. Daily mean temperatures were higher during the maize silking months of June to July and ranged from 25 to 29^{o}C. The lowest mean temperature of 18^{o}C was recorded in North Carolina in 2016 while the highest mean temperature of 29^{o}C was recorded in Texas in both years (Table 4.2).

Total accumulated rainfall recorded at the field sites ranged from 104 to 602 mm in April to July of 2016 and 2017 (Table 4.2). In 2016, total rainfall in April to May was low in Mississippi (147 mm) and North Carolina (168 mm), while high in Texas (358 mm). The corresponding total rainfall in June and July was low in Texas (140 mm) and Mississippi (170 mm) while high in North Carolina (602 mm). In 2017, total rainfall was lowest in Texas in April to May (104 mm) and June to July (246 mm). Total rainfall in the other states ranged from 279 to 353 mm in April to May, and 272 to 409 mm in June to July. Total rainfall recorded in the field sites were higher than their 10-year historical data except for Mississippi in April to May of 2016, Alabama in April to July of 2017, and Texas in April to May of 2017 (Table 4.2).

Soil population densities of *A. flavus* in the field. Mean and maximum population densities of *A. flavus* in the soil increased at harvest as compared to pre-application of biocontrol

treatments in both years in all states except in North Carolina in 2017 (Table 4.3). In 2016, population density prior to treatment application was lowest in Mississippi (3 CFU/g soil) and highest in North Carolina (32 CFU/g soil). Population density at harvest was lowest in Texas (25 CFU/g soil) and highest in Mississippi (369 CFU/g soil). In 2017, population density was lowest in Alabama (6 CFU/g soil) prior to treatment application and in North Carolina (5 CFU/g soil) at harvest. Population density was highest in North Carolina (32 CFU/g soil) before application of biocontrol and in the two field sites in Mississippi (246 and 264 CFU/g soil) at harvest (Table 4.3).

The application of biocontrol treatments increased the soil population densities at harvest (Table 4.3). The highest impact was observed in Mississippi in 2016 and 2017 (Inverness location) where the change in population densities were 123- and 30.8-fold higher at harvest than prior to application of treatments (Table 4.3). Moderate increases in population densities at harvest were observed in Mississippi (13.2-fold increase, Louise location) and Alabama (10.2-fold increase) in 2017. Limited increases in population densities were observed in North Carolina in 2016 (1.3-fold increase) and Texas in both years (2- and 1.6-fold increase, respectively). In contrast, a 0.2-fold decrease in population density was observed in North Carolina in 2017 (Table 4.3).

Genetic diversity in response to application of biocontrol strains. NGMLST using *amdS*, *mfs*, *trpC*, *aflM*, and *aflW* was used to determine the number of unique MLHs at each soil sampling period and assess shifts in genetic structure of *A. flavus* populations after the application of biocontrol treatments. A total of 23 unique MLHs were inferred based on 311 selected *A. flavus* isolates. Field populations exhibited higher number of MLHs prior to application of treatments than at harvest (Table 4.4). The total number of unique MLHs was lowest in North Carolina in 2016 (3 MLH) while the highest was in Alabama in 2017 (11 MLHs). Further, the number of

unique MLHs during sampling periods in Alabama (7 to 8 MLH) and Mississippi (3 to 9 MLH) were generally higher than in North Carolina (3 to 7 MLH) and Texas (4 to 10 MLH) (Table 4.4).

Based on the five loci used for NGMLST, RMb10 and the Afla-Guard® strains were grouped into the same haplotype (H1). Changes in the frequency of H1 isolates between sampling periods varied across states and years. The frequency of H1 isolates increased at harvest in Mississippi (37% increase) and Texas (22% increase) in 2016, and in Alabama (55% increase), North Carolina (22% increase) and Texas (32% increase) in 2017. The frequency of H1 isolates in North Carolina in 2016 (83%) did not change between sampling periods. On the other hand, the frequency of H1 isolates decreased at harvest in the two field sites in Mississippi in 2017 (22% decrease in Inverness and 43% decrease in Louise) (Figure 4.1).

Frequency and distribution of mating type genes and aflatoxin gene cluster type among haplotypes. The *A. flavus* populations in almost all field sites did not significantly ($P > 0.05$) deviate from the 1:1 mating type ratio in both uncorrected and haplotype corrected data using the exact binomial test (Table 4.5). The only exception was the near non-significant mating type ratio ($P = 0.0495$) of uncorrected data at pre-application of biocontrol treatments in Mississippi in 2016 wherein the population is skewed towards *MAT1-2* (Figure 4.2).

Isolates with full aflatoxin gene cluster were predominant for both uncorrected and haplotype corrected data among sampling periods across states in both years (Table 4.6; Figure 4.3). Despite their predominance, the frequency of isolates with full cluster generally decreased at harvest as compared to pre-application of biocontrol treatments. Highest decrease was observed in the haplotype corrected data in North Carolina and Texas in 2017. On the other hand, the number of isolates with missing cluster in the haplotype corrected data increased at harvest in Mississippi in both years and in North Carolina in 2017. In addition, *A. flavus* isolates with partial cluster

emerged at harvest in Mississippi in 2016 and in Mississippi, North Carolina, and Texas in 2017 (Table 4.6; Figure 4.3).

Population genetics and phylogenetic analyses. Nucleotide diversity (π) estimates varied across the five NGMLST loci within states, sampling periods and years (Tables 4.7 and 4.8). The specific ranges of π for the different loci were 196.372 to 230.946 for *aflM*, 77.186 to 205.286 for *aflW*, 7.796 to 45.500 for *amdS*, 16.512 to 170.339 for *mfs*, and 26.173 to 136.09 for t*rpC* (Table 4.7). When averaged across all loci, π was higher in North Carolina (π = 132.061) and Mississippi (π = 105.492) as compared to Texas (π = 95.871) and Alabama (π = 76.796) (Table 4.8). In terms of years, π was higher in 2016 (π = 116.148) than in 2017 (π = 88.747). Similar π estimates were observed between pre-application of biocontrol treatments (π = 103.905) and at harvest (π = 106.158) (Table 4.8).

The population scaled mean mutation rate (θ) averaged across all loci was slightly higher in Alabama (θ = 13.015), intermediate in North Carolina (θ = 12.135) and Texas (θ = 12.687), and lower in Mississippi (θ = 11.352) (Table 4.8). In addition, θ in 2016 (θ = 12.936) was higher than in 2017 (θ = 10.735). There were no observed differences in θ between sampling periods, where θ estimates was 12.321 prior to application of biocontrol treatments and 12.836 at harvest (Table 4.7).

Deviations from neutral mutation hypothesis and population size constancy were examined using Tajima's *D* and Fu's *Fs*. Tajima's *D* for all examined populations did not show significant ($P > 0.05$) deviations from neutrality (Table 4.8). Despite non-significance, positive Tajima's *D* values suggest excess of intermediate-frequency alleles and the populations were undergoing population subdivision or balancing selection. On the other hand, the significant ($P < 0.05$)

deviations from neutrality and negative values of Fu's *Fs* (Table 4.8) signify excess number of rare alleles as what is expected from a recent population growth or from genetic hitchhiking.

The multi-locus phylogenetic tree showed a high degree of homoplasy and low bootstrap values (<70%) for many internal branches (Figure 4.4). The majority of the isolates belonged to lineage IB which includes both RMb10 and Afla-Guard® strains. For both RMb10 and the Afla-Guard® strain, patristic distances were close to 0 across *amdS, mfs and trpC* suggesting extensive clonality within lineage IB while incongruent patristic distances across the three loci suggested recombination between lineages IB and IC.

Aflatoxin contamination in harvested grain. Levels of aflatoxin contamination in harvested maize kernels from treated and untreated plots in this study were generally very low except in Texas in 2016 (Figure 4.5). Aflatoxin contamination in Alabama, Mississippi and North Carolina only ranged from 0 to 9 ppb in 2016 to 2017. In the Texas field site in 2016, aflatoxin contamination in plots treated with RMb10 (48 ppb) and Afla-Guard® (54 ppb) were significantly ($P < 0.05$) lower than the untreated control plots (268 ppb) where aflatoxin contamination was reduced by 82% and 80%, respectively.

DISCUSSION

Aspergillus flavus is considered as a threat to maize production due to its ability to contaminate kernels with the carcinogen aflatoxin (Klich 2007; Mitchell et al. 2016). At the same time, the use of non-aflatoxigenic strains of *A. flavus* through biocontrol is currently the most promising strategy to reduce pre-harvest aflatoxin contamination in maize and other crops (Ehrlich et al. 2015; Ojiambo et al. 2018). Afla-Guard® and AF36 are the only two commercial biocontrol products registered in the United States. AF36 is limited for use in maize in Arizona and Texas

(EPA 2015) while Afla-Guard® is not restricted to specific states (EPA 2013). Both biocontrol products are of the mating type *MAT1-2*, while no *MAT1-1* biocontrol strain has yet been reported. In addition, the populations of native *A. flavus* in field soils are very diverse in terms of morphology, sclerotia production and/or aflatoxin biosynthesis (Geiser et al. 2000) and may respond differently to the applied biocontrol strain (Abbas 2011). Thus, it is unlikely that a particular biocontrol strain will be the "one size fits all" strategy and outcompete native populations in all locations (Ehrlich 2014). This led to an increasing interest to identify new biocontrol strains that match the genetic structure and can compete with native *A. flavus* populations. In this study, we assessed the impact of using a candidate biocontrol strain RMb10 on the population dynamics of native *A. flavus* populations and in mitigating aflatoxin contamination in maize fields in the southern United States. Genetic variability among isolates within each field site was examined using next generation multi-locus sequence typing (NGMLST) of the *amdS*, *mfs*, *trpC*, *aflM* and *aflW* genes. A total of 23 unique multi-locus haplotypes were detected in the study with RMb10 and Afla-Guard® biocontrol strains being designated as haplotype H1.

Differences in the densities of *A. flavus* populations in the soil were observed among states. Prior to application of biocontrol treatments, *A. flavus* populations were high in North Carolina, moderate in Texas, low in Alabama, and variable in Mississippi. These differences in population densities may be attributed to differences in temperature, frequency of drought, crop history, soil composition, management practices and cropping systems (Horn and Dorner 1998). Growth of the fungus is favored by temperatures ranging between 25°C to 42°C with an optimum temperature of 37°C (Payne 1998; Schmidt-Heydt et al. 2009). At harvest, high to moderate increases in population densities were observed in Mississippi and Alabama, while limited increases or

decrease in population densities were observed in North Carolina and Texas. The observed increase in *A. flavus* populations in Mississippi in 2016, Alabama in 2017, and Texas in both years can be attributed to the successful growth and spread of RMb10 and Afla-Guard® biocontrol strains as evidenced by the increase in the frequency of H1 isolates at harvest in these field sites. The increase in *A. flavus* populations in Mississippi in 2017 may be caused by other ecological factors instead of simple dose-response to the application of biocontrol strains (Lewis et al. 2019) as the frequency of H1 isolates decreased by 22 to 43% in the two field sites. Despite the limited increase (2016) or decrease (2017) in *A. flavus* populations in North Carolina, the frequency of H1 isolates remained high (61 to 83%) between sampling periods in both years implying that the soil population probably consists of non-aflatoxigenic strains even before application of biocontrol.

The biocontrol strains used in this study belong to different mating types. RMb10 belongs to *MAT1-1*, while Afla-Guard® belongs to *MAT1-2.* In *A. flavus*, the *MAT1-1* gene encodes an α-domain transcription factor, while *MAT1-2* gene encodes a high mobility group-domain transcription factor (Ramirez-Prado et al. 2008). A greater number of *MAT1-2* haplotypes were observed in the different field sites in 2016, while the frequency of *MAT1-1* haplotypes increased in 2017. However, the mating type distribution of the different *A. flavus* populations did not deviate from the 1:1 mating type ratio in both uncorrected and haplotype corrected data when examined using exact binomial test. This observation is suggestive of recombining populations underdoing sexual reproduction. The only exemption was with the uncorrected data prior to application of biocontrol treatments in Mississippi in 2016 though the mating type ratio was nearly non-significant (P = 0.0495) and progressed to 1:1 mating type distribution at harvest. Similar occurrences of recombination in field samples have been previously reported (Ramirez-Prado et al. 2008; Horn et al. 2016; Lewis et al. 2019).

Changes in the frequency of isolates with full, partial, and missing aflatoxin gene clusters were observed between sampling periods and years. Aflatoxin gene cluster type was identified based on the presence or absence of *aflC*, *aflM* and *aflW* genes. Both RMb10 and Afla-Guard® biocontrol strains have missing clusters. Isolates with intact full clusters have the potential to produce aflatoxin while those with gene deletions (partial clusters) and missing clusters have lost their aflatoxin-producing ability (Chang et al. 2005). Although there was predominance of isolates with full clusters throughout the duration of the study, the frequency of isolates with missing clusters at harvest increased in North Carolina in 2017 and in Mississippi in both years. This increased frequency of isolates with missing clusters provides further support that the biocontrol strains have successfully grown and spread into the field populations. Isolates with partial clusters was first observed at harvest in Mississippi in 2016. Similarly in 2017, isolates with partial clusters were observed at harvest in Mississippi (Louise location), North Carolina and Texas and most likely resulted from sexual recombination between the applied biocontrol strains and native population. As observed by Molo (2018), sexual recombination in treated plots occurs three months after application of biocontrol. The emergence of isolates with partial clusters may also be due to migration of individuals with partial clusters from surrounding areas into these fields. Isolates with full, partial, and missing clusters were observed in both sampling periods in Alabama indicating that the native *A. flavus* populations within this field are diverse, as further supported by high number of unique MLH in this state in both sampling periods.

There have been concerns that recombination between biocontrol and native strains has the potential to generate highly aflatoxigenic progenies within the population (Moore 2014). However, there is no documentation showing increased aflatoxin concentrations in fields that were applied with AF36 (Grubisha and Cotty 2015) or other biocontrol products. In addition, unlike AF36 which

has a full aflatoxin cluster (Ehrlich and Cotty 2004), RMb10 and Afla-Guard® have missing clusters and are expected to have lower probabilities of generating aflatoxigenic progeny strains. As shown by Olarte et al. (2012), the incidence of producing aflatoxigenic progenies with Afla-Guard® as parent (36%) was lower than crosses which involved AF36 (58%) because replacement with a functional *pksA* gene in AF36 progeny can promote aflatoxin biosynthesis while the re-acquisition of the full aflatoxin gene cluster in Afla-Guard® progeny is unlikely to occur.

Deviations from the hypothesis of neutral mutation was examined using Tajima's *D* and Fu's *Fs*. Tajima's *D* for all populations were not significant but the positive values observed from the five loci indicate a model of population subdivision or balancing selection. As observed, individuals with both mating types and different in aflatoxin gene cluster composition are maintained in the populations. Values for Fu's *Fs* were all significant and negative indicating that the population is undergoing population growth as has been shown with the increase in soil densities at harvest. The maximum likelihood phylogeny inferred using 311 *A. flavus* isolates showed that RMb10, Afla-Guard®, and most of the collected isolates belong to lineage IB. This lineage is comprised of non-aflatoxigenic strains, low-aflatoxin-producing strains and *A. oryzae* (Geiser et al. 2000). The predominance of lineage IB isolates suggest that the soil populations in the fields can be shifted to a more non-aflatoxigenic IB lineage (Lewis et al. 2019). A sizeable number of isolates belong to lineage IC which is composed of both aflatoxigenic and non-aflatoxigenic strains (Geiser et al. 2000). Four isolates belong to lineage IA which is a lineage composed of toxigenic strains (Geiser et al. 2000). No distinct clustering of strains was observed based on mating type, sampling period, state, or year which suggests active genetic exchange between isolates in the population. The presence of blue, red and intermediate colors in the patristic

distance trees inferred using *amdS*, *trpC*, and *mfs* indicate a mixed genetic background and recombination between strains from lineages IB and IC.

The aflatoxin levels in this study were generally very low except in Texas in 2016. Despite being conducive for the growth of *A. flavus*, weather conditions were not ideal for aflatoxin production. Additionally, the soil density of *A. flavus* does not necessarily predict the frequency of seed infection and hence aflatoxin contamination (Horn and Dorner 1998). The ideal temperature for aflatoxin production is between 29 to 30ºC and levels are significantly reduced at temperatures beneath 25°C or approaching 37°C and above (Bhatnagar et al. 2006; Schmidt-Heydt et al. 2009). High temperatures accompanied by periods of drought during the reproductive stages of the crop, which corresponds to June to July in this study, increase the chances of aflatoxin contamination (Kebede et al. 2012). The small window of temperatures conducive for aflatoxin production partly explains why significant levels of aflatoxin were detected only in Texas in 2016. Moreover, total accumulated rainfall was higher in Alabama, Mississippi and North Carolina. Other factors such as soil pH, corn variety and farmer practices may have also affected the observed differences in aflatoxin levels. It is also possible that aflatoxin was not produced due to high proportion of native non-aflatoxigenic isolates in the soil such as in North Carolina. The significantly lower aflatoxin contents in corn kernels treated with RMb10 and Afla-Guard® compared to the untreated plots suggests that RMb10 is a promising candidate as a biocontrol strain against aflatoxin contamination in corn. As suggested by Molo et al. (2019), it is also likely that a biocontrol product that is formulated to contain both RMb10 and Afla-Guard could potentially provide a more sustainable reduction in aflatoxin levels. Additional competition studies with single and combinations of RMb10 and Afla-Guard are recommended to assess the effectiveness of this hypothesis.

ACKNOWLEDGMENTS

This study was supported by a grant from Aflatoxin Mitigation Center for Excellence and the National Corn Growers Association Award No. 2016-0949. We thank Yaken Samah Ameen and Greg O'Brian for their assistance in soil sample collection and processing of *A. flavus* isolates; Richard Gell for guidance in designing experiments for amplicon sequencing; and, James White for assistance in using the toolkits in DeCIFR.

REFERENCES

Abbas HK, Zablotowicz RM, Horn BW, Phillips NA, Johnson BJ, Jin X, Abel CA. 2011. Comparison of major biocontrol strains of non-aflatoxigenic *Aspergillus flavus* for the reduction of aflatoxins and cyclopiazonic acid in maize. *Food Addit Contam* **28**:198-208.

Bandyopadhyay R, Ortega-Beltran A, Akande A, Mutegi C, Atehnkeng J, Kaptoge L, Senghor AL, Adhikari BN, Cotty PJ. 2016. Biological control of aflatoxins in Africa: current status and potential challenges in the face of climate change. *World Mycotoxin J* **9**:771-789.

Bhatnagar D, Cary JW, Ehrlich K, Yu J, Cleveland TE. 2006. Understanding the genetics of regulation of aflatoxin production and *Aspergillus flavus* development. *Mycopathologia* **162**:155-166.

Callahan BJ, McMurdie PJ, Rosen MJ, Han AW, Johnson AJA, Holmes SP. 2016. DADA2: high resolution sample inference from Illumina amplicon data. *Nature Methods* **13**:581-583.

Carbone I, White JB, Miadlikowska J, Arnold AE, Miller MA, Magain N, U'Ren JM and Lutzoni F. 2019. T-BAS version 2.1: Tree-Based Alignment Selector toolkit for evolutionary placement of DNA sequences and viewing alignments and specimen metadata on curated and custom trees. *Microbiol Resourc Announc* **8**:e00328-19. Doi: 10.1128/MRA.00328-19.

Carbone I, White JB, Miadlikowska J, Arnold AE, Miller MA, Kauff F, U'Ren JM, May G, Lutzoni F. 2017. T-BAS: Tree-Based Alignment Selector toolkit for phylogenetic-based placement, alignment downloads, and metadata visualization; an example with the Pezizomycotina tree of life. *Bioinformatics* **33**:1160-1168.

CAST. 2003. Mycotoxins: risks in plant, animal, and human systems. Council for Agricultural Science and Technology, pp. 1-199. *Task Force Report*. Ames, IA.

Chang PK, Horn BW, Abe K, Gomi K. 2014. *Aspergillus*, p 77-82. *In* Batt CA, Tortorello ML (ed), *Encyclopedia of food microbiology, Vol 1*. Academic Press, Elsevier Ltd.

Chang PK, Abbas HK, Weaver MA, Ehrlich KC, Scharfenstein LL, Cotty PJ. 2012. Identification of genetic defects in the atoxigenic biocontrol strain *Aspergillus flavus* K49 reveals the presence of a competitive recombinant group in field populations. *Int J Food Microbiol* **154**:192-196.

Chang PK, Horn BW, Dorner JW. 2005. Sequence breakpoints in the aflatoxin biosynthesis gene cluster and flanking regions in nonaflatoxigenic *Aspergillus flavus* isolates. *Fungal Genet Biol* **42**:914-923.

Cotty PJ, Bayman DS, Egel DS, Elias KS. 1994. Agriculture, aflatoxins and *Aspergillus*, p 1-27. *In* Powell K (ed), *The genus Aspergillus*. Plenum Press, New York.

Cotty PJ. 1989. Virulence and cultural characteristics of two *Aspergillus flavus* strains pathogenic on cotton. *Phytopathology* **79**:808-814.

Damann KJ. 2015. Atoxigenic *Aspergillus flavus* biological control of aflatoxin contamination: what is the mechanism? *World Mycotoxin J* **8**:235-244.

Diener UL, Cole RJ, Sanders TH, Payne GA, Lee LS, Klich MA. 1987. Epidemiology of aflatoxin formation by *Aspergillus flavus*. *Annu Rev Phytopathol* **25**:249-270.

Dorner JW. 2005. Biological control of aflatoxin crop contamination, p 333-352. *In* Abbas HK (ed), *Aflatoxin and food safety*. CRC Press, Boca Raton, Florida.

Dorner JW, Cole RJ, Lomax LG, Gosser HS, Diener UL. 1983. Cyclopiazonic acid production by *Aspergillus flavus* and its effects on broiler chickens. *Appl Environ Microbiol* **46**:698-703.

Ehrlich KC, Moore GG, Mellon JE, Bhatnagar D. 2015. Challenges facing the biological control strategy for eliminating aflatoxin contamination. *World Mycotoxin J* **8**:225-233.

Ehrlich KC. 2014. Non-aflatoxigenic *Aspergillus flavus* to prevent aflatoxin contamination in crops: advantages and limitations. *Front Microbiol* **5**:1-9.

Ehrlich K, Cotty P. 2004. An isolate of *Aspergillus flavus* used to reduce aflatoxin contamination in cottonseed has a defective polyketide synthase gene. *Appl Microbiol Biotechnol* **65**:473-478.

EPA. 2015. *Aspergillus flavus* AF36 Prevail. United States Environmental Protection Agency. Retrieved Oct 1, 2018. Available from https://www3.epa.gov/pesticides/chem_search/ppls/071693-00002-20150625.pdf.

EPA. 2013. Afla-Guard® GR. United States Environmental Protection Agency. Retrieved Oct 1, 2018. Available from https://www3.epa.gov/pesticides/chem_search/ppls/000100-01469-20130805.pdf.

Fu YX, Li WH. 1993. Statistical tests of neutrality of mutations. *Genetics* **133**:693-709.

Geiser DM, Dorner JW, Horn BW, Taylor JW. 2000. The phylogenetics of mycotoxin and sclerotium production in *Aspergillus flavus* and *Aspergillus oryzae*. *Fungal Genet Biol* **31**: 169-179.

Grubisha LC, Cotty PJ. 2015. Genetic analysis of the *Aspergillus flavus* vegetative compatibility group to which a biological control agent that limits aflatoxin contamination in U.S. crops belongs. *Appl Environ Microbiol* **81**:5889-5899.

Horn BW, Gell RM, Singh R, Sorensen RB, Carbone I. 2016. Sexual reproduction in *Aspergillus flavus* sclerotia: acquisition of novel alleles from soil populations and uniparental mitochondrial inheritance. *PLoS One* **11**:e0146169. Doi:10.1371/journal.pone.0146169.

Horn BW, Dorner JW. 1998. Soil populations of *Aspergillus* species from section *Flavi* along a transect through peanut-growing regions of the United States. *Mycologia* **90**:767-776.

Huang C, Jha A, Sweany R, DeRobertis C, Damann KEJ. 2011. Intraspecific aflatoxin inhibition in *Aspergillus flavus* is thigmoregulated, independent of vegetative compatibility group and is strain dependent. *PloS One* **6**:e23470. Doi:10.1371/journal.pone.0023470.

Islam MS, Callicott KA, Mutegi C, Bandyopadhyay R, Cotty PJ. 2018. *Aspergillus flavus* resident in Kenya: high genetic diversity in an ancient population primarily shaped by clonal reproduction and mutation-driven evolution. *Fungal Ecol* **35**:20-33.

Kebede H, Abbas HK, Fisher DK, Bellaloui N. 2012. Relationship between aflatoxin contamination and physiological responses of corn plants under drought and heat stress. Toxins **4**:1385-1403.

King ED, Bassi ABJ, Ross DC, Druebbisch B. 2011. An industry perspective on the use of "atoxigenic" strains of *Aspergillus flavus* as biological control agents and the significance of cyclopiazonic acid. *Toxin Rev* **30**:33-41.

Klich MA. 2007. *Aspergillus flavus*: the major producer of aflatoxin. *Mol Plant Pathol* **8**:713-722.

Klich MA. 2002. Identification of common *Aspergillus* species, p 1-116. Centraalbureau voor chimmelcultures, Utrecht, Netherlands.

Leslie JF, Klein KK. 1996. Female fertility and mating type effects on effective population size and evolution in filamentous fungi. *Genetics* **144**:557-567.

Lewis MH, Carbone I, Luis JM, Payne GA, Bowen KL, Hagan AK, Kemerait R, Heiniger R, Ojiambo PS. 2019. Biocontrol strains differentially shift the genetic structure of indigenous soil populations of *Aspergillus flavus*. *Front Microbiol* **10**:1738. doi: 10.3389/fmicb.2019.01738

Li H, Fu YX. 2003. NeutralityTest: novel software for performing tests of neutrality. *Bioinformatics*, submitted.

Linde CC, Zala M, Ceccarelli S, McDonald BA. 2003. Further evidence of for sexual reproduction in *Rhynchosporum secalis* based on distribution and frequency of mating-type alleles. *Fungal Genet Biol* **40**:115-125.

Mitchell NJ, Bowers E, Hurburgh C, Wu F. 2016. Potential economic losses to the USA corn industry from aflatoxin contamination. *Food Addit Contam* **33**:540-550.

Molo MS, Heiniger RW, Boerema L, Carbone I. 2019. Trial summary on the comparison of various non-aflatoxigenic strains of *Aspergillus flavus* on mycotoxin levels and yield in maize. *Agron J* **111**:942-946.

Molo M, Heiniger R, Boerema L, Carbone I. 2019. A response to the letter to the editor from Ortega-Beltran and Bandyopadhyay. *Agron J* **111**:1–3.

Molo MS. 2018. Population genetics of biological control in *Aspergillus flavus*. Ph.D. dissertation, North Carolina State University. Retrieved Sep 26, 2019. Available from https://repository.lib.ncsu.edu/handle/1840.20/35756.

Moore GG. 2014. Sex and recombination in aflatoxigenic Aspergilli: global implications. *Front Microbiol* **5**:32. Doi: 10.3389/fmicb.2014.00032.

Moore GG, Elliot JL, Singh R, Horn BW, Dorner JW, Stone EA, Chulze SN, Barros GG, Manjunath KN, Wright GC, Hell K, Carbone I. 2013. Sexuality generates diversity in the aflatoxin gene cluster: evidence on a global scale. *PloS Pathogens* **9**:e1003574. Doi:10.1371/journal.ppat.1003574.

Moore GG, Singh R, Horn BW, Carbone I. 2009. Recombination and lineage-specific gene loss in the aflatoxin gene cluster of *Aspergillus flavus*. *Mol Ecol* **18**:4870-4887.

Nei M, Li WH. 1979. Mathematical model for studying genetic variation in terms of restriction endonucleases. *Proc Natl Acad Sci USA* **76**:5269-5273.

NCGA. 2018. World of corn 2018. National Corn Growers Association. Retrieved Sep 24, 2018. Available from http://www.worldofcorn.com/#/.

Ojiambo PS, Battilani P, Cary JW, Blum BH, Carbone I. 2018. Cultural and genetic approaches to manage aflatoxin contamination: recent insights provide opportunities for improved control. *Phytopathology* **108**:1024-1037.

Olarte RA, Horn BW, Dorner JW, Monacell JT, Singh R, Stone EA, Carbone I. 2012. Effect of sexual recombination on population diversity in aflatoxin production by Aspergillus flavus and evidence for cryptic heterokaryosis. *Mol Ecol* **21**:1453-1476.

Payne GA. 1998. Process of contamination by aflatoxin producing fungi and their impacts on crops, p 279-300. *In* Sinha KK, Bhatnagar D (eds). *Mycotoxins in Agriculture and Food Safety*. Marcel Dekker Inc., New York.

Probst C, Bandyopadhyay R, Price LE, Cotty PJ. 2011. Identification of atoxigenic *Aspergillus flavus* isolates to reduce aflatoxin contamination of maize in Kenya. *Plant Dis* **95**:212-218.

Ramirez-Prado JH, Moore GG, Horn BW, Carbone I. 2008. Characterization and population analysis of the mating-type genes in *Aspergillus flavus* and *Aspergillus parasiticus*. *Fungal Genet Biol* **45**:1292-1299.

Raper KB, Fennell DI. 1965. The genus *Aspergillus*, p 1-686. The Williams & Wilkins Co, Baltimore.

Schmidt-Heydt M, Abdel-Hadi A, Magan N, Geisen R. 2009. Complex regulation of the aflatoxin biosynthesis gene cluster of *Aspergillus flavus* in relation to various combinations of water activity and temperature. *Int J of Food Microbiol* **135**:231-237.

Stamatakis A, Hoover P, Rougemont J. 2008. A rapid bootstrap algorithm for the RAxML web servers. *Systemic Biol* **57**:758-771.

Statista. 2018a. Global grain production by type, 2016/2017 | Statistic. The Statistics Portal. Retrieved Sep 25, 2018. Available from https://www.statista.com/statistics/272536/ acreage- of-grain-worldwide-by-type/.

Statista. 2018b. Grain production worldwide by type, 2017/2018 | Statistic. The Statistics Portal. Retrieved Sep 25, 2018. Available from https://www.statista.com/statistics/263977/world-grain-production-by-type/.

Sukumaran J, Holder MT. 2010. DendroPy: a Python library for phylogenetic computing. *Bioinformatics* **26**:1569-1571.

Tajima F. 1989. Statistical method for testing the neutral mutation hypothesis by DNA polymorphism. *Genetics* **123**:585-595.

USDA-FAS. 2018. Grain: World markets and trade. United States Department of Agriculture - Foreign Agricultural Service. Retrieved Sep 24, 2018. Available from https://apps.fas.usda.gov/psdonline/circulars/grain.pdf.

USDA-NASS. 2018. National Statistics for Corn. United States Department of Agriculture - National Agricultural Statistics Service. Retrieved Sep 24, 2018. Available from https://www.nass.usda.gov/Statistics_by_Subject/.

Villers P. 2014. Aflatoxins and safe storage. *Front Microbiol* **5**:158. Doi: 10.3389/fmicb.2014.00158

Watterson GA. 1975. On the number of segregating sites in genetical models without recombination. *Theor Popul Biol* **7**:256-276.

Wild CP. 2007. Aflatoxin exposure in developing countries: the critical interface of agriculture and health. *Food Nutr Bull* **28**:S380. Doi:10.1177/15648265070282S217.

Table 4.1. Preliminary assessment of candidate biocontrol strains for reducing aflatoxin contamination in maize. Aflatoxin concentration (parts per billion, ppb) and percent reduction in aflatoxin contamination are based on co-inoculation of biocontrol strains with toxigenic *A. flavus* strain NRRL 3357.

Strain	State	Mating type	Aflatoxin concentration (ppb)			Reduction (%)		
			Greenhouse[a]	Field	Mean	Greenhouse[a]	Field	Mean
13RMb16	North Carolina	*1-1*	783	877	825	1.5	16	6
12ALb84	Alabama	*1-1*	243	553	334	69.5	47	62
12RMa41	North Carolina	*1-2*	307	136	263	61.5	87	70
12RMb10	North Carolina	*1-1*	88	84	88	89	92	90
K49	Mississippi	*1-2*	684	804	729	14	23	17
Afla-Guard®	Georgia	*1-2*	56	136	79	93	87	91
Control	--	--	795	1044	878	439	1044	878

[a] Aflatoxin concentration and percent reduction values indicated in the columns are average of two greenhouse trials. All trials were conducted in Mississippi in 2015 and values are a mean of four replications.

Table 4.2. Daily mean, maximum, minimum air temperatures, and accumulated rainfall recorded at the field sites in Alabama, Mississippi, North Carolina and Texas in April to July of 2016 and 2017.

Weather Variable	2016			2017				Historical Average (2009 - 2018)			
	MS	NC	TX	AL[a]	MS	NC	TX	AL	MS	NC	TX
Mean Temperature (°C)											
April - May	20	18	21	21	19	20	22	21	18	19	21
June - July	28	26	29	26	25	26	29	28	26	25	29
Max Temperature (°C)											
April - May	26	23	26	27	27	26	27	26	27	25	27
June - July	33	32	34	31	32	31	34	31	32	29	33
Min Temperature (°C)											
April - May	14	12	16	14	16	14	16	14	15	11	13
June - July	22	20	24	22	22	20	23	25	21	20	24
Accumulated Rainfall (mm)											
April - May	147	168	358	353	279	290	104	361	170	147	173
June - July	170	602	140	409	335	272	246	625	165	150	104

[a] No soil samples were collected in Alabama in 2016.

Table 4.3. Soil population densities of *A. flavus* prior to application of RMb10 and Afla-Guard® biocontrol strains, and at harvest in maize fields in southern United States.

Year	State	Pre-application (CFU/g soil)[a]		Harvest (CFU/g soil)[a]		ΔCFU[b]
		Mean	Maximum	Mean	Maximum	
2016[c]	Mississippi	3	14	369	979	123.0
	North Carolina	32	138	63	197	2.0
	Texas	20	47	25	88	1.3
2017	Alabama	6	18	61	541	10.2
	Mississippi_1	8	33	246	851	30.8
	Mississippi_2	20	184	264	1208	13.2
	North Carolina	32	76	5	19	-0.2
	Texas	14	43	22	95	1.6

[a] Maximum and mean numbers of colony forming units (CFU) per gram of soil were calculated from 20 soil samples collected at each field site per sampling period.

[b] ΔCFU indicates positive or negative change in CFU at harvest relative to CFU at pre-application of biocontrol agents. ΔCFU = (x/y), where x refers to CFU at harvest, and y refers to CFU at pre-application of biocontrol agents.

[c] Soil samples were not collected in Alabama in 2016.

Table 4.4. Number of unique multi-locus haplotypes (MLHs) inferred from populations of *A. flavus* in maize fields in southern United States treated with RMb10 and Afla-Guard® biocontrol strains in 2016 and 2017.

Year	Sampling period	Alabama	Mississippi_1	Mississippi_2	North Carolina	Texas
2016[a]	Pre-application	-- [a]	9 (21)	-- [a]	3 (12)	4 (25)
	Harvest	-- [a]	6 (17)	-- [a]	3 (21)	5 (14)
	Total[c]	-- [a]	10 (38)	-- [a]	3 (33)	4 (39)
2017	Pre-application	8 (25)[b]	3 (8)	7 (16)	7 (23)	10 (24)
	Harvest	7 (22)	9 (19)	7 (15)	3 (24)	5 (23)
	Total[c]	11 (47)	10 (27)	10 (31)	4 (47)	8 (47)

[a] In 2016, soil samples were not collected in Alabama, and soil samples were only collected in one field site in Mississippi.

[b] Numbers presented in parentheses refer to number of isolates examined.

[c] Totals refer to the sum of the number of unique MLHs in each state for each year.

Table 4.5. Frequency of the mating type (*MAT*) genes among *A. flavus* isolates in maize fields in southern United States treated with RMb10 and Afla-Guard® biocontrol strains in 2016 and 2017.

Year	State	Sampling period[a]	Genetic scale[b]	Mating type frequency[c]		*P*-value[d]
				MAT1-1	*MAT1-2*	
2016	Mississippi	Pre-application	Uncorrected	28.6 (6)	71.4 (15)	0.0495
			Haplotype Corrected	40.0 (4)	60.0 (6)	0.5271
		Harvest	Uncorrected	35.3 (6)	64.7 (11)	0.2253
			Haplotype Corrected	37.5 (3)	62.5 (5)	0.4795
	North Carolina	Pre-application	Uncorrected	58.3 (7)	41.7 (5)	0.5637
			Haplotype Corrected	75.0 (3)	25.0 (1)	0.3173
		Harvest	Uncorrected	31.8 (7)	68.2 (15)	0.0881
			Haplotype Corrected	40.0 (2)	60.0 (3)	0.6547
	Texas	Pre-application	Uncorrected	40.7 (11)	59.3 (16)	0.3359
			Haplotype Corrected	40.0 (2)	60.0 (3)	0.6547
		Harvest	Uncorrected	40.0 (6)	60.0 (9)	0.4386
			Haplotype Corrected	50.0 (4)	50.0 (4)	1.0000
2017	Alabama	Pre-application	Uncorrected	60.0 (15)	40.0 (10)	0.3173
			Haplotype Corrected	70.0 (7)	30.0 (3)	0.2059
		Harvest	Uncorrected	45.5 (10)	54.5 (12)	0.6698
			Haplotype Corrected	33.3 (3)	66.7 (6)	0.3173
	Mississippi_1	Pre-application	Uncorrected	37.5 (3)	62.5 (5)	0.4791
			Haplotype Corrected	25.0 (1)	75.0 (3)	0.3173
		Harvest	Uncorrected	35.0 (7)	65.0 (13)	0.1797
			Haplotype Corrected	30.0 (3)	70.0 (7)	0.2059
	Mississippi_2	Pre-application	Uncorrected	56.3 (9)	43.8 (7)	0.6171
			Haplotype Corrected	60.0 (6)	40.0 (4)	0.5271
		Harvest	Uncorrected	66.7 (10)	33.3 (5)	0.1967
			Haplotype Corrected	75.0 (6)	25.0 (2)	0.1573
	North Carolina	Pre-application	Uncorrected	60.9 (14)	39.1 (9)	0.2971
			Haplotype Corrected	66.7 (6)	33.3 (3)	0.3173
		Harvest	Uncorrected	66.7 (16)	33.3 (8)	0.1025
			Haplotype Corrected	60.0 (3)	40.0 (2)	0.6547

Table 4.5 (continued)

Texas	Pre-application	Uncorrected	58.3 (14)	41.7 (10)	0.4142
		Haplotype Corrected	66.7 (8)	33.3 (4)	0.2482
	Harvest	Uncorrected	62.5 (15)	37.5 (9)	0.2207
		Haplotype Corrected	57.1 (4)	42.9 (3)	0.7055

[a] Sampling period indicates the time when soil samples were collected from the field in relation to the application of biocontrol strains.

[b] Mating type designation was based on either uncorrected or corrected haplotype data. Haplotype correction was implemented by counting the total number of unique multi-locus haplotypes (MLHs) in each *MAT1-1* and *MAT1-2* category.

[c] Numbers presented in parentheses refer to number of individuals for uncorrected genetic scale or number of unique MLHs for corrected genetic scale.

[d] Probability from a two-tailed exact binomial test performed under the null hypothesis of no significant difference in the frequency of isolates with *MAT1-1* and *MAT1-2* genes.

Table 4.6. Frequency of aflatoxin gene cluster types among *A. flavus* isolates in maize fields in southern United States treated with RMb10 and Afla-Guard® biocontrol strains in 2016 and 2017.

Year	State	Sampling period[a]	Genetic scale[b]	Aflatoxin gene cluster[c]		
				Full	Partial	Missing
2016[d]	Mississippi	Pre-application	Uncorrected	13	0	8
			Haplotype Corrected	7	0	1
		Harvest	Uncorrected	8	1	8
			Haplotype Corrected	5	1	3
	North Carolina	Pre-application	Uncorrected	9	0	3
			Haplotype Corrected	3	0	1
		Harvest	Uncorrected	10	2	9
			Haplotype Corrected	3	0	1
	Texas	Pre-application	Uncorrected	18	0	7
			Haplotype Corrected	4	0	1
		Harvest	Uncorrected	9	0	5
			Haplotype Corrected	4	0	1
2017	Alabama	Pre-application	Uncorrected	14	3	8
			Haplotype Corrected	6	1	2
		Harvest	Uncorrected	9	2	11
			Haplotype Corrected	6	1	1
	Mississippi_1	Pre-application	Uncorrected	3	0	5
			Haplotype Corrected	3	0	1
		Harvest	Uncorrected	5	5	9
			Haplotype Corrected	4	5	1
	Mississippi_2	Pre-application	Uncorrected	9	0	7
			Haplotype Corrected	7	0	1
		Harvest	Uncorrected	7	0	8
			Haplotype Corrected	5	0	3
	North Carolina	Pre-application	Uncorrected	10	0	13
			Haplotype Corrected	7	0	1
		Harvest	Uncorrected	8	2	14
			Haplotype Corrected	3	1	2
	Texas	Pre-application	Uncorrected	15	1	8
			Haplotype Corrected	8	1	2
		Harvest	Uncorrected	14	2	7
			Haplotype Corrected	4	2	1

[a] Sampling period indicates the time when soil samples were collected from the field in relation to the application of biocontrol strains.

[b] Aflatoxin gene cluster type was based on either uncorrected or corrected haplotype data. Haplotype correction was implemented by counting the total number of unique multi-locus haplotypes in each aflatoxin gene cluster category.

[c] Full, partial and missing cluster types were based on the presence or absence of three genes (*aflC*, *aflM* and *aflW*) in the *A. flavus* aflatoxin gene cluster.

[d] Soil samples were not collected in Alabama in 2016.

Table 4.7. Parameter estimates of *A. flavus* populations in maize fields in southern United States treated with RMb10 and Afla-Guard® biocontrol strains in 2016 and 2017. Neutrality tests were based on Tajima's *D* and Fu's *Fs* for five NGMLST loci (*aflM*, *aflW*, *amdS*, *mfs* and *trpC*).

State	Sampling period/ year	*aflM*		*aflW*		*amdS*		*mfs*		*trpC*	
		Tajima's D[a]	Fu's Fs[b]	Tajima's D	Fu's Fs	Tajima's D	Fu's Fs	Tajima's D	Fu's Fs	Tajima's D	Fu's Fs
Alabama	Pre-application	1304.3	-23.4*[c]	43.5	-14.8*	11.3	-22.7*	0.1	-11.9*	0.324	-9.7*
	Harvest	1299.7	-22.9*	27.3	-10.9*	*nss*[d]	*nss*[d]	0.4	-8.3*	-0.444	-9.3*
	2016	--[e]	--[e]	--[e]	--[e]	--[e]	--[e]	--[e]	--[e]	--[e]	--[e]
	2017	1270.4	-21.0*	37.1	-19.7*	11.5	-22.4*	0.9	-20.3*	0.552	-19.8*
Mississippi	Pre-application	1220.8	-20.4*	80.8	-21.6*	9.1	-20.8*	10.7	-21.5*	4.025	-16.3*
	Harvest	1168.7	-20.1*	66.6	-20.9*	10.6	-19.9*	6.8	-19.8*	3.032	-21.0*
	2016	1227.9	-20.0*	82.0	-20.8*	9.9	-20.2*	19.7	-18.2*	4.863	-10.6*
	2017	1170.7	-21.6*	72.0	-20.3*	15.1	-20.0*	-0.7	-19.6*	1.665	-20.8*
North Carolina	Pre-application	115.6	-20.4*	81.0	-20.8*	10.1	-20.6*	11.5	-21.0*	10.186	-14.2*
	Harvest	1299.8	-21.8*	93.7	-21.0*	81.8	-20.8*	16.2	-19.5*	5.963	-17.6*
	2016	*nss*[d]	*nss*[d]	83.6	-20.3*	11.9	-20.4*	22.5	-22.5*	14.617	-8.6*
	2017	118.9	-21.0*	90.9	-19.9*	70.2	-20.9*	6.5	-20.4*	0.975	-20.4*
Texas	Pre-application	126.1	-20.6*	58.1	-20.1*	13.8	-21.4*	5.1	-21.2*	5.37	-18.5*
	Harvest	114.8	-21.5*	64.5	-19.8*	13.8	-21.6*	3.7	-11.6*	3.739	-11.6*
	2016	112.5	-21.9*	51.5	-20.1*	13.8	-20.0*	6.6	-15.1*	6.187	-11.1*
	2017	653.7	-22.7*	68.3	-21.3*	13.9	-20.6*	3.12	-20.6*	2.285	-20.2*

[a] Tajima's *D* measures departure from neutrality based on Tajima (1989). Significant tests indicate balancing selection. Negative values suggest rapid population growth, while positive values indicate population contraction.

[b] Fu's *Fs* measures departure from neutrality based on Fu and Li (1993). Significant tests suggest population growth or genetic hitchhiking. Negative values are evidence for an excess number of alleles and suggest recent population growth, while positive values are evidence for a deficiency of alleles from a recent bottleneck.

[c] Asterisk (*) indicates values with significant ($P < 0.05$) deviation from neutrality.

[d] No soil samples were collected from Alabama in 2016.

[e] *nss* indicates no segregating sites detected.

Table 4.8. Mean estimates of nucleotide diversity (π) and mutation rates (θ) of *A. flavus* populations in maize fields in southern United States treated with RMb10 and Afla-Guard® biocontrol strains in 2016 and 2017. Values were estimated using five NGMLST loci (*aflM*, *aflW*, *amdS*, *mfs* and *trpC*).

State/Sampling period/Year	Nucleotide diversity (π)[a]	Watterson's θ [b]
Alabama	76.890	13.015
Mississippi	105.492	11.352
North Carolina	132.061	12.135
Texas	95.871	12.687
Pre-application	103.905	12.321
Harvest	106.158	12.836
2016	116.148	12.936
2017	88.747	10.735

[a] π denotes nucleotide diversity based on Nei and Li (1979).
[b] Watterson's θ estimates the population-scaled mean mutation rate based on Watterson (1975).

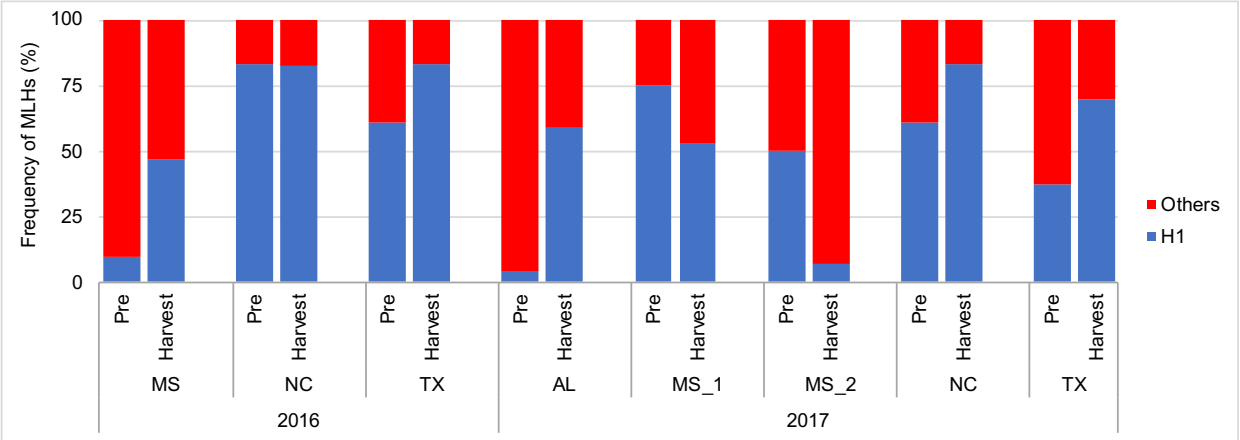

Figure 4.1. Frequency of multi-locus haplotypes (MLHs) recovered as a proportion of the total number of MLHs observed at each sampling period from maize fields in Alabama, Mississippi, North Carolina and Texas in 2016 and 2017 using combined five next generation multi-locus (*aflM*, *aflW*, *amdS*, *mfs* and *trpC*) sequence data. Pre denotes sampling time before application of RMb10 and Afla-Guard® biocontrol strains. Both RMb10 and Afla-Guard® belong to haplotype H1.

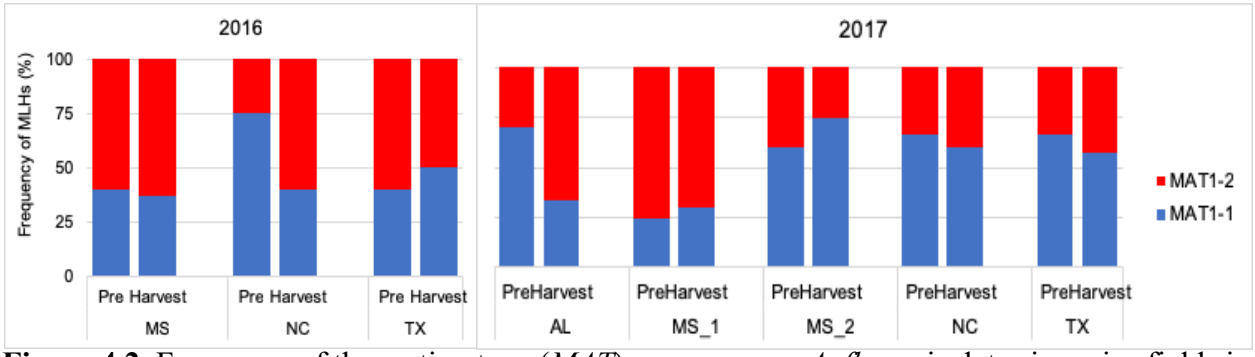

Figure 4.2. Frequency of the mating type (*MAT*) genes among *A. flavus* isolates in maize fields in southern United States treated with RMb10 and Afla-Guard® biocontrol strains in 2016 and 2017.

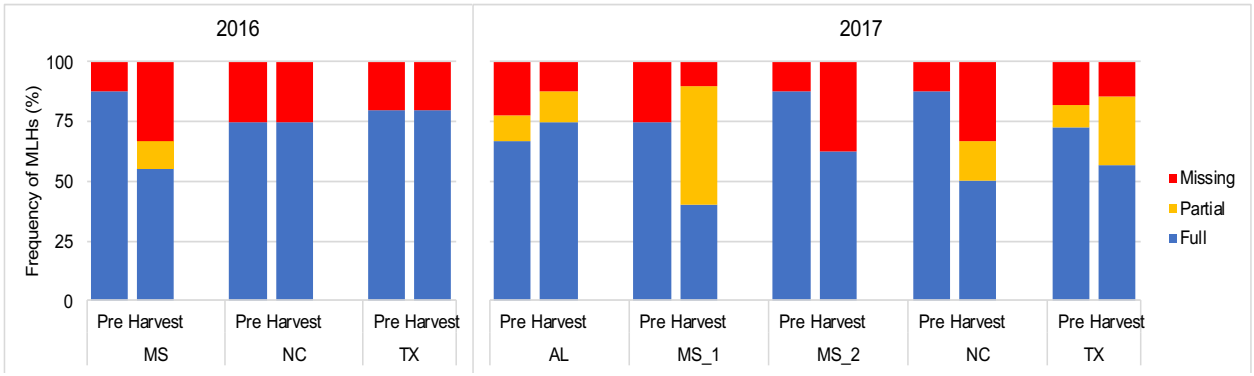

Figure 4.3. Frequency of aflatoxin gene cluster types among *A. flavus* isolates in maize fields in southern United States treated with RMb10 and Afla-Guard® biocontrol strains in 2016 and 2017. Full, partial and missing cluster types were based on the presence or absence of three genes (*aflC, aflM* and *aflW*) in the *A. flavus* aflatoxin gene cluster. Pre denotes sampling time before application of RMb10 and Afla-Guard® biocontrol strains. Both RMb10 and Afla-Guard® biocontrol strains have missing aflatoxin gene clusters.

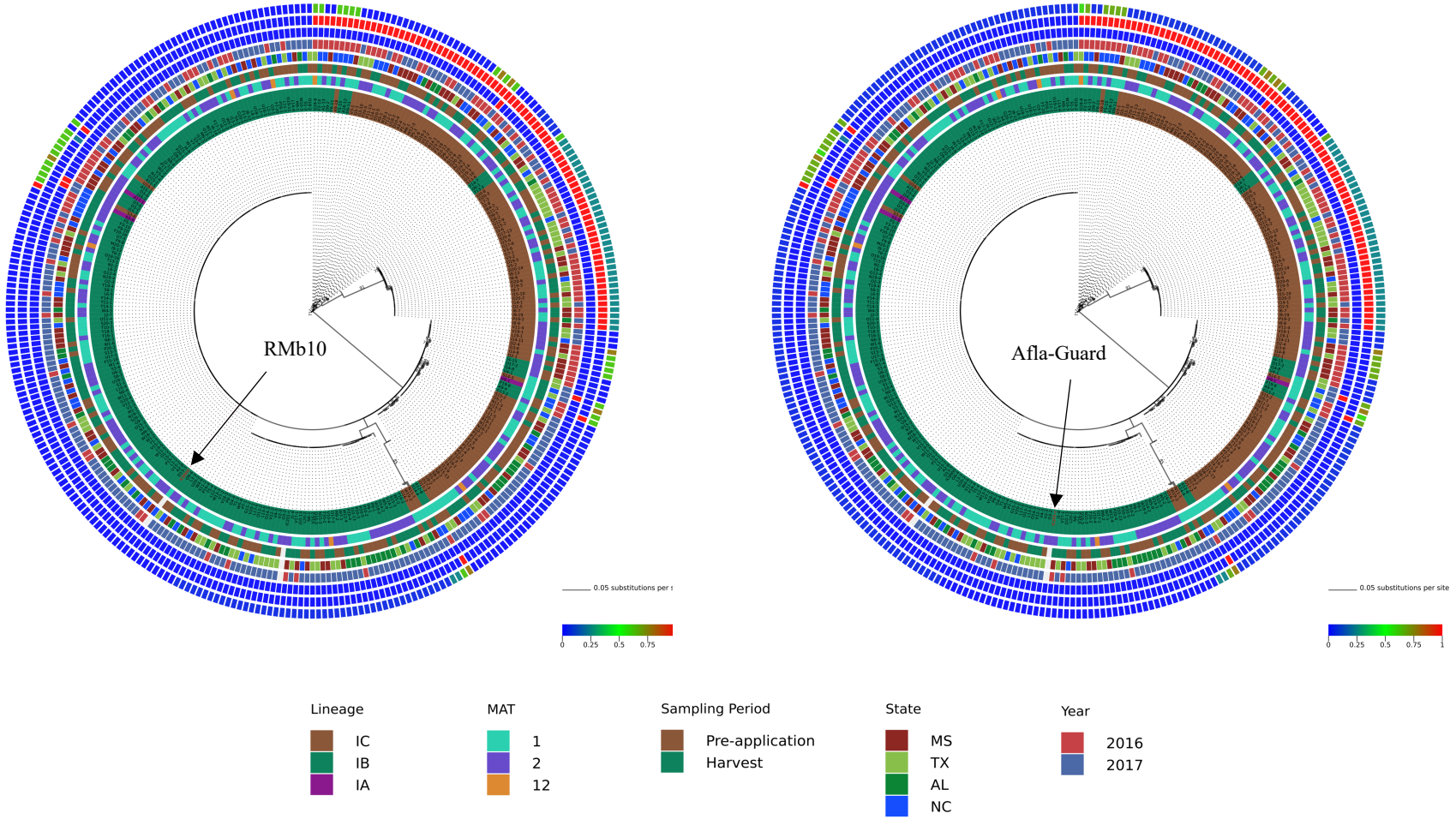

Figure 4.4. Phylogenetic relationships showing patristic distances of 311 *A. flavus* isolates to RMb10 (radial tree on left) or Afla-Guard® (radial tree on right) biocontrol strains. In the center of each radial ring is the best maximum likelihood tree for the combined NGMLST loci using *amdS*, *mfs* and *trpC* with branches drawn to scale. The five innermost rings represent *A. flavus* lineage, mating type, sampling period, state, and year respectively. The three outermost rings represent patristic distances for *amdS*, *mfs* and *trpC*, respectively. The distance of each isolate from RMb10 or Afla-Guard® as a reference is shown using a heat map, where a value of 0 (blue) indicates high genetic similarity of the isolate to the reference and a value of 1 (red) is high genetic dissimilarity.

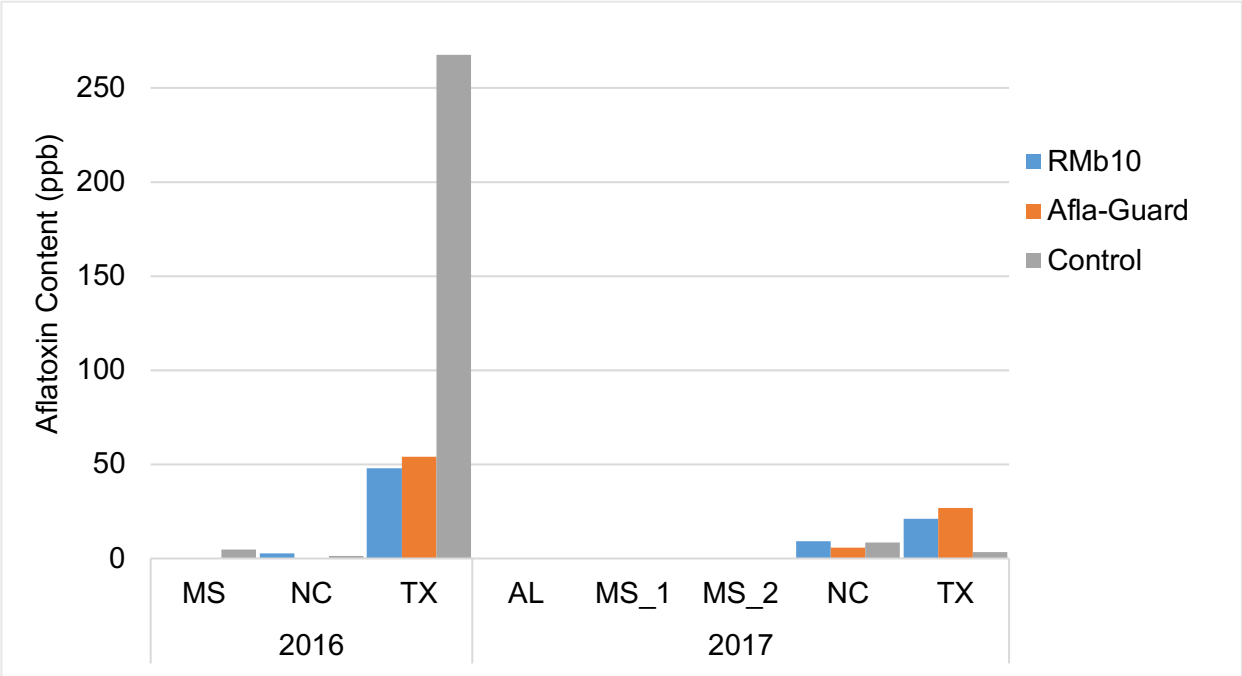

Figure 4.5. Aflatoxin contamination in grain harvested from maize fields in southern United States treated with RMb10 and Afla-Guard® biocontrol strains in 2016 and 2017. Aflatoxin values, quantified in parts per billion (ppb), were calculated from three to five replicate plots per field site. Similar letters indicate no significant statistical difference ($P < 0.05$) in aflatoxin values between treatments.

CHAPTER 5

Conclusion

Aflatoxin contamination of maize following infection by aflatoxigenic *A. flavus* continues to be serious problem worldwide. Biocontrol using non-aflatoxigenic strains of *A. flavus* offer the greatest potential in mitigating contamination. As such, there have been tremendous interest in improving the efficacy of biocontrol based on knowledge gained from studies on the biology of *A. flavus*. This study was specifically conducted to characterize the processes that occur during sexual reproduction within the stromata of *A. flavus* and to assess the effect of applying a novel *MAT1-1* biocontrol strain in the dynamics of native populations of *A. flavus* in the soil.

In Chapter 2, the first documentation of the morphological changes that occur within the stromata when a sclerotium-producing female strain with high level of fertility is crossed with a conidium-producing male strain of the opposite mating type is provided. Early events during sexual reproduction examined using green fluorescent protein (eGFP)-labeled and mCherry (mCH)-labeled strains showed the germination of the conidium-producing strain towards the base of the sclerotium-producing strain within 24 hours of crossing, production of interlocking hyphal networks at 72 hours incubation, and observation of the conidium-producing strain within the stromatal matrix of the sclerotium-producing strain at 5 weeks of incubation. Difference in morphological structures became apparent between fertilized stromata and unfertilized sclerotia at 4 weeks of incubation when ascocarps, internal hyphae and croziers formed within the stromatal matrix of the high fertility cross but not in the low fertility cross or unmated sclerotia. Further branching and coiling of the croziers produced numerous ascospore-bearing asci observed at 6 to 8 weeks of incubation. These results broadened our knowledge on the morphological features of sexual reproduction while providing a basis for relating metabolomic and transcriptomic properties

associated with the formation of sexual structures within stromata exhibiting high levels of female fertility. Perhaps one of the major finding of this work relates to the mechanism of sexual reproduction in *A. flavus* where the results suggest that genetic information from the male parent is likely transferred into the stroma possibly through anastomosis of hyphae originating from both conidia and sclerotia on the exterior of the sclerotia.

The impact of female fertility on metabolomic and transcriptomic profiles between reciprocal crosses that exhibit different levels of female fertility is documented in Chapter 3. Eighteen secondary metabolites, including the carcinogen aflatoxin B1 (AFB_1), were detected in the study. AFB_1 decreased over time in samples from the high fertility cross which used the aflatoxigenic strain NRRL 29507 as the sclerotial parent and the biocontrol strain NRRL 21882 as the conidial parent, supporting previous reports that a non-aflatoxigenic strain has the potential to reduce AFB_1 when crossed with an aflatoxigenic strain via sexual reproduction. Hierarchical and PCA analyses identified the elevated abundance of hydroxyaflavazole, an indole diterpene isomer, and an aflavinine isomer in samples from the high fertility cross at time-points that are consistent with the formation of sexual structures identified in Chapter 2. Further, transcriptional analysis identified the possible involvement of the genes *brlA, chiB, gprD, ppoC, rodA* and several backbone genes that encode enzymes in the *A. flavus* secondary metabolism gene clusters in the process of sexual reproduction in *A. flavus*. Integration of these metabolomic and transcriptomic results with the morphological data could be used to further explore the biochemical mechanism underlying sexual reproduction in *A. flavus* and inform possible strategies to screen *A. flavus* strains with high levels of female fertility.

Finally, Chapter 4 documents the change in the population dynamics of native *A. flavus* in southern United States as influenced by the application of a novel *MAT1-1* biocontrol strain,

RMb10. RMb10 and Afla-Guard®, both biocontrol strains belonging to lineage IB and has missing aflatoxin gene clusters, were applied in large-scale field trials in Alabama, Mississippi, North Carolina and Texas in 2016 and 2017. *A. flavus* populations collected from soil samples prior to application of biocontrol and at harvest exhibit signatures of recombination consistent with ongoing sexual reproduction. Recombination is further evidenced by emergence of isolates with partial aflatoxin gene clusters at harvest. The frequency of isolates belonging to the same haplotype as RMb10 and Afla-Guard® as well as the frequency of isolates with missing aflatoxin gene cluster increased at harvest, indicating successful proliferation of these biocontrol strains into the native *A. flavus* populations. Further, levels of aflatoxin contamination from Texas in 2016 showed that RMb10 and Afla-Guard® had comparable efficacy in reducing aflatoxin contamination in maize kernels. Thus, RMb10, is a promising candidate as a biocontrol agent against aflatoxin contamination in maize. Availability of a biocontrol strain with *MAT1-1* mating type could be useful in soil populations whose predominant native population are *MAT1-2* whereby sexual recombination can shift the toxigenic population towards a non-aflatoxigenic population and thereby result in more sustainable mitigation of aflatoxin contamination.